Towards the analysis of translational regulation during male meiosis and dissection of pollen development via mutants in cell cycle control factors in *Arabidopsis thaliana*.

Dissertation submitted to obtain the doctoral degree (Dr. rer. nat.)
at the Faculty of Mathematics, Informatics und Natural Sciences,
Department of Biology
University of Hamburg

Submitted by
Wojciech Jan Urban

Hamburg

Evaluators:

Prof. Dr. Arp Schnittger

Prof. Dr. Stefan Hoth

Examination commission:

Dr. Dirk Warnecke

Prof. Dr. Julia Kehr

Prof. Dr. Wilhelm Schäfer

8th of October 2018

“ Szxdsc c fcxbnbc v b cvgnbnb m „.redfc “

Wiktor Urban – 9 months

Table of contents

1. Introduction

One of characteristic plant traits is that during their lifetime they develop two different generations, which are different in terms of ploidy. In flowering plants the haploid gametophyte, responsible for creating gametes, is confined within a diploidal sporophyte, which grows to sustain the former. The female gametophyte produces two gametes one egg cell and one central cell, whereas the male gametophyte produces two sperm cells as gametes.

1.1. Formation of microspore mother cells

Anther development starts with periclinal divisions of the hypodermal cells in the anther primordium leading to the formation of the archesporial cells in the primordium corners. Different layers of the anther are formed from subsequent mitotic divisions of those cells. This process begins with two layers of cells, namely the outer parietal cells and inner primary sporogenous cells. The former divides into endothecial cells and secondary paretial cells (Figure 1.F), which will later create the middle cell layer and the tapetum (Figure 1.G and H). The inner primary cells undergo a small number of divisions and form mother cells of the male germline, which further develop into microsporocytes and then in pollen (Figure 1.D; Wilson and Zhang, 2009).

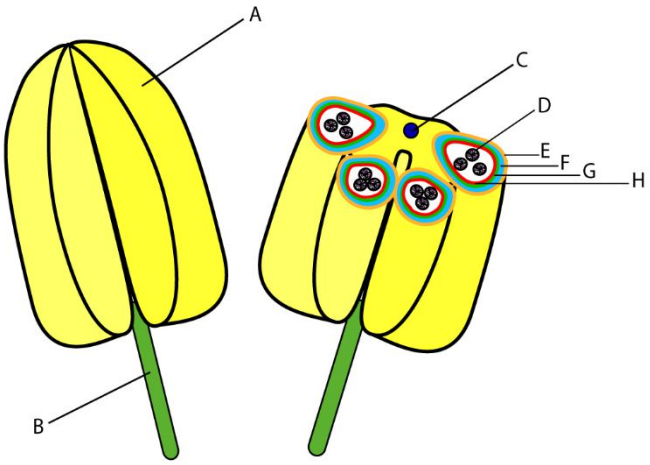

Figure 1. Anther morphology

(based on Cardarelli and Cecchetti, 2014)

A. anther; B. filament; C. vasculature; D. male gametophyte (pollen); E. epidermis; F. endothecium; G. middle layer; H. tapetum.

1.2. Meiotic division in pollen development

The first meiotic division occurs after the pollen mother cell (PMC; Figure 2.A) grows into a microsporocyte (Figure 2.B) and results in the creation of a cell with two haploid nuclei (Figure 2.C). The second meiotic division doubles the number of nuclei in the cell. Afterwards, the nuclei are separated from each other by a callose wall. This formation is called a tetrad and marks the end of the meiotic part of pollen development which is named microsporogenesis (Figure 2.D; Wijnker and Schnittger, 2013). The foundation for this division is already laid down when the genetic material is doubled in the pre-meiotic S-phase of the cell cycle (Figure 2.b). The first stage of meiosis is called prophase (Figure 2.c) and consists of 5 distinguishable sub-phases (Figure 3). The first one, called leptotene, starts with chromosome condensation, after which double strand breaks (DSB; Figure 3.A) are introduced. Afterwards, the 5' end is resected so the other end can invade the structure of the second homolog (Edlinger and Schloglehofer, 2010).

Subsequently, the zygotene stage commences, this stage is characteristic for the formation of the synaptonemal complex (Figure 3.D) and recombination progression. The next pachytene is categorized by further recombination, fully manifested crossing-over and finally the degradation of the synaptonemal complex. Highly condensed chromosomes as well as chiasmata representing the crossing-overs may be easily observed in the last two phases, named diplotene and diakinesis (Wijnker and Schnittger, 2013). Next, the chromosomes line up in the central axis of the dividing cell in methaphase I and - thereafter are pulled as whole to the opposite poles in anaphase I. Afterwards, instead of decondensation, cells are undergoing another division, but in this case only the chromatids will be separated, instead of whole chromosomes, which leads to the creation of haploid gametes. This division ends with a telophase and cytokinesis, during which the haploid genetic material is surrounded by the new nuclear envelope. The result of this division is the creation of four genetically diverse cells (Edlinger and Schloglehofer, 2011; Osman et al.,2011; Wijnker and Schnittger, 2013).

1.2.1. Progression of meiosis in male germline

Among different species, meiosis is evolutionarily conserved on a cellular level, but in spite of that, the mechanisms of molecular initiation of meiosis are miscellaneous (Pawlowski, 2007). Throughout the progression of meiosis as well as the entire cell cycle – *CDKs* (*CYCLIN DEPENDENT KINASES*), cyclins, and *APC/C* (*ANAPHASE-PROMOTING COMPLEX/CYCLOSOME*) play a major role. *CDKs* are serine/threonine kinases that, in Arabidopsis, are categorized into seven different groups depending on the motif responsible for interacting with cyclins. *CDKA;1* is an only representative of the A-group of kinases and is known to have high activity peaks during both metaphases in meiosis, driving the cell through this part of the cell cycle (Vandepoele et al., 2002; Menges et al., 2005; Harashima and Schnittger, 2012). Cyclins in Arabidopsis are represented by an assembly of at least 50 genes gathered into 10 different groups. The most characteristic feature of those genes is their interaction with *CDKs,* and the influence on CDK activity. This influence depends on the combination between various CDKs and CYCLINs of the CDK-CYCLIN complex. The role of APC/C is to degrade cyclins which will decrease the activity of the CDKs and move the cell into anaphase (Figure 2; Osman et al., 2011; Harashima and Schnittger, 2012; Mercier et al., 2015).

Interactions between the CDK/CYCLIN complex and the APC/C complex are not the only mechanism controlling the progression of the cell cycle. In fact, there is a second layer of interactions that circles around a very important cyclin. It is one of the cyclins from the A-group which alone plays a major role in the control of transitions in meiosis, from prophase to meiosis I and from meiosis I to meiosis II. Mutants of *CYCLINA1;2*, also called *TAM (TARDY ASYNCHRONUS MEIOSIS*), fail to enter the second meiotic division, which results in unreduced (2n) gametes. In Arabidopsis, this can be observed by the formation of dyads instead of tetrads, and subsequently larger pollen grains (d'Erfurth et al., 2010). When combined with *spo11* and *rec8* mutants (see below) *tam* mutant plants are producing 2n gametes that are identical to parental cells, just like in a process similar to mitosis, which, in turn, is very similar to the *osd1* (*OMISSION OF SECOND DIVISION 1*) mutants (d'Erfurth et al., 2010). Mutations in *OSD1* lead to a premature exit from meiosis, before the second meiotic division and in the subsequent creation of diploid gametes. *OSD1* also takes part in suppressing ectopic endomitosis by inhibiting the *APC/C* complex (Figure 2; Cromer et al., 2012). When those two genes (T*AM* and *OSD1*) are mutated

together, it results in the failure in transition from prophase to meiosis I and production of completely unreduced tetraploid gametes (d'Erfurth et al., 2010).

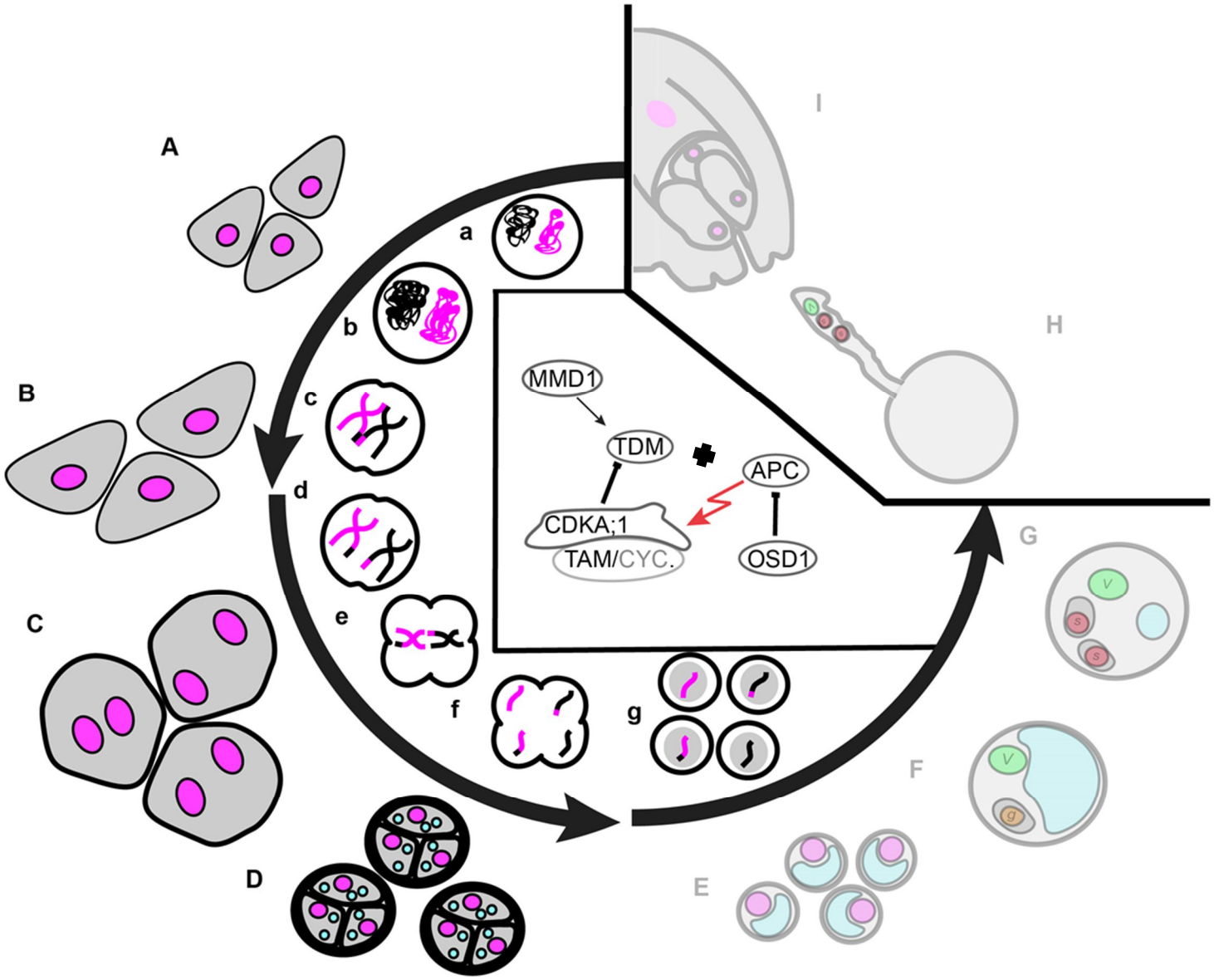

Microspore development:

A. Pollen mother cells (PMC)
B. PMC grows into a microsporocyte
C. First meiotic division
D. Second meiotic division and tetrad formation

Meiotic division:

a. Interphase
b. S-phase – doubling of genetic material
c. Prophase + Metaphase I
d. Anaphase I
e. Metaphase II
f. Anaphase II
g. Telophase and cytokinesis

Figure 2. Microsporogenesis highlighted (A-D). Meiotic division (a-g). The scheme in the middle of the figure explains the interactions between some of the important meiotic regulators significant for the progression of meiosis. *OSD1* –acts as an APC/C inhibitor, TDM is proposed to act together with APC/C and its directly activated by MMD1 and phosphorylated by the CDKA;1/TAM complex. The role of APC/C lies in CYCLIN degradation.

The next gene involved in meiotic progression is *TDM1/MS5 (THREE DIVISION MUTANT1/MALE STERILE 5*), which is responsible for termination of meiosis after the second meiotic division and prevents an atypical third division. Moreover, it is known for interacting with the Anaphase-Promoting Complex and is showing similarities to some of the APC/C components. Additionally, when a CDK phosphorylation site in *TDM1* is mutated, it results in a premature meiosis termination and production of diploid gametes. Typically, this process is prevented by the CDKA;1/TAM complex, which stops the premature exit from meiosis by phosphorylating TDM1 (Cromer et al,. 2012; Cifuentes et al., 2016).

TDM is directly activated by *MMD1 (MALE MEIOCYTE DEATH 1),* also called *DUET*, which encodes a PHD finger protein. Mutants of *mmd1* are showing collapsing meiocytes, defective chromosome condensation, delayed progression and occasional arrest at metaphase I. Moreover, organelle band during interkinesis is absent in mutant cells which subsequently leads to forming lethal dyads and triads, instead of tetrads. This transcriptional regulator is also known to influence proper organization of microtubules during meiosis II (Andreuzza et al., 2014).

1.2.2. Important events during meiosis

Successful meiosis relies on pairing and synapsis of homologous chromosomes during the meiotic prophase. This process is governed by synaptonemal complex, a structure that compromises of a central element, which is polymerized between two axial elements (in later stages called lateral elements) (Figure 3. D; Higgins et al., 2005; Mercier et al., 2015). So far, in plants, only one conserved gene was identified to be a part of the central element of the synaptonemal complex in more than one species. *ZYP1* (*ZIPPER1*), which is a homolog of *ZIP1* from yeast, was identified in rice (*OsZEP1*; Wang et al., 2010), barley (*ZIP1*, Barakate et al., 2014) and in Arabidopsis (as a duplicated gene – *ZYP1a/ZYP1b*; Higgins et al., 2005).

ASY 1 and *3* (*ASYNAPTIC 1* and *3*) are the two genes that were identified as part of plant lateral elements of the synaptonemal complex. ASY1 is a HORMA protein and ASY3 contains a coiled-coil domain towards its C-terminus. Deficiency in the abundance of one of these proteins leads to defects during recombination (because of missing synapsis; Figure 3 D; Ferdous et al., 2012; Mercier et al., 2015).

Another complex necessary for successful division whichever mitotic or meiotic, is the cohesion complex. When it functions properly, it manages the cohesion between replicated chromosomes, either by holding them together or releasing them if needed. Main body of this complex consists of two proteins encoded by genes *SMC1* and *3* (*STRUCTURAL MAINTENANCE OF CHROMOSOME 1 and 3*). Proteins from this family possess several conserved domains, such as an N-terminal NTP binding motif, a C-terminal DA box and two central coiled-coil domains separated by a hinge domain. Plants with those genes mutated show premature sister chromatid separation and problems with segregation of the chromosomes (Lam et al., 2005). Proteins encoded by *SMC1* and *3* are fastened together by either *RAD21* (*RADIATION-SENSITIVE 21*) in mitosis or its homologue - *REC8* (*RECOMBINATION 8*) in meiosis. Mutants of the latter exhibit defective meiotic cohesion and chromosome condensation, which results in their subsequent fragmentation and polyads formation (Cai et al., 2003). Cleavage of *RAD21* after metaphase - anaphase transition releases the binding between the chromatids and enables them to be transported to the opposite poles of the mitotic spindle. Unlike most eukaryotes, there are three *RAD21*-like homologs - *AtRAD21.1*, *AtRAD21.2* and *AtRAD21.3* in Arabidopsis (Figure 3.B; Costa Nunes et al., 2006)

Before any recombination occurs in meiosis, it is necessary to form double strand breaks (DSB) enabling the DNA strand to infiltrate through the break and finally relegate the ends of the broken strands. This is possible thanks to a conserved eukaryotic gene *SPO11* (*SPORULATION 11*; Mercier et al., 2015). In plants it has at least two homologues (*SPO11-1* and *SPO11-2*) which are required for recombination. Mutants of those two genes show a huge decrease in meiotic recombination rate, which leads to achiasmatic univalents caused by the absence of DSB (Hartung and Puchta, 2000; Muyt et al. 2008).

After the strands are broken, two important genes need to act, *RAD51 (RADIATION-SENSITIVE 51)* and *DMC1 (DNA MEIOTIC RECOMBINASE 1)*. Those genes are recombinases responsible for forming nucleoprotein presynaptic filaments that are bound to the 3' end

of the single strand DNA. Their role is to invade the homologous DNA duplexes, find homologies and form stable molecules so it would be possible to exchange strands. *RAD51* is present in both mitotic and meiotic cells, whereas the other *DMC1* is present only during meiosis. Mutating both of those genes leads to failure in chromosome synapsis. Mutants of *rad51* exhibit chromosome fragmentation during the first metaphase, whereas in the case of the *dmc1* mutants it is possible to observe univalent chromosomes (Osman et al., 2011). Later the single strand extends into the direction of the homologues chromosome, the D-loop captures the other overhanging single strand and then the gaps are filed via DNA synthesis (depicted as pink arrows). Ligation of the DNA creates an intricate structure where two DNA molecules are connected by transferring parts of a DNA strand from each duplex (Figure 3.C.I). Resulting assembly shows two X - like shaped structures called double Holliday junctions (Osman et al., 2011; Mercier et al., 2015). Stabilization of the progenitor Holliday junction is performed by *MSH4* and *5* (*MUTS HOMOLOG 4* and *5*; Mercier et al., 2015). Mutating those genes heavily impacts chiasmata frequency, distribution and delays the overall progression of prophase I (Higgins et al., 2008; Lu et al., 2008). A very similar mutant phenotype may be observed with *PTD* (*PARTING DANCERS*) mutants. The function of these genes is not entirely known so far but there is some indication that it is required for dHj resolution (Osman et al., 2011). This resolution occurs together with DNA ligation and cross over formation and happens after the double Holliday junction is cleaved in an asymmetric matter (black arrows; Figure 3.C.II). After the cleavage and subsequent DNA ligation the cross over is formed (Figure 3.C.III).

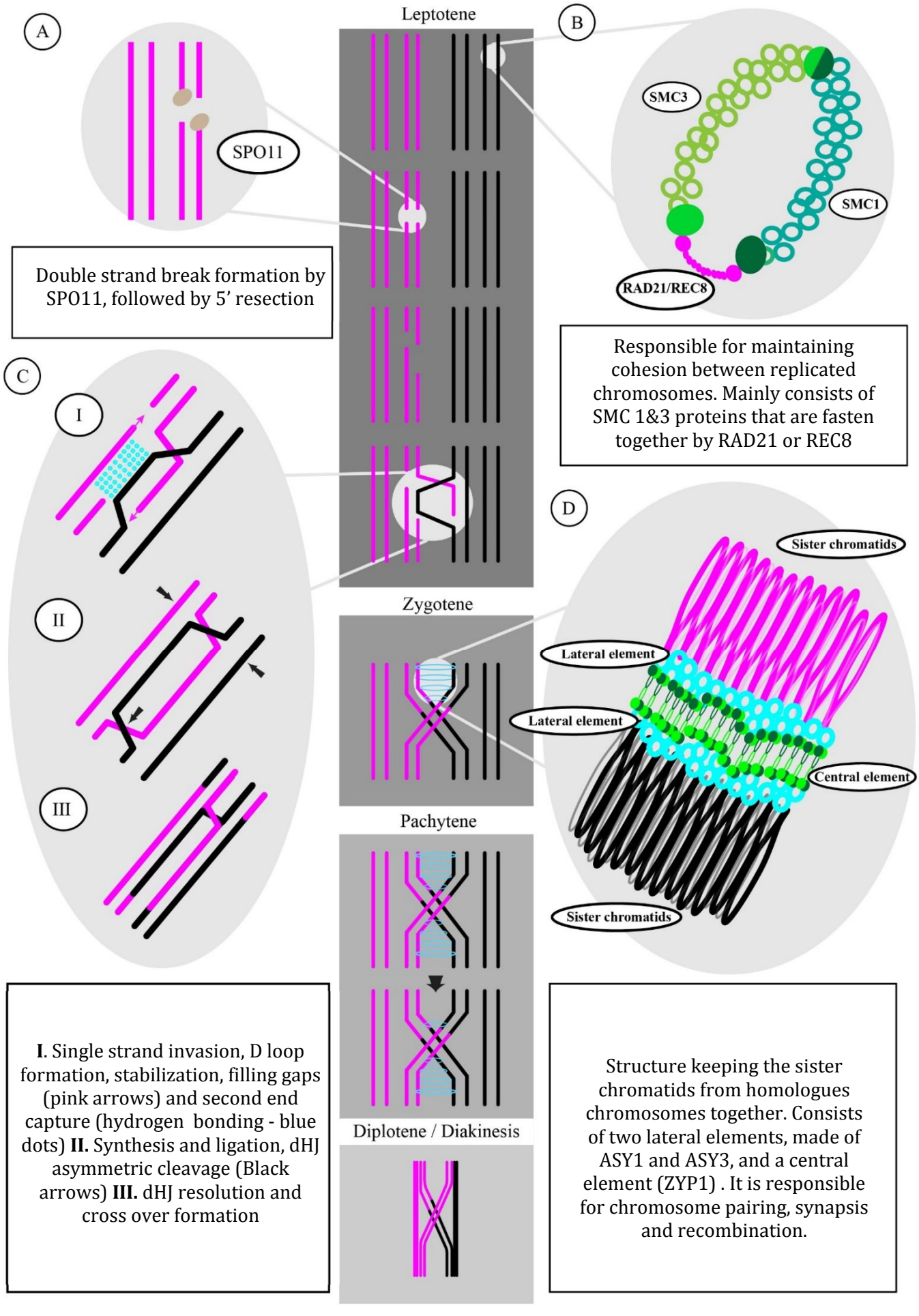
A
SPO11
Leptotene
B
SMC3
SMC1
RAD21/REC8
Double strand break formation by SPO11, followed by 5' resection
Responsible for maintaining cohesion between replicated chromosomes. Mainly consists of SMC 1&3 proteins that are fasten together by RAD21 or REC8
C
I
II
III
Zygotene
D
Sister chromatids
Lateral element
Lateral element
Central element
Sister chromatids
Pachytene
Diplotene / Diakinesis
I. Single strand invasion, D loop formation, stabilization, filling gaps (pink arrows) and second end capture (hydrogen bonding - blue dots) **II.** Synthesis and ligation, dHJ asymmetric cleavage (Black arrows) **III.** dHJ resolution and cross over formation
Structure keeping the sister chromatids from homologues chromosomes together. Consists of two lateral elements, made of ASY1 and ASY3, and a central element (ZYP1) . It is responsible for chromosome pairing, synapsis and recombination.

Figure 3. Important events during meiosis. A. Double strand break formation **B**. Cohesion complex. **C**. Homologous recombination. **D.** Synaptonemal complex.

1.2.3. Transcript expression during meiosis

In the preparatory work of our lab Hirofumi Harashima obtained high-resolution transcriptional maps of meiotic progression in Arabidopsis using CATMA microarrays (Figure 4.A). The plants were beforehand synchronized and the microarrays were showing discrepancies in transcription between different days after synchronization induction. At the day when meiosis occurs, the differences between that day and the day before are scarce, which is astonishing in regard to the complexity of meiosis. Subsequently, a quantitative expression analysis was performed, where some of the meiosis specific genes exhibited expression that did not correlate with the onset of meiosis. Some of the genes transcripts appeared few days before meiosis (*REC8*) and some of them were present through the whole experiment (*TAM*; Figure 4.B). These two experiments are suggesting extensive translation control.

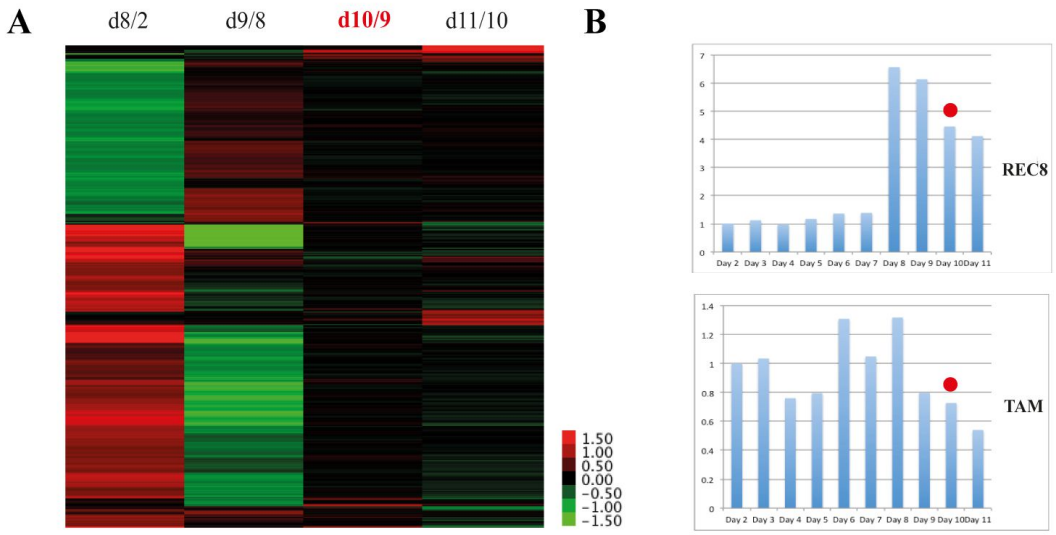

Figure 4. Transcript expression during meiosis. A. CATMA microarray B. qPCR experiment for REC8 and TAM genes (unpublished results from H. Harashima, M. Heese, D. Gey, S. Balzergue)

1.2.4. Translation control in plants

Control of translation is a mechanism that is able to quickly influence protein formation in reply to developmental and external signals. With great precision in time and

space it can control protein synthesis by coordination of many different factors. This type of control happens mostly during translation initiation and is typically directed towards its machinery (Muench et al., 2012).

1.2.4.1. Translation initiation

Translation can be divided in three phases, initiation, elongation and termination. Initiation can be mediated by the cap structure at the beginning of mRNA, this structure consists of 7-methylguanylate, three phosphate groups and an instance of any base. The other way for translation to start is via internal ribosome entry sequence (IRES), located in the 5'UTR or open reading frame which can recruit a ribosome directly to an internal site on the mRNA strand (Gebauer and Hentze, 2004).

The process of translation initiation via the cap structure starts when the initiator mRNA, loaded with methionine, binds with eIF2 (Eukaryotic initiation factor 2), which is coupled with a GTP and finally yields a ternary complex. Subsequently, it becomes a part of the 43S pre-initiation complex together with the small ribosome subunit and four other eIF's (eIF1, eIF1A, eIF3 and eIF5; Figure 5.D). With the usage of ATP this complex will bind to the mRNA via establishing a connection between the eIF3 and scaffold protein eIF4G, which is a part of the eIF4F complex that is bound to the cap structure of the mRNA. The other parts of this cap binding complex are factor 4E, which is binding directly to the mRNA cap and 4A, which is a DEAD box RNA helicase that unwinds any secondary structures during the subsequent scanning event (Gebauer and Hentze, 2004; Browning, 2004). The 4G scaffold protein is also responsible for establishing a connection with the poly(A)-binding protein (PABP), which is accountable for circularisation of the mRNA molecule (Figure 5.C; Gebauer and Hentze, 2004).

Apart from the canonical 4F complex, plants possess a second form of this complex called eIF(iso)4F. This significantly smaller cousin of the 4F complex (smaller in about 100 kDa) was extensively studied in terms of it connection with reaction to virus infection in plants (Bush et al., 2015). It has much higher affinity to mRNA caps that are hypomethylated in comparison to canonical 4F. Also a double knock-out mutant of the *iso4G 1* and *2* redundant genes showed multiple phenotypic effects but no influence in general translation of the plant. This can indicate that this isoform may regulate translation of some specific physiologically important mRNAs (Muench et al., 2012).

After binding to the 4F complex the 43S pre-initiation complex will scan the mRNA in order to find an AUG start codon. Factors eIF1 and eIF1A are responsible for scanning. This scanning uses ATP and when the pre-initiation complex stumbles upon a start codon it will bind to it, establishing the 48S initiation complex. This activates eIF5 which is responsible for promoting GTP hydrolysis in order to separate other initiation factors from the small ribosome subunit. This allows the big ribosome subunit to bind, form a 80S initiation complex and finally start the formation of the first peptide bound (Gebauer and Hentze, 2004; Muench et al., 2012).

1.2.4.2. Global control

Global control, involves regulatory aspects that influence most of the mRNA translation in the cell. Global control is mostly executed by modifying initiation factors. There are two most common mechanisms of global control in eukaryotes. First involves a 4E-BP (4E binding protein), which, by binding to the 4E Factor, blocks the formation of the 4F complex impossible and therefore prevents translation initiation. It can block the 4E protein before or after it establishes connection with the mRNA cap (Figure 5.A; Gebauer and Hentze, 2004). The 4E-BP was identified in mammals with another 4E binding factor – 4e-T that controls nuclear transport of 4E (Freire et al., 2005). In Drosohpila 4E-BP has one homologue - THOR which is involved in regulating *OSCAR* mRNA translation (Nakamura et al., 2003; Wilhelm et al., 2003 Freire et al., 2005). Yeast possess two homologues of 4E-BP, *p20* and *EAP1*. In plants, up to now, no protein was identified as a homologue of 4E-BP, also no other protein is known to globally control translation via binding to eIF4E, although there are other proteins that are binding to the 4E factor. One of them is encoded by the *AtLOX2* gene (*ARABIDOPSIS THALIANA TYPE LIPOXYGENASE* 2) and its involved in the synthesis of specific regulatory substrates, such as jasmonic acid (Freire et al., 2000; Browning, 2004). Almost 7000 other proteins with motif characteristic for 4E binding were found and it is very likely that among them there is a protein that is controlling translation initiation in a global manner, just like 4E-BP (Sesma et al., 2016)

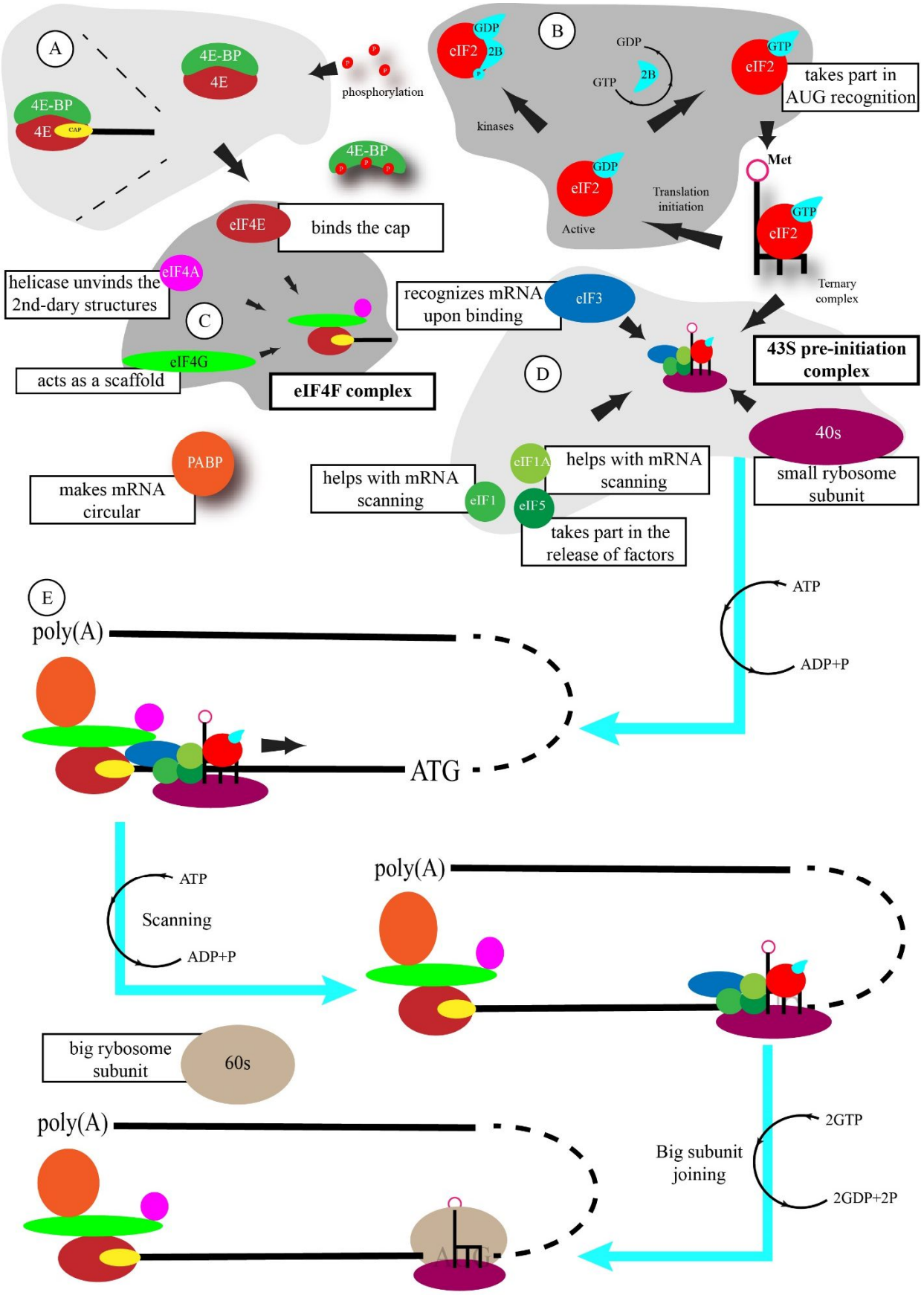

Figure 5. Translation initiation mechanism and global translation control. A.Global control - eIF4E-binding proteins. 4E-BPs binds to eIF4E, either when its already interacting with the CAP or before, preventing its interaction

interaction with eIF4G and so inhibiting translation Phosphorylation of this binding protein releases the 4E factor subsequently allowing the translation to proceed. **B.** Global control – eIF2 phosphorylation, eIF2 is a part of the ternary complex, together with the initiator RNA (black L-like shape), methionine and GTP. The GTP is hydrolyzed when the AUG codon is recognized during translation initiation, resulting in eIF2 bounded to GDP. If the eiF2 is phosphorylated by a kinase, the exchange between GDP/GTP is blocked therefore reducing the dissociation rates between the eIF2 and the 2B factor which then prevents the 2B factor from catalyzing the GDP -GTP exchange and stops the eIF2 molecule from being recycled. **C.** eIF4F complex consists from eIF4E protein that binds the cap structure at the beginning of the mRNA; eIF4G protein which acts as an scaffold for other proteins; eIF4A which is a helicase that unwinds any secondary structures present on the mRNA strand. **D.** 43S pre-initiation complex comprises of the ternary complex, small ribosome subunit, the eIF3 protein – responsible for mRNA recognition upon binding, eIF1 and 1A that are helping with the scanning procedure and finally the eIF5 which takes part in the release of other factors when the AUG codon is recognized. **E.** Translation initiation. After the ternary complex forms the 43S pre-initiation complex with other factors and the 40S ribosome subunit it binds to the 4F complex that is already bounded to the mRNA. Afterwards the pre-initiation complex will scan in search of the AUG codon. When the complex recognizes the start of translation it forms a stable connection with it, after that the large subunit binds to the complex and all of the initiation factors are being released from the complex which marks the beginning of translation (based on Gebauer and Hentze, 2004).

The second global mechanism revolves around the 2nd initiation factor, which forms the ternary complex together with the initiator tRNA and GTP, which will be hydrolyzed during translation initiation. If the eIF2 is being phosphorylated, the dissociation rates with the eIF2B factor are reduced in consequence blocking the GDP-GTP exchange reaction. This deters the regeneration of eIF2 therefore hindering translation initiation (Gebauer and Hentze, 2004; Muench et al., 2012). There are two kinases in plants known for phosphorylation of eIF2. Genes coding those proteins are called *GCN 1* and *2* (*GENERAL CONTROL NON-DEREPRESSIBLE 1* and *2*), and are deeply connected to plant response to different kinds of stress. *GCN2* is active after starvation, UV light, wounding, a pathogen attack and oxidative or cadmium stress. The *GCN1* gene seems to react to stress caused by low temperatures. Those two genes are responsible for blocking mRNA translation in plants in those specific stress conditions (Gebauer and Hentze, 2004; Wang et al., 2016).

1.2.4.3. Local control

Apart of the previously described global control, eukaryotic organisms possess a more specific way of controlling translation. Local control mostly relies on regulating translation via proteins that are reacting with specific elements, which are placed in the untranslated regions of mRNA (Gebauer and Hentze, 2004). Often the way of influencing the translation initiation on a local matter involves blocking the formation of the 4F complex. This interference can happen when certain proteins will recognize a specific element (sequence) located in the 3' UTR and, at the same time, will bind to the 4E factor,

simultaneously blocking the translation. This process can happen directly via activity of one protein or indirectly via two proteins working together. The former can be represented by the Bicoid protein that recognizes the Bicoid response element (BRE) and interacts with the 4E element and blocks translation of caudal mRNA at the anterior pole of *Drosophila melanogaster* embryo (Figure 6.A; Kronja and Weaver, 2011). The latter process, which happens during oocyte maturation in vertebrates, thanks to interaction of two proteins MASKIN and CPEB (cytoplasmic-polyadenylation-element-binding protein) where the first one is binding to the 4E factor and the second is recognizing the *CPE* (*cytoplasmic polyadenylation element*) sequence (Figure 6.A; Yamashita and Takeuchi, 2017).

One of the ways to influence translation initiation requires presence of stem loop motif in a certain distance to the cap structure and a eIF4 complex present at the site. This specific motif is recognized by a protein molecule, which hinders the recruitments of the 43S pre-initiation complex. In this case, the 4F complex normally binds to the mRNA. An excellent example of this mechanism can be observed in the case of iron regulatory protein (IRP) and *iron responsive element* (*IRE*), that are controlling translation of ferritin- which is a iron storage protein (Figure 6.B; Zhou and Tan, 2017).

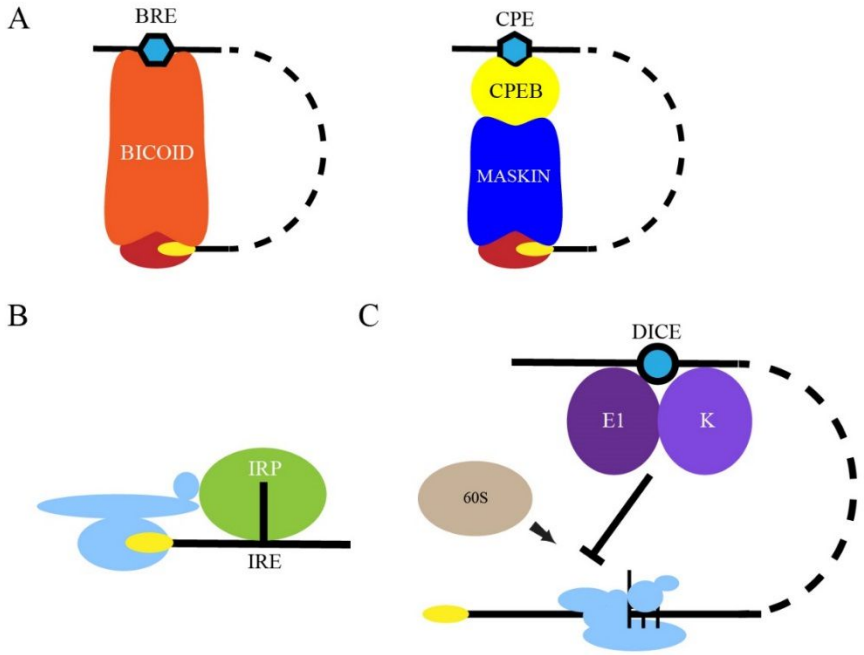

Figure 6. Local control A. Mechanisms of mRNA-specific regulation via 4E / 3' end binding. **B.** Steric blockage **C.** Regulation at post-recruitment steps (based on Gebauer and Hentze, 2004).

Translation can be also inhibited after the translation machinery has been loaded onto the mRNA strand and already started scanning. This type of control happens to the

lipoxygenase (*LOX*) mRNA during early erythroid differentiation. In this case, two binding proteins hnRNP K and E1 (heterogenous nuclear ribonulcleoprotein K and E1) prevent the large ribosome subunit from forming the 80S initiation complex by binding to the *DICE* element (*differentiation-control element*) and *ipso facto* blocking translation (Figure 6.C; Gebauer and Hentze, 2004).

1.2.4.4. Upstream open reading frames (uORF)

Another type of post recruitment translational control involves upstream open reading frames (uORF). Those usually short open reading frames are located before the start of the main frame. There are certain factors that are influencing how efficient in translation repression uORFs are : that is distances to the cap or the main ORF, length of the uORF, sequence of the uORF, number of uORF present or if there is any secondary structures at the site (Figure 7.A; Barbosa et al., 2013).

One of the examples of uORF influence on translation is the *GCN4 (GENERAL CONTROL NONDEREPRESSIBLE 4)* gene in yeast. This gene is responsible for amino acid biosynthesis and contains four upstream ORF's, Translation of *GCN4* relies on re-initiation, efficient retranslation of the main ORF depends on the amount of amino acids available and the consequent number of ternary complexes formed and active. If the levels of amino acids is high there are a lot of ternary complexes present, which leads to greater possibility of forming the 43S pre initiation complex before the last uORF. This results in translation of that frame and following dissociation of the 60S subunit. Finally, this hinders the reassembly of the pre-initiation complex before the main frame. Only in the case when the number of ternary complexes is low, the possibility of the complex formation before the last uORF is low, which increases the chances for the formation before the main frame (Figure 7.B and C; Gebauer and Hentze, 2004). In plants, there are several studies illustrating the influence of uORF. As in the case of *bZIP11 (*BASIC LEUCINE ZIPPER 11) gene, an uORF can cause ribosome stalling (Figure 7.D) that prevents re-initiation, physically blocking other scanning ribosomes from passing through the uORF cluster and reaching the main ORF (Hou et al., 2016). It also might be possible that uORF are causing the whole mRNA molecule to decay before the main ORF is translated. This is caused by premature recognition of the uORFs stop codon which triggers

nonsense-mediated mRNA decay. This happens especially if the uORF overlaps the main ORF or if it is unusually long (Arnim et al.,2013, Kalyna et al.,2011).

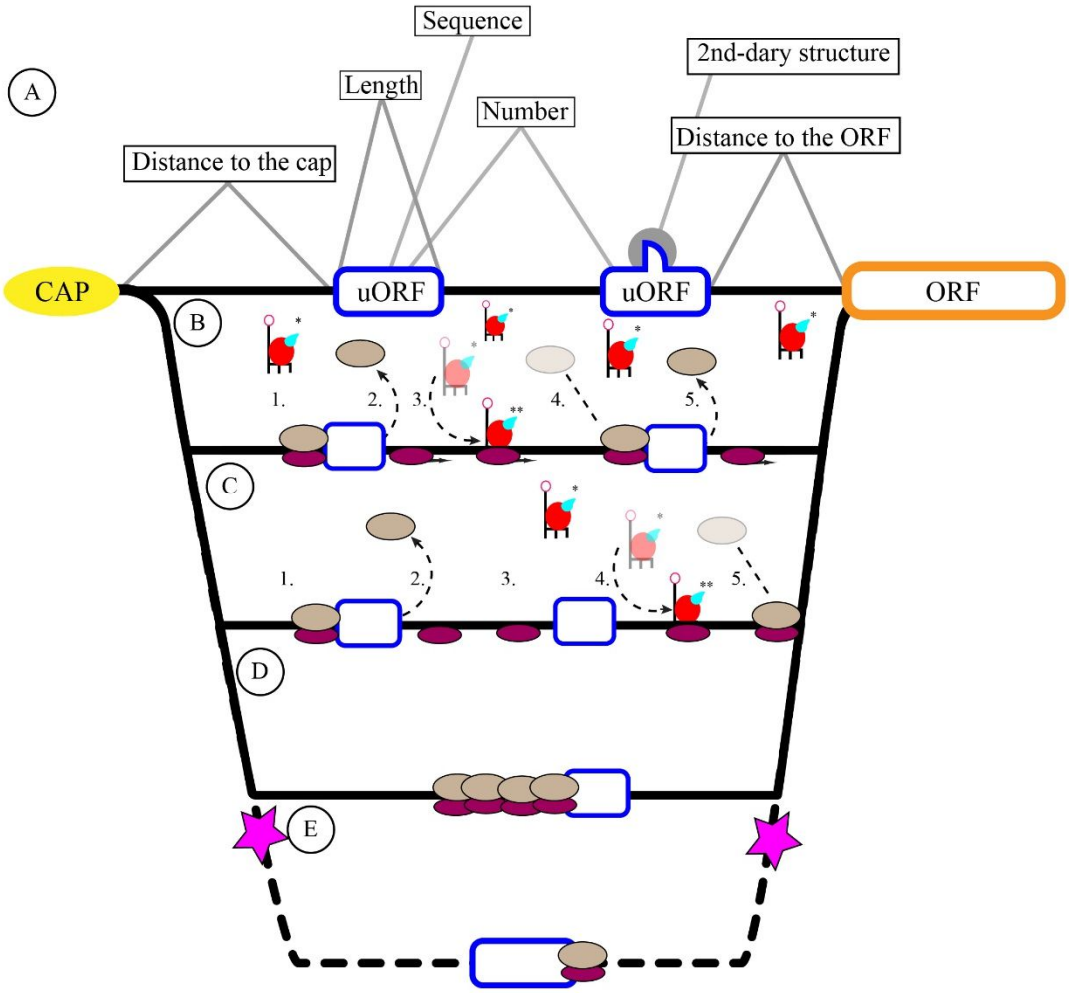

Figure 7. Upstream open reading frame and translation control.

A. Factors influencing uORFs efficiency

B. uORF influence on *GCN4* gene in high amino acid concentrations

1. 80S initiation complex starts the translation of the first uORF
1. After the STOP codon the big ribosome subunit dissociate from the mRNA
2. One of the plenty ternary complexes binds to the 40S ribosome subunit forming the 43S-preinitiation complex which resumes scanning
3. After reassembly of the 80S initiation complex the second uORF is being translated
4. Ending the translation the big subunit disassemble and then the 40S subunit will traverse by the main ORF before the next ternary complex binds which end up in the main ORF being not translated

C. uORF influence on *GCN4* gene in low amino acid concentrations

1. 80S initiation complex starts the translation of the first uORF
2. After the STOP codon the big ribosome subunit dissociate from the mRNA
3. Because of the scarcity of the ternary complexes the 40S subunit will traverse the next uORF without translation
4. One of the scarce ternary complexes will then bind to the 40S ribosome subunit forming the 43S-preinitiation complex which resumes scanning
5. In the last step the 60S subunits forms the 80S complex and starts translation of the main ORF

D. Ribosome stalling

E. Nonsense-mediated mRNA decay

1.3. Mitotic divisions in pollen development

Mitosis is a type of division where the cell divides in two identical cells. Mitosis consists of four main parts, starting with the prophase stage when the chromosomes condense and the mitotic spindle starts to form. The next phase is metaphase which starts with the nuclear envelope break down, in this stage, the spindle binds to the chromosomes, which are then placed in the equatorial plane. In the subsequent stage, anaphase, sister chromatids are being disconnected from each other and pulled to the opposite poles of the cell. At the end of mitosis, during the telophase, a new nuclear envelope is formed around the two chromosome sets. Directly after mitosis, the cytoplasm is divided during cytokinesis and two diploid cells are created (Figure 8.a to f; Criqui et al 2002).

After the meiotic divisions of pollen development ends, resulting in the creation of four haploid microspore cells, the callose wall of the tetrad is removed by the enzyme callase. This event, called microspore release marks the beginning of the second part of pollen development, called microgametogenesis. A microspore is the first cell of the haploid generation, which, after its release, will increase in volume and change shape from a lightly flatten triangle to a round shape. During its development a microspore cell starts to polarize, when the nucleus moves to the so-called generative pole, most of the other organelles move to the opposite side to the so-called vegetative pole. All of the vacuoles in that pole will form one big vacuole and the whole cell will prepare for the first asymmetric mitotic division. This division creates two different cells – a small generative

cell and much bigger vegetative cell, which is engulfing the other cell in its cytoplasm. The vegetative cell exits the cell cycle and plays a crucial role in pollen tube formation and sperm delivery. The generative cell will later undergo another division, dividing into two male gametes, the sperm cells (Figure 8.E to I; McCormick, 2004; Borg et al., 2009 ;Twell, 2011).

1.3.1. Wiring of the cell cycle gene network during premitotic s-phase

Genetic dissection of the cell cycle wiring shows various interactions between different genes. Mutants of *cdka;1+/-* as well as mutants in the F-Box protein encoding *FBL17* (*F-BOX- LIKE 17*) gene produced single sperm pollen, likely through a pathway that controls *CDKA;1* activity (Kim et al., 2008; Gusti et al., 2009; Zhao et al., 2012). This pathway appears to involve the upstream acting transcription factor *E2F*, which is well known from studies in animals to control entry into the DNA replication phase of the cell cycle (Dick and Rubin, 2013). In plants, *E2F* is kept in an inactive state by binding with the pocket protein called *RETINOBLASTOMA RELATED 1* (*RBR1*; Sabelli and Larkins, 2009; Gutzat et al., 2012; Kuwabara and Gruissem, 2014; Desvoyes et al., 2014; Harashima and Sugimoto, 2016;). A major target of E2F is FBL17 which mediates, as a part a SKIP-CULLIN-F-BOX (SCF) complex, the degradation of KRP proteins that are inhibitors of CDKA;1 (Gusti et al., 2009; Kim et al., 2008,; Zhao et al., 2012,; Noir et al., 2015,). Hence, loss of *FBL17* results in higher *KRPs* levels and subsequently lower *CDKA;1* activity. Interestingly, the concomitant loss of *CDKA;1* and *FBL17* gave rise to plants that produced single-celled pollen at anthesis (Zhao et al., 2012). Similarly, loss of *E2F* activity in combination with *fbl17+/-* mutants also resulted in single celled pollen (Zhao et al., 2012).

As presented earlier, CDKs need a specific cyclin for activation and the same applies to the pre-mitotic S-phase. In 2010, studies performed by Van Leene et al. pointed out that there are two groups of cyclins, A-type (*CYCA*) and D-type (*CYCD*), which are interacting with *CDKA;1*. Both of those groups count 10 genes each. Arrangement of the genes to each group is based on different sequence similarities. The *CYCAs* are assembled in three subgroups *CYCA1, 2* and *3*, on the other hand the D group is made of 7 subclasses (Vandepoele et al., 2002; Wang et al., 2004). Genes from the A group are expressed at G1/S transition and through the whole S-phase and the D-type cyclins are mostly up-regulated in the G1/S transition stage (Menges et al., 2005; Van Leene et al., 2010). It is still not

known if some of those genes are more important during mitotic divisions or if they are highly redundant. Experiments presenting results from the interaction studies between the *CDKA;1* and D-type cyclins are presented in this PhD thesis.

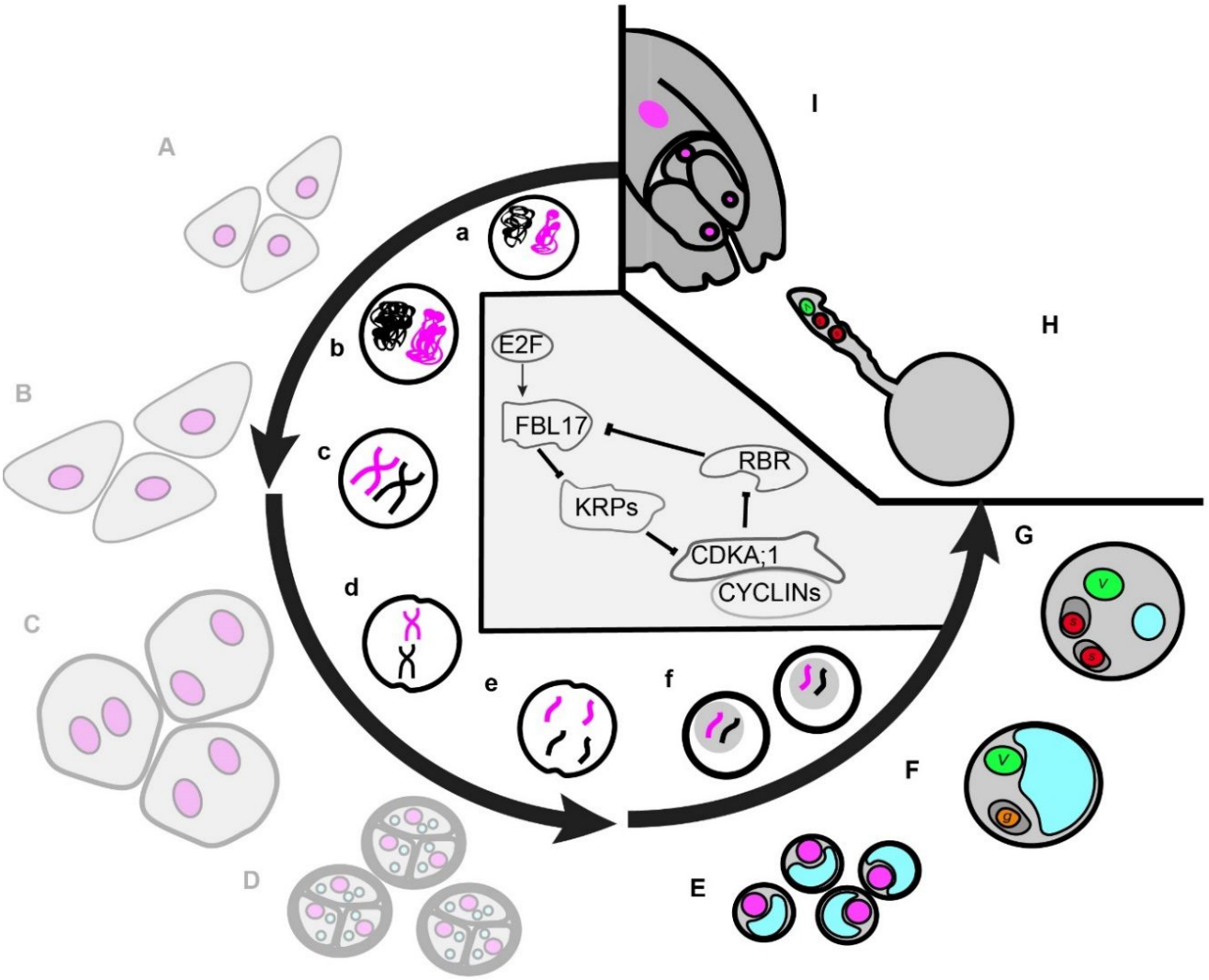

Microgametogenesis:

E. Microspore release
F. First mitotic division, generation of the generative cell an vegetative cell
G. Second mitotic division resulting in the creation of two sperm cells
H. Mature pollen with a developed pollen tube
I. Ovule

Mitotic division:

a. Interphase
b. S-phase – doubling of genetic material
c. Prophase + Metaphase
d. Anaphase
e. Telophase and cytokinesis
f. Identical daughter cells

Figure 8 Microgametogenesis (E-F), mitotic division (a-f) and gene network during premitotic S-phase – *E2F* transcription factor activates *FBL17* which inhibits the *KRP* genes, which are inhibiting *CDKA;1*. *CDKA;1* forms a complex with a CYCLIN. This complex will then interact with RBR – the inhibitor of *FBL17*

1.4. Transposons, end of mitosis and pollen adulthood

A striking characteristics of the vegetative cell differentiation is the de-repression of transposable elements (TEs; Slotkin et al., 2009; Calarco et al., 2012; Ibarra et al., 2012). This de-repression is thought to serve as a source of siRNAs (small interfering RNAs), which accumulate in the sperm cell and drive post-transcriptional silencing of TEs (Slotkin et al., 2009; Martinez et al., 2016).

In plant gametes transposable elements are repressed by epigenetic silencing, which is thought to help halting transposon activity in the next generation. In *Arabidopsis thaliana*, transposons are repressed in the sperm cells and in the vegetative cell by *DDM1* (*DECREASE IN DNA METHYLATION 1*). This gene is a heterochromatin re-modelling ATPase and a main repressor of transposon activity. It makes the H1 - containing heterochromatin accessible for DNA methyltransferases which are then able to silence transposable elements. A characteristic feature of this gene is that in the vegetative cell it is active only until the end of the second mitotic division. After this division the sperm cells are formed and the transposons start to be active in the vegetative nucleus (Slotkin et al., 2009; Zilberman et al., 2013).

When a pollen grain is fully developed it still needs to prepare itself for its life outside the anther. Firstly, it accumulates carbohydrates, as storage of energy and pollen tube wall components (Yang et al., 2010). Secondly, it dehydrates - entering a dormant state with inactive metabolism (Johnson and McCormick, 2001).

1.5. Pollen tube development and guidance

After the male gametophyte is fully developed, in *Arabidopsis thaliana*, the anthers are reaching the stigma and self-pollination occurs. When a pollen grain adheres to the stigma it rehydrates, intakes the water from stigma's papillary surface and activates its metabolism. After that, Ca^{2+} intake causes the reorganization of the cytoskeleton and subsequent polarization of the vegetative cell in the direction of the adhesion site. Those events are followed up by pollen tube germination (Johnson and McCormick, 2001; Yang, 2010).

After germinating, it is growing from the tip thanks to the materials secreted by the Golgi apparatus. The apical dome of the pollen tube is the only part that is growing, this region is at the same time plastic enough to allow expansion of the tube and sufficiently rigid to prevent the cell from bursting under the turgor pressure (Grebnev et al., 2017). From the female side chemical gradients of different factors attract the pollen tube. Among them are: oligomerizing arabinogalactans, plantacyanin's or nitric oxide (NO) which is produced by the cells of the micropylar opening of the ovule (Cheung et al., 1995; Dong et al., 2005; Prada et al., 2008). Furthermore, it was shown that NO influences Ca^{2+} signaling, therefore directly influencing growth of the pollen tube. Other different molecules like peptides or small proteins are produced by the ovule to successfully guide the pollen tube when it is already in close proximity to the female gametes (which is about 100/200 μm; Dresselhaus and Franklin-Tong, 2013).

1.6. Pollen as a model system for studying cell cycle

Pollen grain starts its development as a microspore mother cell and only after meiotic and mitotic divisions it becomes an fully functional gametophyte. This developmental process provides insight into every stage of the cell cycle. Pollen grains residing in the anther are easily accessible and abundant, which makes them easier to quantify by using different methods like DAPI staining or Alexander staining. Pollen development inside of the anther is mostly synchronized but still there are usually very few meiocytes at the same developmental stage regarding the whole plant. This means that the amount of nucleic acids or protein produced by those few meiocytes would be too small to perform any stage correlated experiments Therefore, in order to research the translatome/proteome of Arabidopsis, it is necessary to obtain a decent amount of mRNAs/proteins. This can be only done by synchronizing the development of all flowers in one plant. In Arabidopsis it is possible firstly, by creating a double mutant of *apetala1* (*ap1*) and *cauliflower* (*cal*). Those two genes are redundantly initiating flower development and their lack of activity leads to massive over-proliferation of inflorescence-like meristems, demonstrated by cauliflower-like appearance. Secondly, those mutants must be transformed by a construct containing a glucocorticoid receptor, the *apetala1* gene and a consecutive promoter. In the cell, the receptor is bound by a heat shock protein (HSP) which blocks the whole fusion protein from entering the nucleus

(Figure 9.A). Although, when a synthetic glucocorticoid (dexamethasone) is added, the conformation of the receptor changes, subsequently dislodging the HSP and allowing the protein to enter the nucleus (Figure 9.B). Spraying the whole plant with dexamethasone will lead to synchronized development of all meristems of the cauliflower – like structure (Kaufmann et al., 2010)

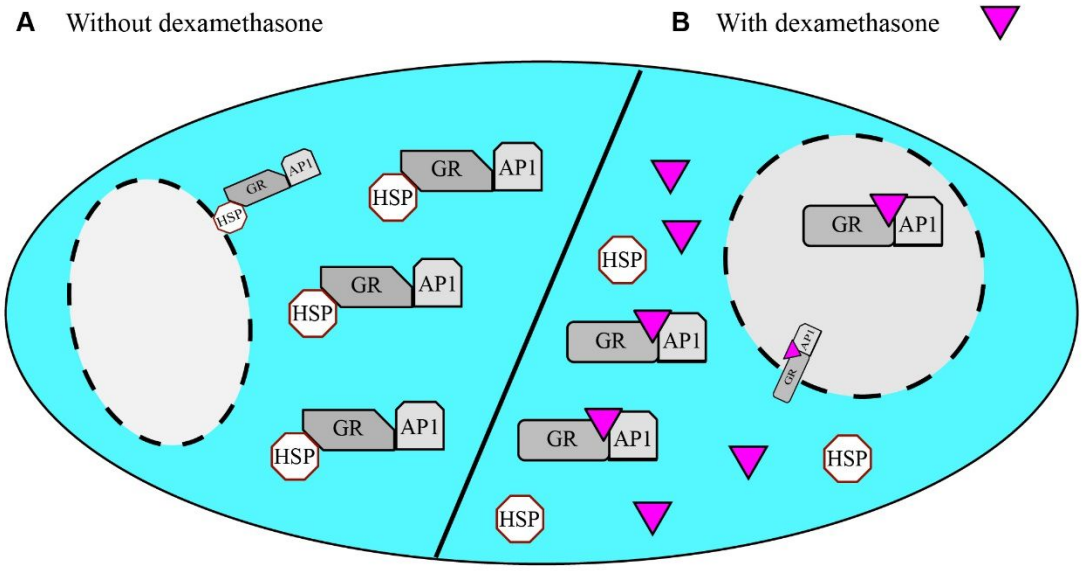

Figure 9. Arabidopsis synchronisation model. **A**. State of the cell without dexamethasone treatment; **B.** State of the cell with dexamethasone treatment – initiation of flower development. GR- glucocorticoid receptor, AP1 – apetala 1 protein, HSP- heat shock protein

Since a failure to progress through one or more pollen mitoses leads to pollen that has a reduced cell number, interfering with cell division control is a promising approach for untangling the function of individual cells. A fine example of using pollen as a model system for unveiling the mechanism of cell cycle is the work of Zhao et al. from 2012. In their research they established a system for discovering the nature of interactions between genes during the pre-mitotic S-Phase. In this case, the method rests on the importance of the *CDKA;1* gene and the fact that a certain level of activity of this gene is necessary for progression though the first and second mitotic divisions. By crossing mutants of the investigated gene with a *cdka;1+/-* mutant itself or a mutant in the *FBL17* gene that lies upstream of *CDKA:1*, it is possible to observe a phenotype change which would indicate the placement of the investigated gene in the network or its general importance. Namely it would influence the distribution of mutant (monocellular and bicellular) and WT pollen (tricellular) produced by the double/triple/etc. mutant plant in comparison to a single mutant of *cdka;1 +/-* or *fbl17 +/-* (Figure 10).

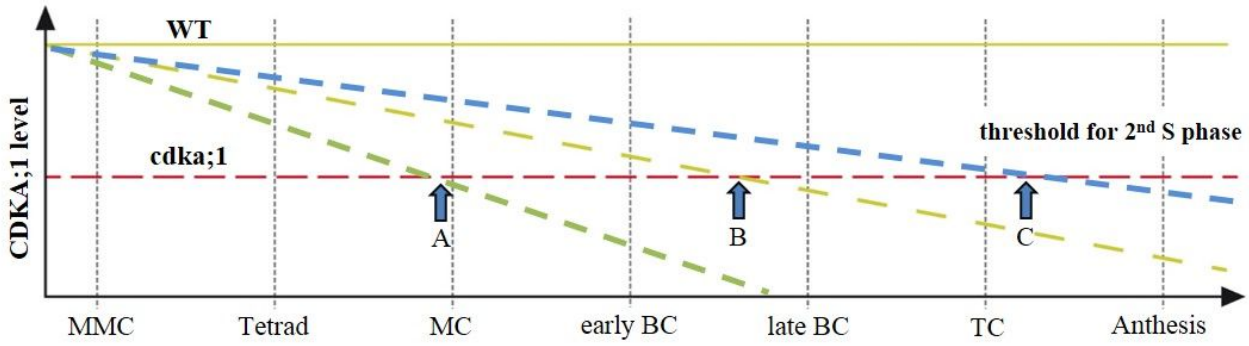

Figure 10. **Cell Cycle Mutant System**. Since *CDKA;1* is an very important regulator of the plant cell cycle, so changing it's activity influences the phenotype of the pollen and so the ratio between the number of cells in pollen. The yellow continuous line represents the assumed level of activity of the *CDKA;1* in WT plant. The red dashed line is the level of activity necessary for divisions. The yellow dashed line represent the level of *CDKA;1* activity in the heterozygous *cdka;1* mutant (**B**). That activity is not high enough for the last division and because of that it is possible to observe mutant phenotype with only two cells. If we cross the *cdka;1* mutant with a mutant of a different gene which is an inhibitor of the *CDKA;1* (**C**) we will observe a different ratio of the tri- an bi-cellular pollen, because the activity of the *CDKA;1* will be higher. This case was observed with the *cdka;1 x krp* mutants. On the opposite side if we cross the *cdka;1* with the *fbl17* mutant which is an inhibitor of the *krp's* it will be possible to observe pollen grains with only one cell (**A**).

2. Aims of this study

My PhD thesis can be divided in the meiosis and mitosis part. In both of them, although they were focused on different elements of the cell cycle, I was using *Arabidopsis thaliana* pollen as a model system. The meiosis project was following up an experiment that revealed, by quantitative expression analysis, that the transcripts of several selected meiosis specific genes do not correlate with entry into meiosis, suggesting extensive translation control. To test this hypothesis, I have adapted a previously developed system by Halstead et al. (2015) to compare, by live cell imaging of meiosis, the mRNA levels with the accumulating levels of the respective proteins. The other aim of this project was to create a live imaging system for investigating translation control in plants in general. The mitosis project was succeeding the research of Barbara Gloecke and was based on *cdka;1+/-* and *fbl17 +/-* mutants. In both of those lines a portion of pollen stops developing before the second mitotic division. My work in this project started with an intention to untangle the network of genes involved in the pre-mitotic S-phase entry. Namely it was to check if one of the D-type cyclins plays a major role in this process. In my studies I checked double mutants of D-type cyclins and *cdka;1+/-* or *fbl17 +/-* in order to understand which of the combinations would show further enhancement of mitotic defects observed in the single mutants. For the rest of the project I used pollen coming from double mutants of *e2fa-/-* and *cdka;1+/-* with *fbl17 +/-.* Those double mutants are showing pollen that will fail to enter the first mitotic division and remain a single cell. This new class of pollen allowed me to study the developmental potential of grains that were lacking both gametes. It made it possible to check if those cells are able to: differentiate into a vegetative cell, create a pollen tube, guide it towards the ovule and if they are able to penetrate it.

3. Results

3.1. Translational control during meiosis in plants

Studying translation requires monitoring mRNA molecules which are processed, modified and degraded in the cytoplasm. Harvesting whole cells and carrying out experiments like Northern blot allows measuring mRNA abundance. Nevertheless, those methods fail to capture the spatiotemporal dynamics of mRNA movement and translation control. To address this, I used techniques that allow visualizing mRNA particles in vivo by modifying the mRNA itself.

3.1.1. MS2-tagging of meiosis specific genes in plants

In the first approach I used vectors containing GFP that were already developed in our lab. Those constructs were created in in order to visualize and localize TAM and REC8 proteins. I modified those vectors by adding stem loops from the MS2 bacteriophage after the GFP. For detection, I used coating protein fused with a nuclear localization signal and an RFP. This protein, by binding specifically to the stem loops already at the moment of transcription, shows exactly the moment when the RFP tagged transcript appears in the cytoplasm. If we then compare the time point of that appearance and the moment when we can detect the GFP signal, I will see if there are any discrepancies (Figure 11). Those differences, if present, strongly indicate that some kind of mechanism is controlling the onset of translation of reviewed genes.

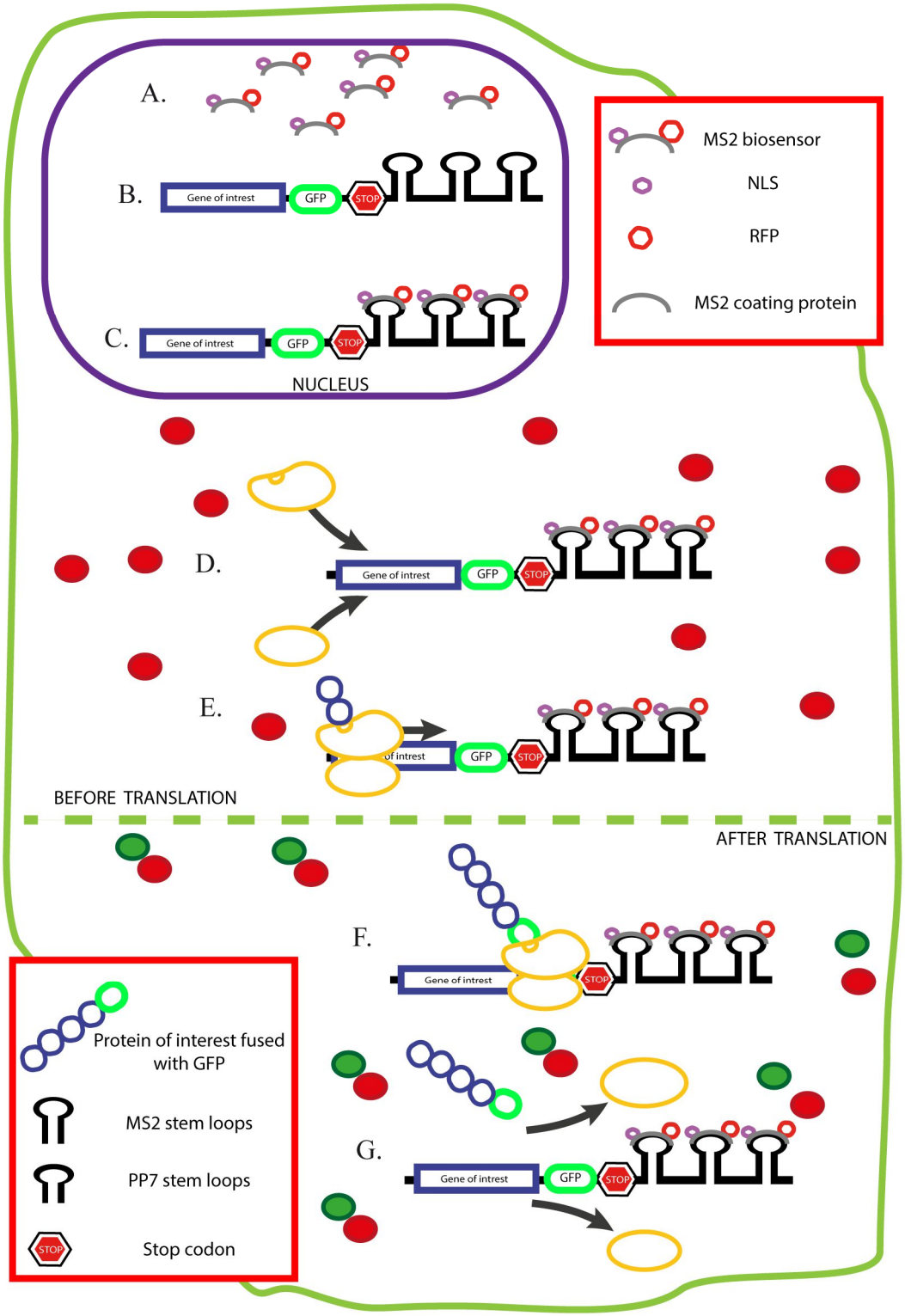

Figure 11. Overview of MS-tagging. A. MS2 binding protein that consists a NLS, a MS2 coating protein and RFP. **B.** Main mRNA construct that consists of the gene of interest transcript followed by a stop codon and stem loops from the MS2 bacteriophage. **C.** Binding of MS2 coating protein to MS stem loops from the main mRNA construct. **D.** Transferring of the complex to the cytoplasm where translation starts (red signal appears in the cytoplasm). **E**. Ribosomal machinery lands on the mRNA main construct and starts translation. **F**. The protein of interest is being translated and GFP is starting to fold. G**.** End of translation, with the fully folded GFP a green signal is appears.

3.1.1.1. Generation of *TAM:GFP:MS2* construct

Thanks to the courtesy of Chao Yang, I received a *TAM:GFPpENTRY2B* construct. With primers number C16 and C18, I introduced two restriction enzyme sites ASCI and PACI, respectively. In the same time another PCR reaction was performed on a commercial plasmid, ordered from Addgene (*pmaxpona 12xTRICK 24xMS2SL*), with primers C11 and C13 to obtain MS2 loops. Also in this case, ASCI / PACI restriction sites were introduced by PCR. After cutting with the respective enzymes it was possible to ligate both fragments, and therefore create a MS-tagged *TAM:GFP* construct (Figure 12).

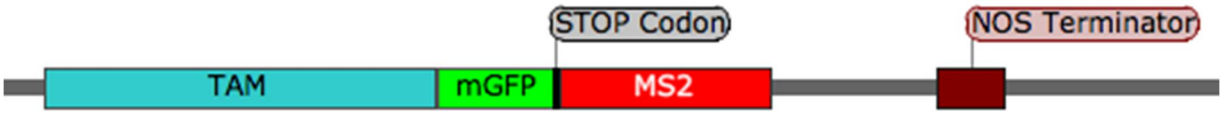

Figure 12. *TAM:GFP:MS2* construct

After obtaining and sequencing the construct, I used the Gateway system to generate the destination vector, which was used to transform *tam* mutants. Subsequently the T_1 generation was genotyped in order to check for presence of the construct (Figure 13).

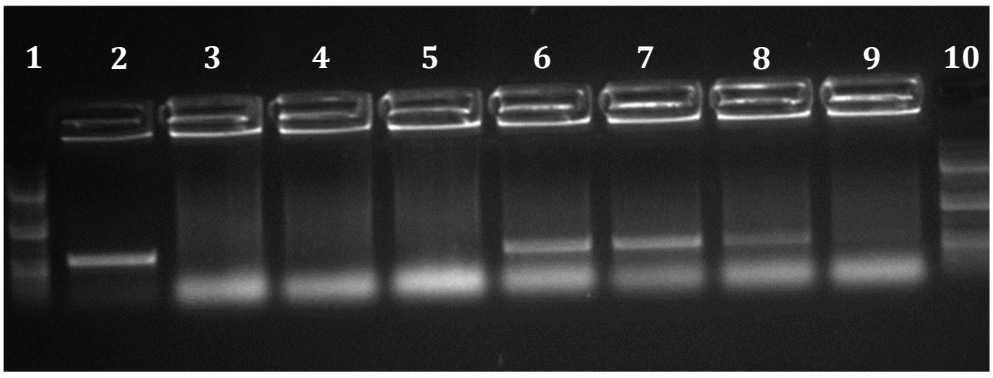

Figure 13. Genotyping example of *TAM:GFP:MS2* construct; using primers "Tam genotyping primer F" and "Tam genotyping primer R" showing the presence of the construct in the plant genome. Pockets 1 and 10 contain the Generuler 1kb DNA Ladder. Pockets 2,6,7 and 8 are showing positive genotyping result with a clear band. In the rest of pockets no PCR product was detected.

As revealed by confocal microscopy, three from ten lines, showed GFP signal that looked similar to the plant lines containing only the vector expressing the TAM:GFP fusion protein (without the MS2 stem loops; Figure 14). Among all lines one exhibited a rescued

phenotype and a GFP signal. From the rest of the lines two showed partial rescue, five showed a rescued phonotype but no GFP signal was detected and the other two exhibited a mutant phenotype

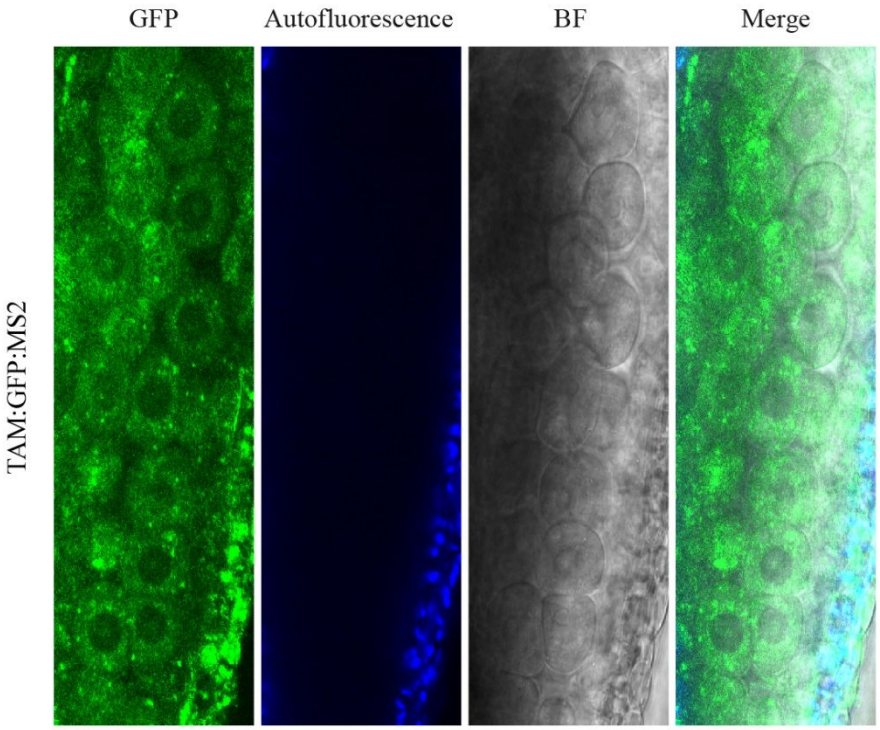

Figure 14. *TAM:GFP:MS2* signal example. First panel represents the GFP signal, second panel demonstrates the signal coming from auto fluorescence, third shows bright field, the last panel displays a merge of first three panels.

3.1.1.2. Generation of *REC8:GFP:MS2* construct

Thanks to the courtesy of Shinichiro Komaki, I obtained a *REC8:GFPpENTR2B* construct. With primers number C14 and C14a, I introduced two restriction sites for ASCI and PACI, respectively. This was done after performing a Klenow reaction to inactivate the already existing ASCI restriction site that was present in the obtained vector. Simultaneously, another PCR reaction was performed on a commercial plasmid, ordered from Addgene (*pmaxpona 12xTRICK 24xMS2SL*), with primers C11 and C13 to obtain MS2 loops. Also in this case, ASCI / PACI restriction sites were introduced by PCR. After cutting with the corresponding enzymes both fragments were ligated, to create a MS-tagged REC8:GFP construct (Figure 15).

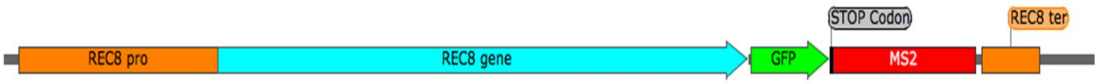

Figure 15. *REC8:GFP:MS2* construct

After obtaining and sequencing the construct, I used Gateway system to generate the destination vector, which was used to transform *rec8* mutants. The plants were transformed, and subsequently the T_1 generation was genotyped to check for presence of the construct (Figure 16).

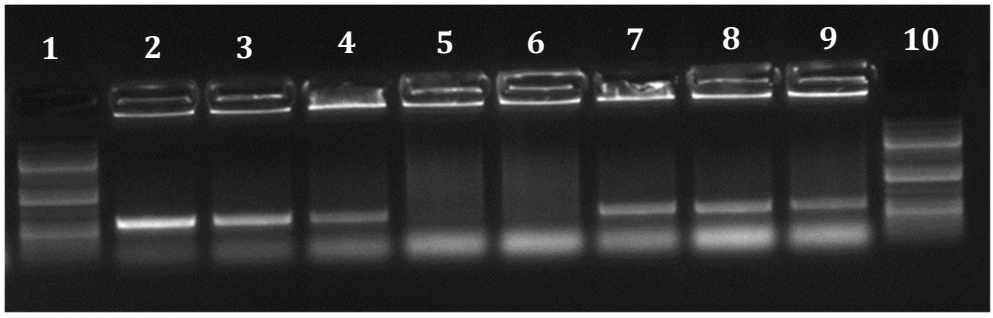

Figure 16. Genotyping example of REC8:GFP:MS2 construct; using primers Rec8 Shini and C53 showing the presence of the construct in the plant genome. Pockets 1 and 10 contain the Generuler 1kb DNA Ladder. Pockets 2,3,4,7,8, and 9 are showing positive genotyping result with a clear band. In the rest of pockets no PCR product was detected.

3.1.1.3. Generation of MS2 binding proteins (MBPs)

3.1.1.3.1. Generation of *PRO$_{CDKA;1}$:MCP:RFP*

To obtain a functional MBP, I used a *UBC NLS-HA-2XMCP-tagRFPt* vector from Addgene as a template for a PCR reaction. Firstly, I inserted a *CDKA;1* promoter that was obtained by PCR directly from Arabidopsis (with primers C19 and C20), via NOTI restriction enzyme site. Afterwards, I used primers C69 and C36a to create a PCR fragment with attb sites added. To generate the destination vector I used the Gateway system. In addition to the promoter, terminator, RFP and MS2 coating protein sequences, there are three other components in the created construct. The first one is the nuclear localization signal (NLS) coming from the simian virus 40 that will move the unbounded biosensor to the nucleus. The following one is a human influenza hemagglutinin tag (HA-tag) for

isolation and purification of the biosensor. And lastly, the Factor Xa protease that can be used for the removal of MS2 binding protein molecules (Figure 17).

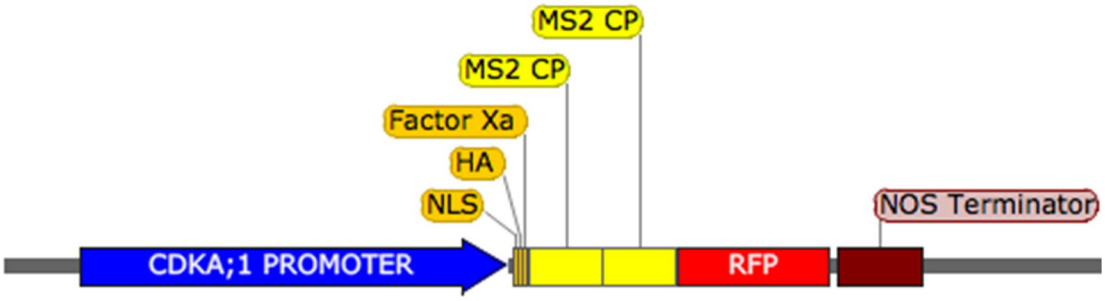

Figure 17. *PRO$_{CDKA:1}$:MCP:RFP* construct

After sequencing the destination vector, it was used to transform wild type Columbia. The resulting T_1 generation was screened by confocal microscopy (Figure 18)

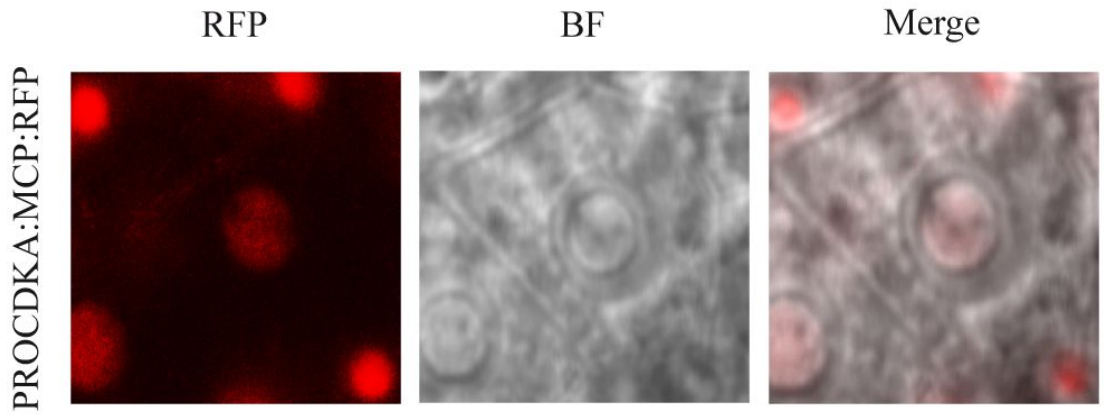

Figure 18. Signal coming from the PRO$_{CDKA:1}$:MCP:RFP is present in microsporocytes. First panel represents the RFP signal, second shows bright field, the last panel displays a merge of the first two panels.

3.1.1.3.2. Generation of *PRO$_{UBIQUITIN}$:MCP:RFP*

To obtain a functional MBP, I used a *UBC NLS-HA-2XMCP-tagRFPt* vector from Addgene as a template for a PCR reaction. Firstly, I inserted a UBIQUITIN promoter, which was obtained by PCR directly from Arabidopsis, via NOTI restriction enzyme site. Afterwards, I used primers C35 and C36a to create a PCR fragment with attb sites added. To generate the destination vector I used the Gateway system In addition to the promoter, terminator, RFP and MS2 coating protein sequences, there are three other components in

the created construct. The first one is the nuclear localisation signal (NLS) coming from the simian virus 40 that will move the unbounded biosensor to the nucleus. The following one is a human influenza hemagglutinin tag (HA-tag) for isolation and purification of the biosensor. And lastly, the Factor Xa protease that can be used for the removal of MS2 binding protein molecules (Figure 19).

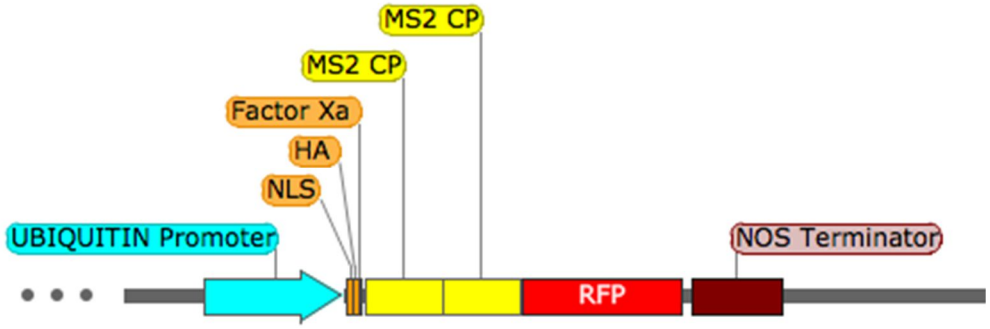

Figure 19. ***PRO$_{UBIQUITIN}$:MCP:RFP***

After sequencing the destination vector, it was used to transform wild type Columbia. The resulting T_1 generation was screened by confocal microscopy (Figure 20).

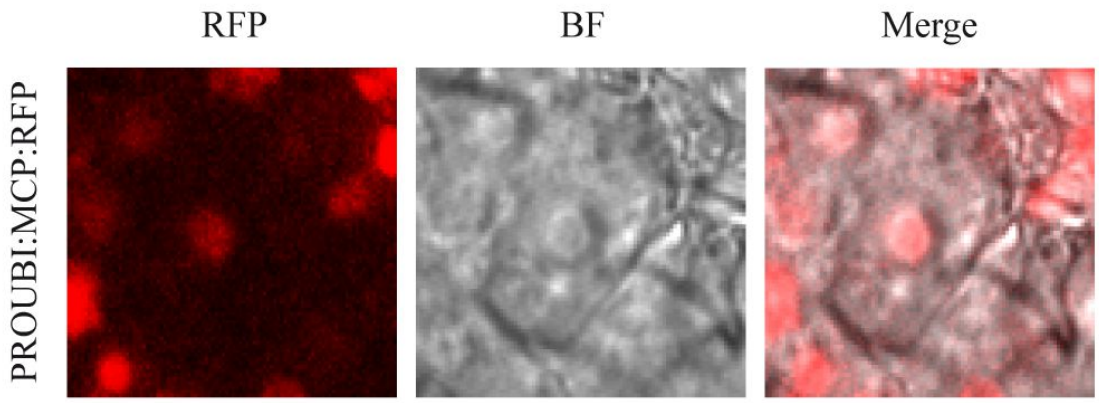

Figure 20. Signal coming from the *PRO$_{UBIQUITIN}$:MCP:RFP* is present in microsporocytes. First panel represents the RFP signal, second shows bright field, the last panel displays a merge of the first two panels.

MS tagging is a technique already established in plants (Christensen et al 2010; Pena and Heinlein, 2016). Together with the GFP, already fused with the genes of interest, MS-tag can be used to decide if there are discrepancies between the timepoints of transcript and protein appearance. This method already can demonstrate if the mRNA of the genes of interest is controlled on a translation level. Since GFP needs time to fold, there

is a period of time before the signal is visible. If some kind of translation control occurs in that period of time it would remain undetectable by using only the MS - tag method. Knowing when the first round of translation happens would allow us to see the whole picture.

3.1.2. Translating RNA imaging by coat protein knockoff (TRICK) of meiosis specific genes in plants

To address this problem, I have adapted a previously developed system by Halstead et al. (2015) to compare the subsequent live imaging results with the MS-tag experiments. This method utilizes the fact that coating proteins from certain bacteriophages (PP7 and MS2) bind specifically to the mRNA stem loops that originate from the matching phages. For this method to work, the presence of two components is required. The main construct which consists of the gene of interest, stem loops from the PP7 bacteriophage, a stop codon and stem loops from the MS2 bacteriophage. The second part are the biosensors which are built of three elements: a nuclear localization signal, bacteriophage coating protein (PP7 or MS2) and a specific fluorescent protein (GFP or RFP). The feature of those biosensors is that the coating protein will bind specifically to the stem loops from the matching bacteriophage. The whole system relies on the placement of elements in the main construct. After the gene of interest, the first set of stem loops is placed (PP7). The second set of different stem loops (MS2) is placed after the STOP codon which is located in between.

In the nucleus, the biosensors are binding to the loops in the mRNA construct that was freshly transcribed. Afterwards, the whole complex moves to the cytoplasm. This moment is visible by appearance of the GFP and RFP signals belonging to the biosensors. When translation occurs, the ribosomal machinery that binds to the mRNA will knock off the first biosensor while sliding and translating the mRNA. Knock off of the second biosensor is prevented by the STOP codon that lies in between. When the first PP7 biosensor is not attached to the mRNA, it moves to the nucleus, which can be detected with the disappearance of the GFP signal (Figure 21).

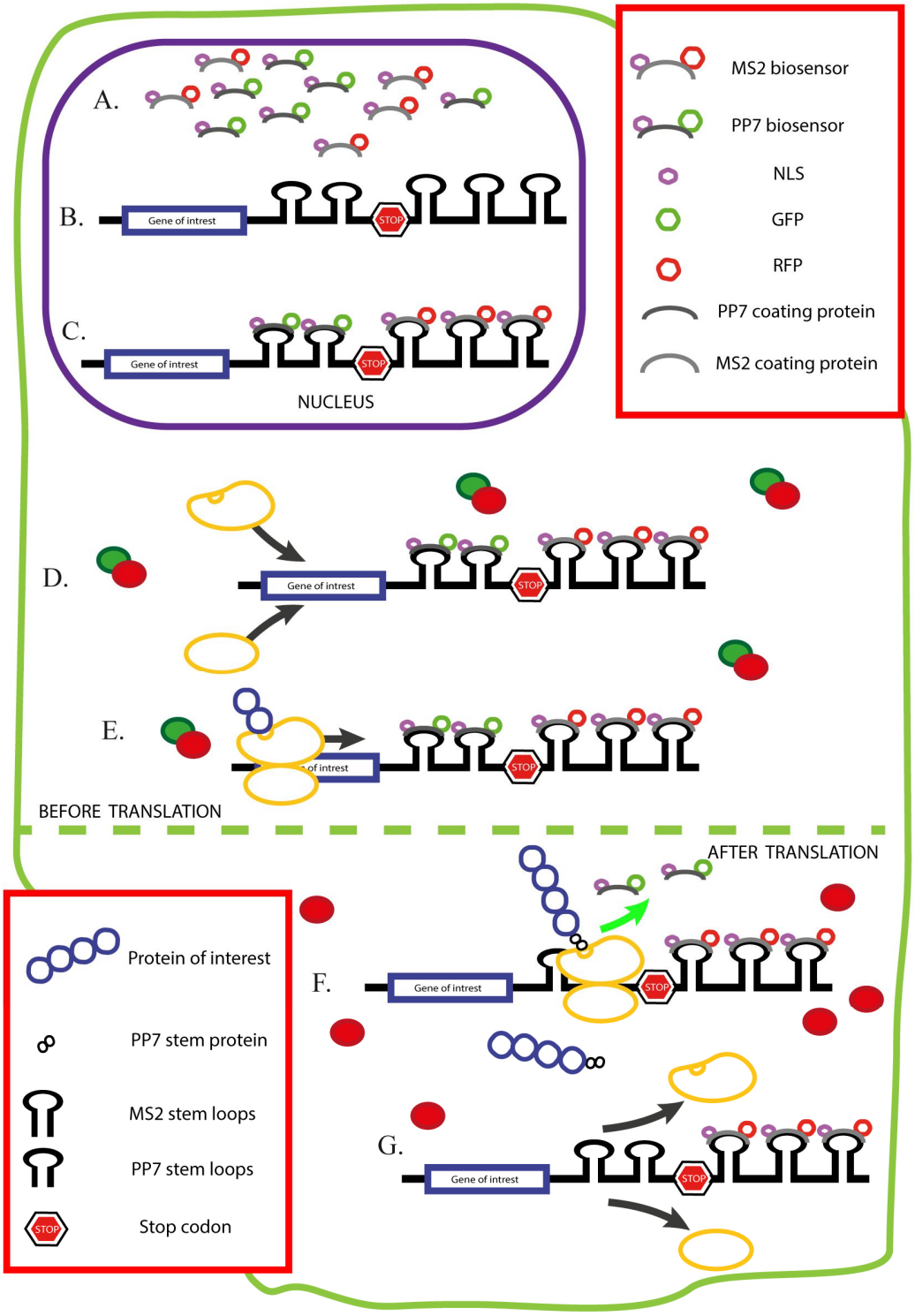

Figure 21. TRICK system explanation. A. MS2 biosensor that consists of NLS, MS2 coating protein and RFP with PP7 biosensor built up from NLS, PP7 coating protein and GFP. **B.** Main mRNA construct that consists of the gene of interest transcript followed by PP7 stem loops, a stop codon and stem loops from the MS2 bacteriophage. **C.** Binding of coating protein to respective stem loops from the main mRNA construct. **D.** Transferring of the complex to the cytoplasm where translation starts (green and red signal appears in the cytoplasm). **E**. Ribosomal machinery lands on the mRNA main construct and starts translation. **F**. The

protein of interest is being translated and PP7 biosensor in knocked off the main mRNA construct. **G.** End of translation, with the PP7 biosensor moving to the nucleus the green signal disappears.

3.1.2.1. Generation of *TAM: PP7:MS2* construct

Thanks to the courtesy of Chao Yang, I received a *TAMpENTR2b* construct. With primers number C17 and C18, I introduced two restriction sites ASCI and PACI, respectively. Simultaneously, another PCR reaction was performed on a commercial plasmid taken from Addgene (*pmaxpona 12xTRICK 24xMS2SL*) where with primers C11 and C12 a PP7/MS2 fragment was obtained. Also in this case, ASCI/PACI restriction sites were introduced by PCR. After cutting with the respective enzymes, it was possible to ligate both fragments, and therefore create a TAM:TRICK construct (Figure 22).

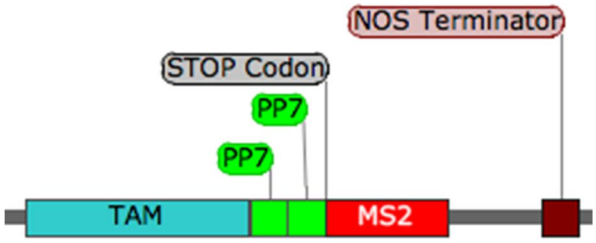

Figure 22. TAM: PP7:MS2 construct.

After sequencing the construct I used Gateway system to generate a destination vector, which was used to transform *tam* mutants. Subsequently the T_1 generation was genotyped in order to check for presence of the construct (Figure 23).

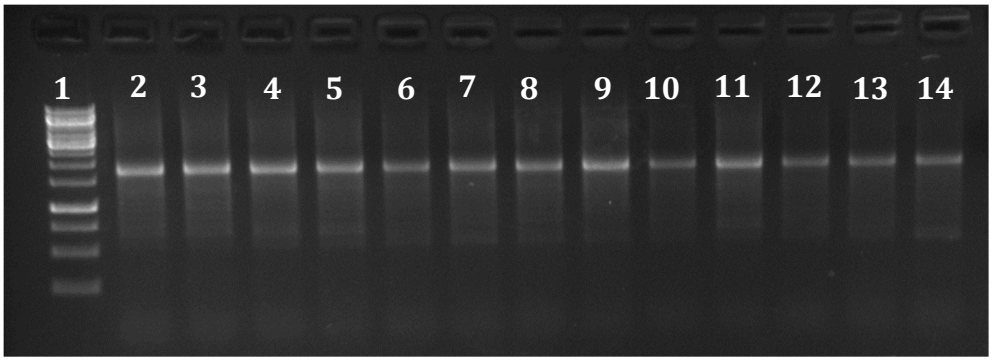

Figure 23. Genotyping example of *TAM: PP7:MS2* construct using primer S10 and C11 showing the presence of the construct in the plant genome. Pocket 1 contain the Generuler 1kb DNA Ladder. All other pockets are showing positive genotyping result with a clear band.

3.1.2.2. Generation of *REC8:PP7:MS2* construct

Thanks to the courtesy of Shinichiro Komaki, I obtained an *REC8pENTR2b* construct. With primers number C27 and C28, I introduced two restriction sites ASCI and PACI, respectively. This was done after performing the Klenow reaction to inactivate the already existing ASCI restriction site that was present in the obtained vector. Simultaneously, another PCR reaction was performed on a commercial plasmid taken from Addgene (*pmaxpona 12xTRICK 24xMS2SL*) where with primers C11 and C12 a PP7/MS2 fragment was obtained. Also in this case, ASCI/PACI restriction sites were introduced by PCR. After cutting with the corresponding enzymes it was possible to ligate both fragments, and therefore create a functional REC8:TRICK construct (Figure 24).

Figure 24. *REC8:PP7:MS2* construct

After sequencing the construct I used Gateway system to generate a destination vector, which was used to transform *rec8* mutants. After the plants were transformed the T_1 generation was genotyped in order to check for presence of the construct.

3.1.2.3. Generation of TRICK biosensors with two-fragment multisite gateway system

3.1.2.3.1. Generation of $PRO_{CDKA;1}$:PCP:GFP:$PRO_{CDKA;1}$:MCP:RFP (R4pGW501) construct

To create a functional TRICK construct, I used two vectors obtained from Addgene (*phage ubcnls ha pcpgfp* and *phage UBC NLS-HA-2XMCP-tagRFPt*), as templates for my experiments. Both of the commercial vectors had a NOTI site, which was used to insert promoter sequences. In this case for both coating proteins a *CDKA;1* promoter was

inserted. Afterwards, I used primers C65 and C30 for the *PP7:GFP* vector and C69 and C67 for the *MS2:RFP* vector to create a PCR fragments with attb sites added.

Both of them were subsequently used as components for the two - fragment multisite gateway system, building up one vector. In addition to the promoters, NOS terminator, fluorescent and coating protein sequences there are three other type components in the created construct. The first one is the nuclear localization signal (NLS) coming from the simian virus 40 that will move the unbounded biosensor to the nucleus. The following one is the human influenza hemagglutinin tag (HA-tag) for isolation and purification of the biosensor. And lastly, the Factor Xa protease can be used for the removal of MS2 binding protein molecules. Two sets of those components are placed before each of the binding proteins (Figure 25).

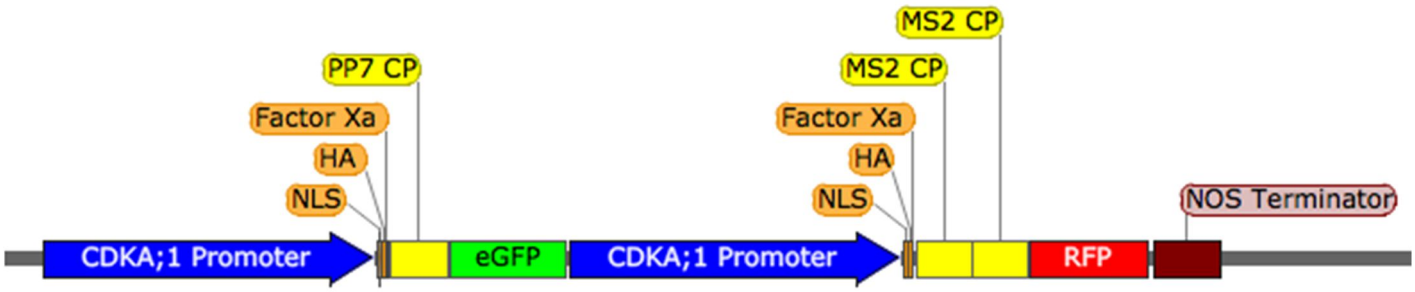

Figure 25. ***PRO*$_{CDKA;1}$*:PCP:GFP:PRO:*$_{CDKA;1}$*:MCP:RFP*** **(R4pGW501) construct.**

After sequencing the destination vector, it was used to transform Columbia wild type plants. Subsequently the T_1 generation was screened with the confocal microscope. Within these combination of promoters no signal was detected both from GFP or RFP despite successful antibiotic selection.

3.1.2.3.1.1. Generation of *PRO*$_{CDKA;1}$*:PCP:GFP:PRO:*$_{UBIQUITIN}$*:MCP:RFP* (R4pGW501) construct

To obtain a functional TRICK construct, I used two vectors obtained from Addgene (*phage ubcnls ha pcpgfp* and phage *UBC NLS-HA-2XMCP-tagRFPt*), as templates for my experiments. Both of the vectors had a NOTI site, which was used to insert promoter sequences into the commercial vectors. In this case for the PP7 coating protein a *CDKA;1* promoter was inserted and the MS2 was fused with an *UBIQUITIN* promoter. Afterwards, I used primers C65 and C30 for the *PP7:GFP* vector and C35 and C36a for the *MS2:RFP* vector to create a PCR fragments with attb sites added.

Both of them were subsequently used as components for the two - fragment multisite gateway system, building up one vector. In addition to the promoters, NOS terminator, fluorescent and coating protein there are three other type components in the created construct. The first one is the nuclear localization signal (NLS) coming from the simian virus 40 that will move the unbounded biosensor to the nucleus. The following one is the human influenza hemagglutinin tag (HA-tag) for isolation and purification of the biosensor. And lastly, the Factor Xa protease that can be used for the removal of MS2 binding protein molecules. Two sets of those components are placed before each of the binding proteins (Figure 26).

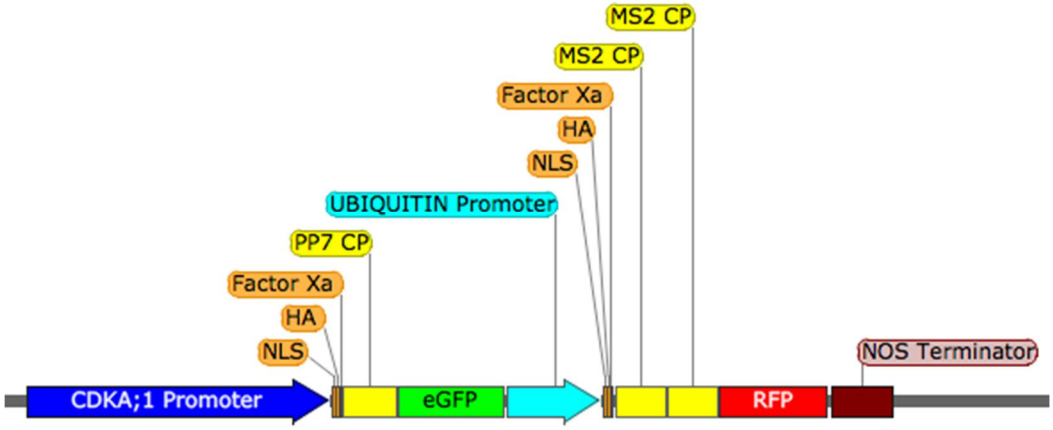

Figure 26. ***PRO$_{CDKA;1}$:PCP:GFP:PRO:$_{UBIQUITIN}$:MCP:RFP*** **(R4pGW501) construct**

After sequencing the destination vector, it was used to transform Columbia wild type plants. Subsequently the T_1 generation was screened with the confocal microscope. Within these combination of promoters signal was detected only in several cells.

3.1.2.3.1.2. Generation of *PRO $_{UBIQUITIN}$:PCP:GFP:PRO:$_{CDKA;1}$:MCP:RFP* (R4pGW501) construct

To obtain a functional TRICK construct, I used two vectors obtained from Addgene (*phage ubcnls ha pcpgfp* and *phage UBC NLS-HA-2XMCP-tagRFPt*), as templates for my experiments. Both of the vectors had a NOTI site, which was used to insert promoter sequences into the commercial vectors. In this case for the PP7 coating protein a *UBIQUITIN* promoter was inserted and the MS2 was fused with a *CDKA;1* promoter. Afterwards, I used primers C29 and C30 for the *PP7:GFP* vector and C69 and C67 for the *MS2:RFP* vector to create a PCR fragments with attb sites added.

Both of them were subsequently used as components for the two - fragment multisite gateway system, building up one vector. In addition to the promoters, NOS terminator, fluorescent and coating protein there are three other type components in the created construct. The first one is the nuclear localization signal (NLS) coming from the simian virus 40 that will move the unbounded biosensor to the nucleus. The following one is the human influenza hemagglutinin tag (HA-tag) for isolation and purification of the biosensor. And lastly, the Factor Xa protease that can be used for the removal of MS2 binding protein molecules. Two sets of those components are place before each of the binding proteins (Figure 27).

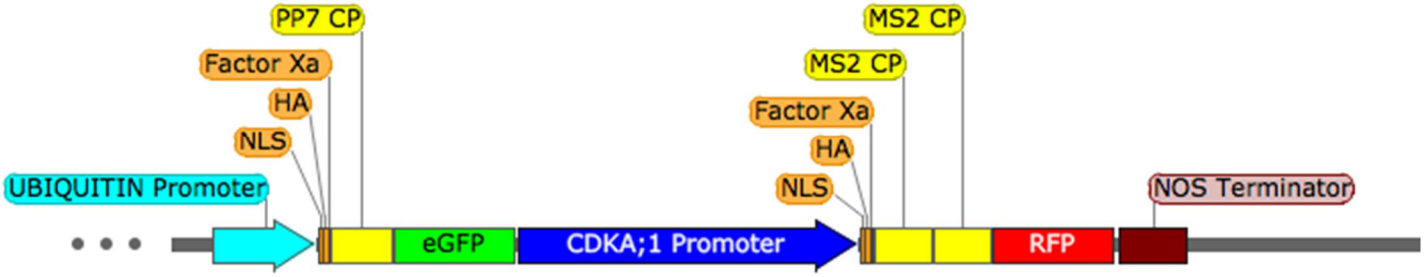

Figure 27. ***PRO*** $_{UBIQUITIN}$***:PCP:GFP:PRO:*** $_{CDKA;1}$***:MCP:RFP*** **(R4pGW501) construct**

After sequencing the destination vector, it was used to transform Columbia wild type plants. Subsequently the T_1 generation was screened with the confocal microscope. Within this promoter combination it was possible to obtain one line that had signal in every cell in all developmental stages. The rest of plants exhibited either GFP or RFP only (Figure 28).

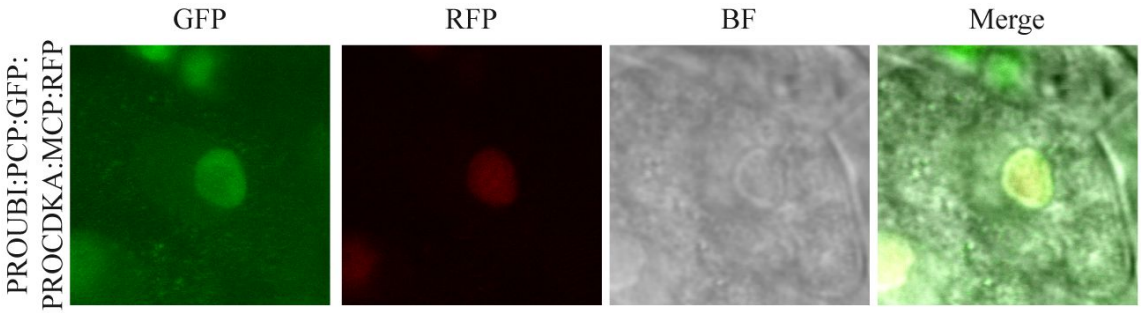

Figure 28. Signal coming from the ***PRO*** $_{UBIQUITIN}$***:PCP:GFP:PRO:*** $_{CDKA;1}$***:MCP:RFP (R4pGW501)*** **construct is present in microsporocytes** First panel represents the GFP signal, second panel demonstrates the signal coming from RFP, third shows bright field and the last one displays a merge of first two panels.

3.1.2.3.1.3. Generation of *PRO UBIQUITIN:PCP:GFP:PRO: UBIQUITIN:MCP:RFP* (R4pGW501) construct

To obtain a functional TRICK construct, I used two vectors obtained from Addgene (*phage ubcnls ha pcpgfp* and *phage UBC NLS-HA-2XMCP-tagRFPt*), as templates for my experiments. Both of the vectors had a NOTI site, which was used to insert promoter sequences into the commercial vectors. In this case for both coating proteins a *UBIQUITIN* promoter was inserted. Afterwards, I used primers C29 and C30 for the *PP7:GFP* vector and C35 and C36a for the *MS2:RFP* vector to create a PCR fragments with attb sites added.

Both of them were subsequently used as components for the two - fragment multisite gateway system, building up one vector. In addition to the promoters, NOS terminator, fluorescent and coating protein there are three other type components in the created construct. The first one is the nuclear localization signal (NLS) coming from the simian virus 40 that will move the unbounded biosensor to the nucleus. The following one is the human influenza hemagglutinin tag (HA-tag) for isolation and purification of the biosensor. And lastly, the Factor Xa protease that can be used for the removal of MS2 binding protein molecules. Two sets of those components are place before each of the binding proteins (Figure 29).

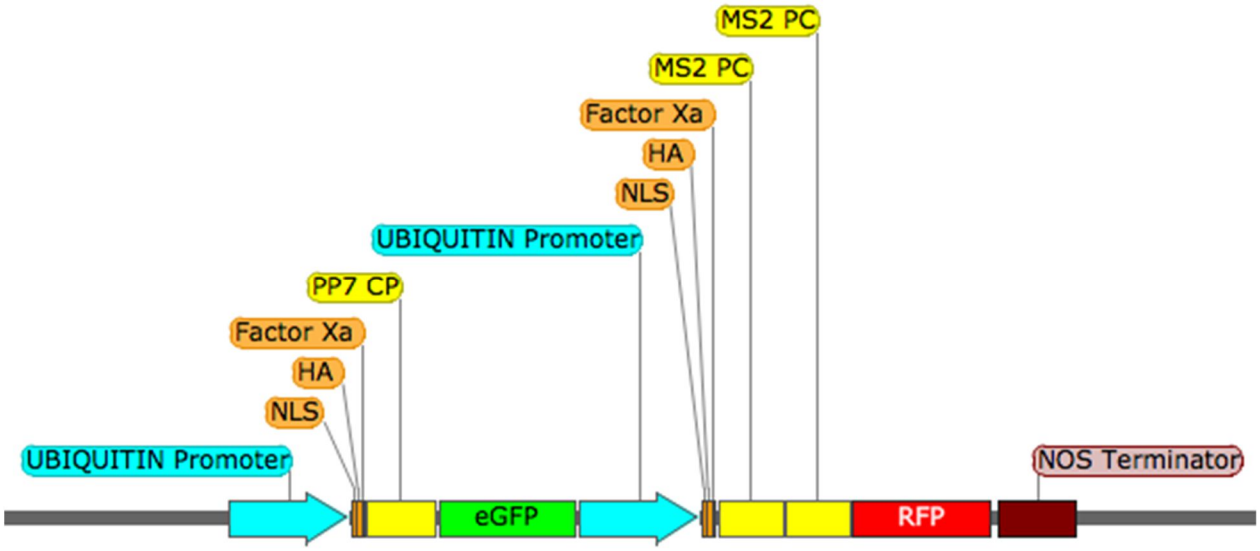

Figure 29. ***PRO UBIQUITIN:PCP:GFP:PRO: UBIQUITIN:MCP:RFP (R4pGW501)*** **construct**

After sequencing the destination vector, it was used to transform Columbia wild type plants. Subsequently the T_1 generation was screened with the confocal microscope. Within this promoter combination it was possible to obtain one line that had signal in

every cell in all developmental stages. The rest of plants showed only either GFP or RFP only (Figure 30).

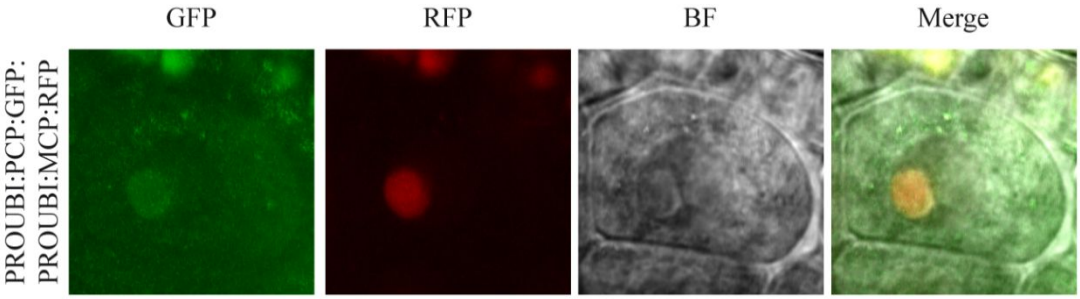

Figure 30. Signal coming from the *PRO$_{UBIQUITIN}$:PCP:GFP:PRO:$_{UBIQUITIN}$:MCP:RFP* (R4pGW501) construct present in microsporocytes First panel represents the GFP signal, second panel demonstrates the signal coming from RFP, third shows bright field, the last panel displays a merge of first two panels.

3.1.2.3.2. Generation of TRICK biosensors with three-fragment multisite gateway system (pB7m34GW)

3.1.2.3.3. Generation of *PRO$_{CDKA;1}$:PCP:GFP:TER:PRO$_{CDKA;1}$:MCP:RFP* (pB7m34GW) construct

To obtain a functional TRICK construct, I used two vectors obtained from Addgene (*phage ubcnls ha pcpgfp* and *phage UBC NLS-HA-2XMCP-tagRFPt*), as templates for my experiments. Both of the vectors had a NOTI site, which was used to insert promoter sequences into the commercial vectors. In this case for both coating proteins a *CDKA;1* promoter was inserted. Afterwards, I used primers C65 and C30 for the *PP7:GFP* vector and C67 and C69 for the *MS2:RFP* vector to create a PCR fragments with attb sites added. In order to enhance the expression of the *PP7:GFP*, I decided to add an additional terminator in between the coating proteins. To achieve the objective, I used primers C31 and C32 to create a PCR fragment with a NOS terminator from the *pGW501* vector inside and attb sites at both ends.

All three of generated fragments were used as components for the three - fragment multisite gateway system. In addition to the promoters, NOS and 35S terminators, fluorescent and coating protein there are three other type components in the created construct. The first one is the nuclear localization signal (NLS) coming from the simian virus 40 that will move the unbounded biosensor to the nucleus. The following one

is the human influenza hemagglutinin tag (HA-tag) for isolation and purification of the biosensor. And lastly, the Factor Xa protease that can be used for the removal of MS2 binding protein molecules. Two sets of those components are placed before each of the binding proteins (Figure 31). After sequencing the destination vector, it was used to transform Columbia wild type plants. In this case the T_1 generation still needs to be generated.

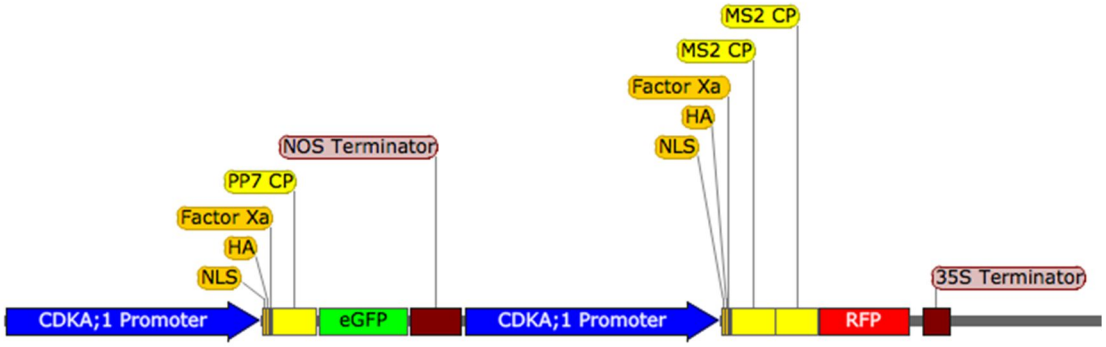

Figure 31. ***PRO$_{CDKA;1}$:PCP:GFP:TER:PRO:$_{CDKA;1}$:MCP:RFP*** **(pB7m34GW) construct.**

3.1.2.3.4. Generation of *PRO$_{CDKA;1}$:PCP:GFP:TER:PRO:$_{UBIQUITIN}$:MCP:RFP* (pB7m34GW) construct

To obtain a functional TRICK construct, I used two vectors obtained from Addgene (*phage ubcnls ha pcpgfp* and *phage UBC NLS-HA-2XMCP-tagRFPt*), as templates for my experiments. Both of the vectors had a NOTI site, which was used to insert promoter sequences into the commercial vectors. In this case for the PP7 coating protein a *CDKA;1* promoter was inserted and the MS2 was fused with a *UBIQUITIN* promoter. Afterwards, I used primers C65 and C30 for the *PP7:GFP* vector and C33 and C34 for the *MS2:RFP* vector to create a PCR fragments with attb sites added. In order to enhance the expression of the *PP7:GFP* I decided to add an additional terminator in between the coating proteins. To achieve the objective, I used primers C31 and C32 to create a PCR fragment with a NOS terminator from the *pGW501* vector inside and attb sites at both ends.

All three of generated fragments were used as components for the three - fragment multisite gateway system. In addition to the promoters, NOS and 35S terminators, fluorescent and coating protein there are three other type components in the created construct. The first one is the nuclear localization signal (NLS) coming from the simian virus 40 that will move the unbounded biosensor to the nucleus. The following one is the

human influenza hemagglutinin tag (HA-tag) for isolation and purification of the biosensor. And lastly, the Factor Xa protease that can be used for the removal of MS2 binding protein molecules. Two sets of those components are place before each of the binding proteins (Figure 32). After sequencing the destination vector, it was used to transform Columbia wild type plants. In this case the T_1 generation still needs to be generated.

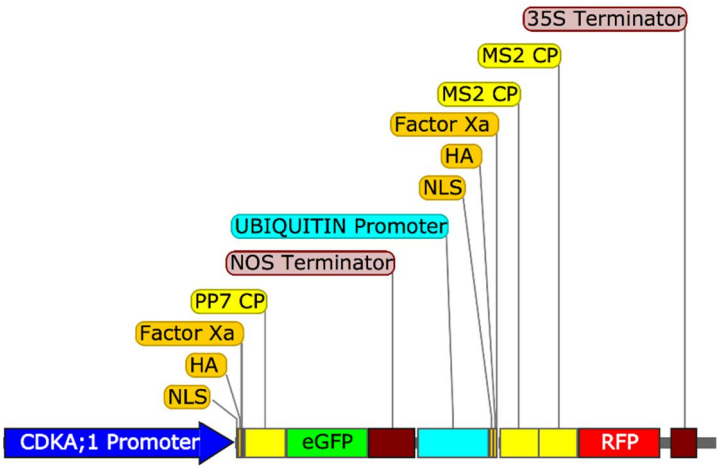

Figure 32. ***PRO*** $_{CDKA;1}$***:PCP:GFP:TER:PRO:*** $_{UBIQUITIN}$***:MCP:RFP*** **(pB7m34GW) construct**

3.1.2.3.5. Generation of *PRO* $_{UBIQUITIN}$*:PCP:GFP:TER:PRO:* $_{CDKA;1}$*:MCP:RFP* (pB7m34GW) construct

To obtain a functional TRICK construct, I used two vectors obtained from Addgene (*phage ubcnls ha pcpgfp* and *phage UBC NLS-HA-2XMCP-tagRFPt*), as templates for my experiments. Both of the vectors had a NOTI site, which was used to insert promoter sequences into the commercial vectors. In this case for the PP7 coating protein a *UBIQUITIN* promoter was inserted and the MS2 was fused with a *CDKA;1* promoter. Afterwards, I used primers C29 and C30 for the *PP7:GFP* vector and C67 and C69 for the *MS2:RFP* vector to create a PCR fragments with attb sites added. In order to enhance the expression of the *PP7:GFP* I decided to add an additional terminator in between the coating proteins. To achieve the objective, used primers C31 and C32 to create a PCR fragment with a NOS terminator from the *pGW501* vector inside and attb sites at both ends. All three of generated fragments were used as components for the three - fragment multisite gateway system. In addition to the promoters, NOS and 35S terminators,

fluorescent and coating protein there are three other type components in the created construct. The first one is the nuclear localization signal (NLS) coming from the simian virus 40 that will move the unbounded biosensor to the nucleus. The following one is the human influenza hemagglutinin tag (HA-tag) for isolation and purification of the biosensor. And lastly, the Factor Xa protease that can be used for the removal of MS2 binding protein molecules. Two sets of those components are place before each of the binding proteins (Figure 33). After obtaining and sequencing the destination vector, it was used to transform Columbia wild type plants.

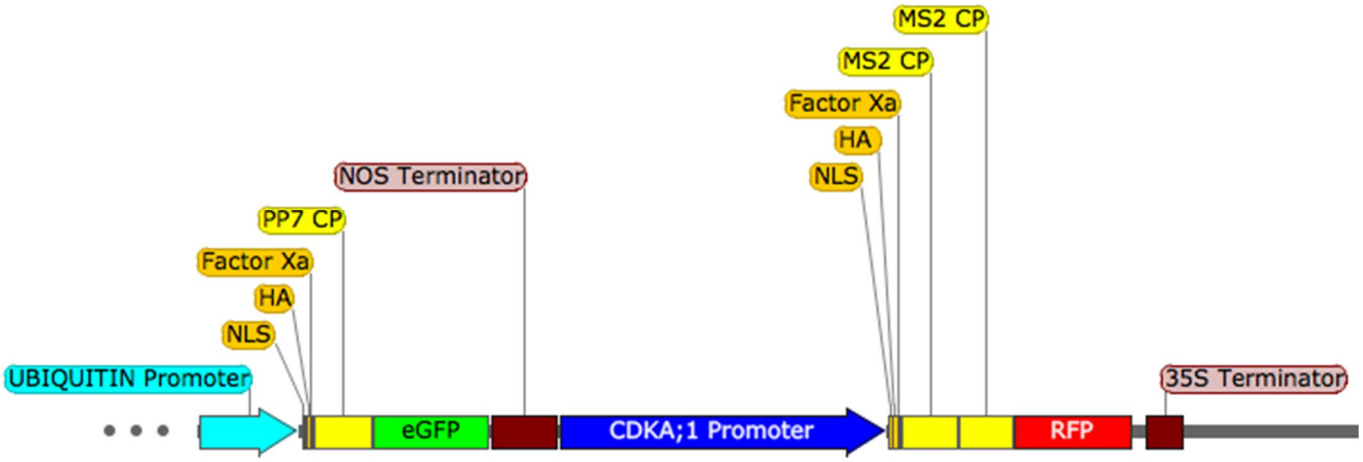

Figure 33. ***PRO*** $_{UBIQUITIN}$***:PCP:GFP:TER:PRO:*** $_{CDKA;1}$***:MCP:RFP*** **(pB7m34GW) construct.**

3.1.2.3.6. Generation of *PRO*$_{UBIQUITIN}$*:PCP:GFP:TER:PRO:*$_{UBIQUITIN}$*:MCP:RFP* (pB7m34GW) construct

To obtain a functional TRICK construct, I used two vectors obtained from Addgene (*phage ubcnls ha pcpgfp* and *phage UBC NLS-HA-2XMCP-tagRFPt*), as templates for my experiments. Both of the vectors had a NOTI site, which was used to insert promoter sequences into the commercial vectors. In this case for both coating proteins a *UBIQUITIN* promoter was inserted. Afterwards, I used primers C29 and C30 for the *PP7:GFP* vector and C33 and C34 for the *MS2:RFP* vector to create a PCR fragments with attb sites added. In order to enhance the expression of the *PP7:GFP* I decided to add an additional terminator in between the coating proteins. To achieve the objective, I used primers C31 and C32 to create a PCR fragment with a NOS terminator from the *pGW501* vector inside and attb sites at both ends. All three of generated fragments were used as components for

the three - fragment multisite gateway system. In addition to the promoters, NOS and 35S terminators, fluorescent and coating protein there are three other type components in the created construct. The first one is the nuclear localization signal (NLS) coming from the simian virus 40 that will move the unbounded biosensor to the nucleus. The following one is the human influenza hemagglutinin tag (HA-tag) for isolation and purification of the biosensor. Then lastly the Factor Xa protease that can be used for the removal of MS2 binding protein molecules. Two sets of those components are place before each of the binding proteins (Figure 34). After sequencing the destination vector, it was used to transform Columbia wild type plants.

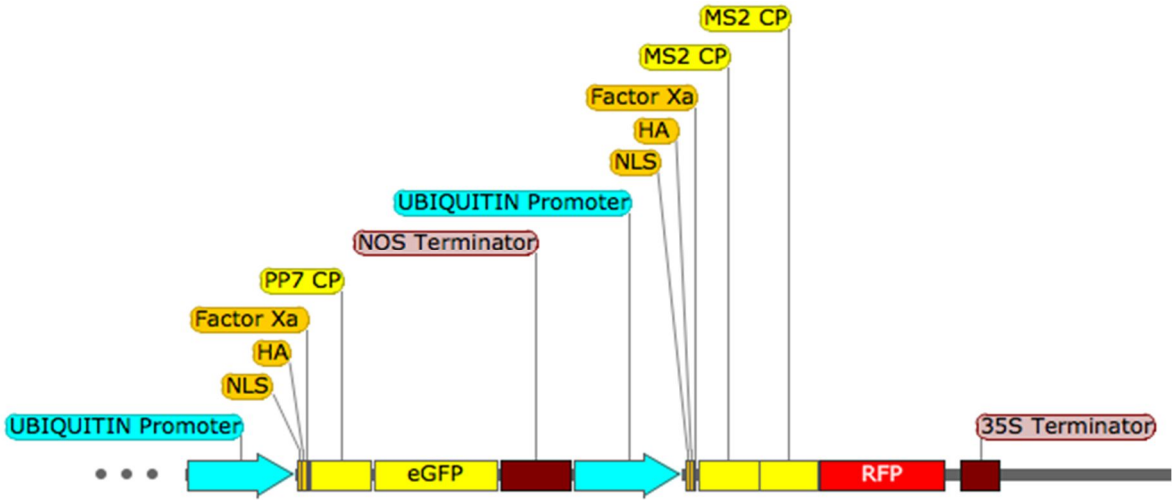

Figure 34. ***PRO*** $_{UBIQUITIN}$***:PCP:GFP:TER:PRO:*** $_{UBIQUITIN}$***:MCP:RFP (pB7m34GW)*** **construct**

3.2. Analysis of mono-cellular pollen mutants

WT pollen development results in a three-celled gametophyte, with two sperm cells and one vegetative cell. Cell cycle mutants are showing a very specific phenotype where some of the mature pollen grains have less cells than usual. Mutants of *cdka;1+/-* or *fbl17+/-* are producing pollen that has only two or even one cell. In double mutants of *cdka;1 +/- fbl17+/-* and *e2fa -/- fbl17+/-* the amount of single celled pollen ranges from 9 to 25 % (Figure 35; Zhao et al 2012).

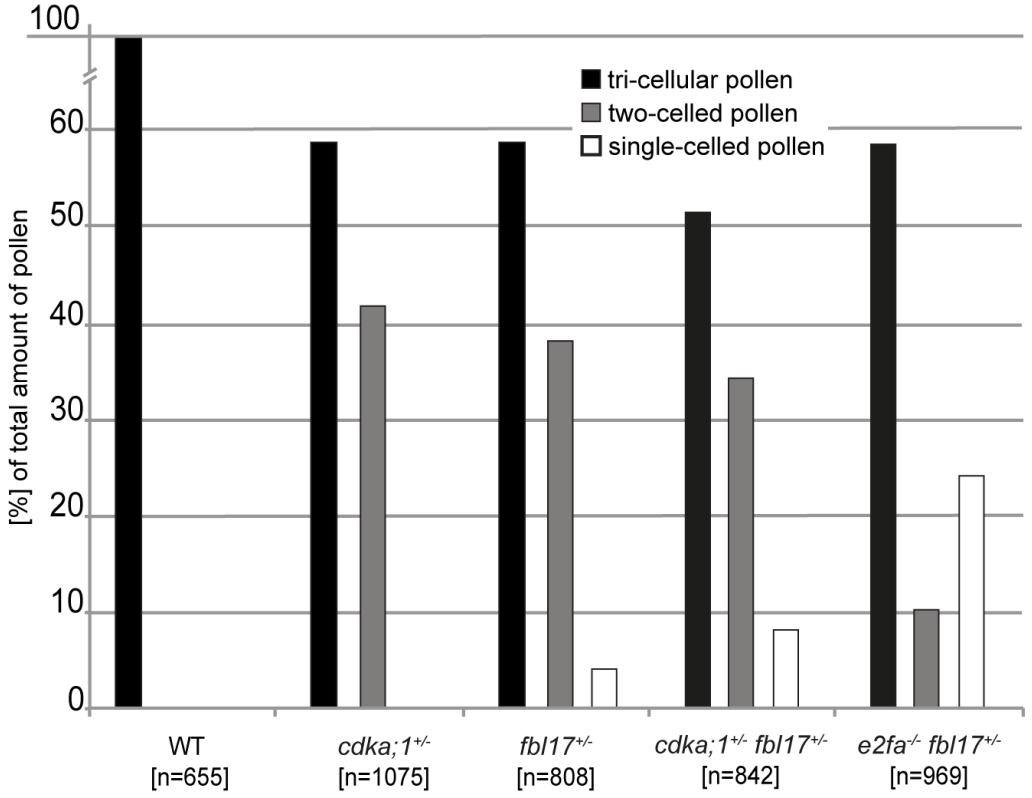

Figure 35. Frequencies of pollen phenotypes. Frequencies of mutant, i.e. single-celled and two-celled, pollen versus wild-type and wild-type like tricellular pollen of the mutants used in this study in comparison with the wildtype.

3.2.1. Analysis of *CYCD x CDKA;1 / FBL17* double mutants

It remains unclear which group of cyclins is involved in forming a complex with *CDKA;1* during the pre-mitotic S-Phase. It is also unknown if one of the cyclins plays a main role in that process or if they are redundant. In 2010, studies performed by Van Leene et al. pointed out that there are two groups of *CYCLINS*, *A-type* and *D-type*, which are interacting with *CDKA;1*. To address that issue, I used a method developed by Zhao et al in 2012. To limit the amount of cyclins to analyze, an *in silico* experiment was performed by Barbara Gloecke where expression of the *D-type CYCLINS* was examined and four candidate genes were chosen. Subsequently, Barbara Gloecke performed a preliminary experiment counting 200 to 300 pollen grains per genotype that showed some promising results. To further confirm those results I performed the same experiments but on a greater scale.

3.2.1.1. CYCLIND1;1 (CYCD 1;1)

The first counting was performed for the *CYCLIN D1;1*. There were four types of controls used, such as wild type Columbia, single mutant of the *cycd1;1* itself, single mutants of *fbl17+/-* and *cdka;1+/-* . In the preparatory work (made by B. Gloecke) the *cycd1;1* mutant was crossed with both *fbl17* and *cdka;1+/-* . In order to count the wild type pollen, three plants were used and 655 pollen grains in total were checked, from which 100% were tricellular. In case of the cyclin also three different plants were used with 677 pollen grains counted, from which 4% of pollen grains showed mutant, bicellular, phenotype, whereas the remaining 96% was characterized as wild type like pollen with three cells. Likewise, for single *fbl17+/-* and *cdka;1+/-* mutants three plants were used for counting's for each genotype. The number of pollen grains counted was 808 for *fbl17+/-* and 1075 for *cdka;1+/-* . In both cases the amount of tricellular pollen was at 58% while the level of bicellular pollen was at the level of 38% for *fbl17+/-* and at 42% for the *cdka;1+/-* . Representing 4% of the whole population of *fbl17+/-* mutant, a new class of unicellular pollen appears. In case of the *cycd1;1* and *fbl17+/-* cross the graph is demonstrating a decrease in numbers of the bicellular class (28%) in favor of the tricellular class (71%), in comparison to the single *fbl17+/-* mutant. However, considering the standard deviation, it is not a significant difference. For this genotype, three different

plants were chosen and 1289 pollen grains were counted. The *cdka;1+/- x cycd1;1* double mutant also showed no significant differences, with the levels of tricellular pollen and bicellular pollen almost at the same levels as *cdka;1+/-* control (57 and 42% respectively). The number of pollen grains was a total of 1489, coming from four plants. In both crosses, it was possible to observe a very small (1%) class of unicellular pollen, which is not statistically relevant (Figure 36).

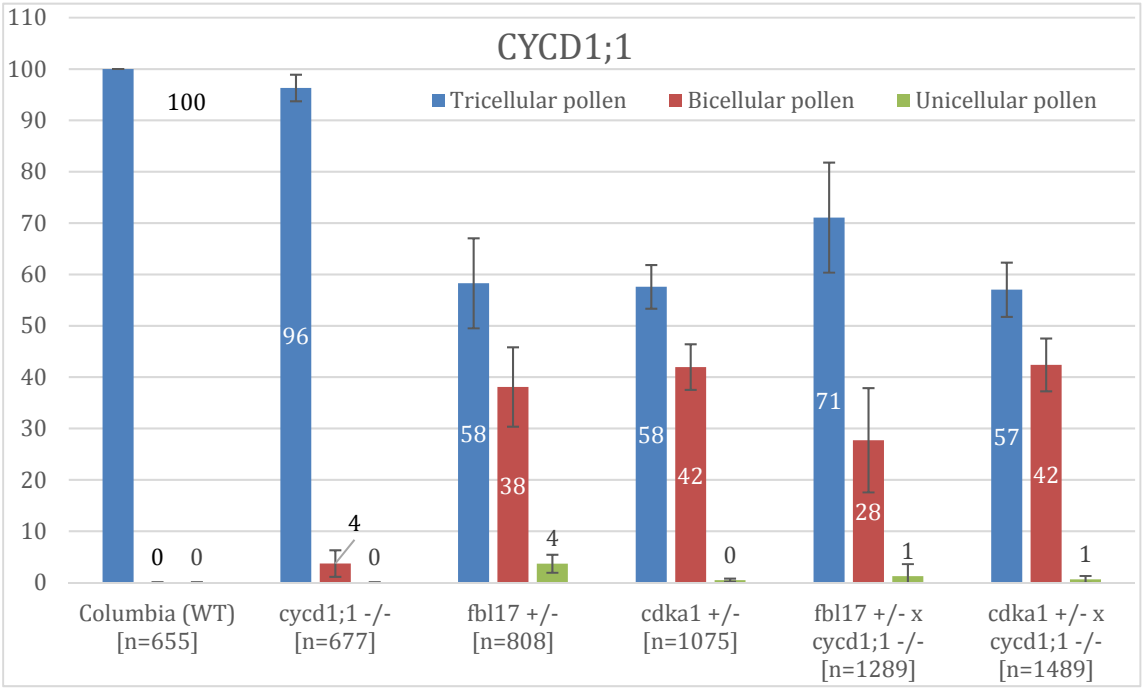

Figure 36. Pollen distribution in the *CYCD1;1* experiment

3.2.1.2. CYCLIND2;1 (CYCD2;1)

The second counting was performed for the *CYCLIND2;1*. There were again four types of controls used, such as wild type Columbia, single mutant of the cyclin itself and single mutants of *fbl17+/-* and *cdka;1+/-* . In the preparatory work (made by B.Gloecke) the *cycd2;1* mutant was crossed with both *fbl17+/-* and *cdka;1+/-* . For the process of counting the wild type pollen, three plants were used and 435 pollen grains in total were checked, from which 100% were tricellular. In case of the *cycd2;1* two different plants were used with 568 pollen grains counted, from which 5% of pollen grains were bicellular, and 1% unicellular, whereas the remaining 94% was characterized as wild type like pollen with three cells. Likewise, for single *fbl17+/-* and *cdka;1+/-* mutants three plants were used for counting each genotype. The number of pollen grains counted was 635 for

fbl17+/- and 634 for *cdka;1+/-* . The amount of tricellular pollen was at 58% for *fbl17+/-* and 59% for *cdka;1+/-* while the level of bicellular pollen was at the level of 42% and 41%, respectively. Representing 1% of the whole population of *fbl17+/-* mutant, a new class of unicellular pollen appeared. For the *cycd2;1* and *fbl17+/-* cross, the graph is demonstrating a decrease in numbers of the bicellular class (47%) in favor of the tricellular class (60%) in comparison to the single *fbl17+/-* mutant. However, considering the standard deviation, it is not a significant difference. For this genotype, four different plants were chosen and 887 pollen grains were counted. The *cdka;1+/- x cycd2;1* double mutant also showed no significant differences, with the levels of tricellular pollen and bicellular pollen at the same levels as *cdka;1+/-* control (59 and 41% respectively). The number of pollen grains was a total of 1156, coming from six plants. In *fbl17+/-* cross it was possible to observe a very small (3%) class of unicellular pollen which is not statistically relevant (Figure 37).

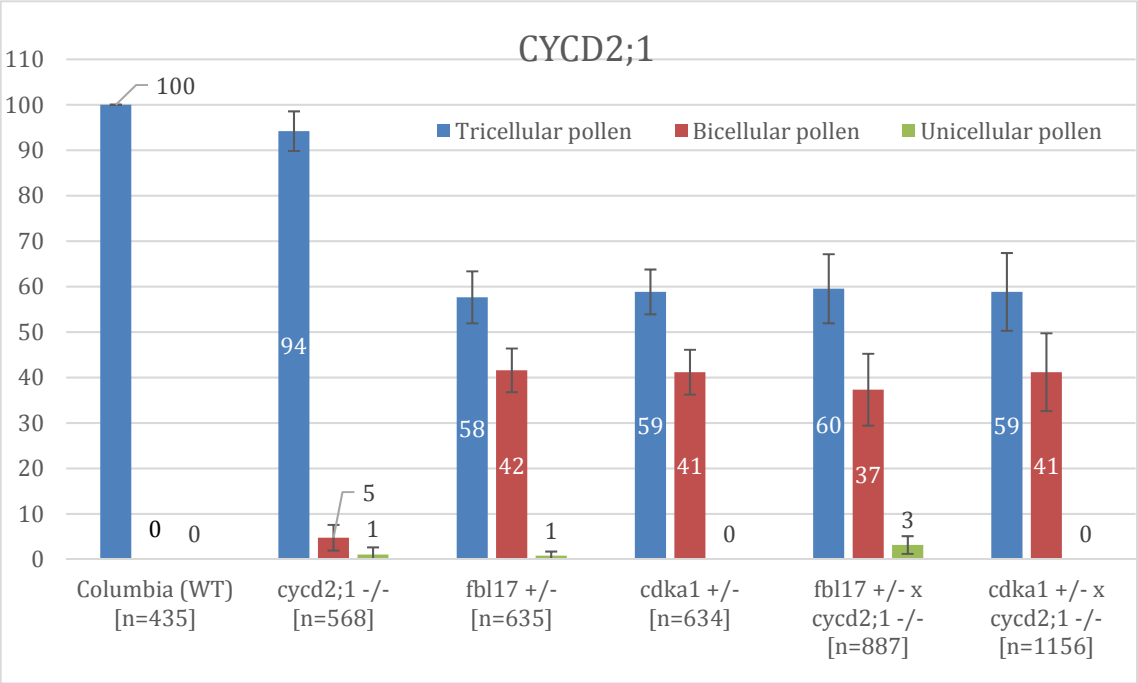

Figure 37. Pollen distribution in the *CYCD2;1* experiment

3.2.1.3. CYCLIND3;2 (CYCD3;2)

The third counting was performed for the *CYCLIND3;2*. There were again four types of controls used, such as wild type Columbia, single mutant of the *cycd3;2* itself and

single mutants of *fbl17* and *cdka;1+/-* . In the preparatory work (made by B.Gloecke) the cyclin mutant was crossed with both *fbl17+/-* and *cdka;1+/-* . In the process of counting of wild type pollen, three plants were used and 552 pollen grains in total were checked, from which 99% were tricellular and only 1% was bicellular. In case of the *cycd3;2* three different plants were used with 548 pollen grains counted, from which 4% of pollen grains showed mutant bicellular phenotype, whereas the remaining 96% was characterized as wild type-like pollen with three cells. Likewise, for single *fbl17+/-* and *cdka;1+/-* mutants three plants were used for counting each genotype. The number of pollen grains counted was 635 for *fbl17+/-* and 884 for *cdka;1+/-* . The amount of tricellular pollen was at 58% while the level of bicellular pollen was at 42% for both *fbl17+/-* and *cdka;1+/-* . Representing 1% of the whole population of *fbl17+/-* mutant a new class of unicellular pollen appeared. For the *cycd3;2* and *fbl17+/-* cross the graph is demonstrating an increase in numbers of the tricellular class by one percent, and a decrease by two percent in the bicellular class in favor of the unicellular class in comparison to the single *fbl17+/-* mutant. However, considering the standard deviation, it is not a significant difference. For this genotype, three different plants were chosen and 1475 pollen grains were counted. The *cdka;1+/- x cycd3;2* double mutant showed a non-significant increase in the bicellular class by 2% altogether, with a decrease in the tricellular class by 2%. The number of pollen grains was a total of 1404, coming from four plants (Figure 38).

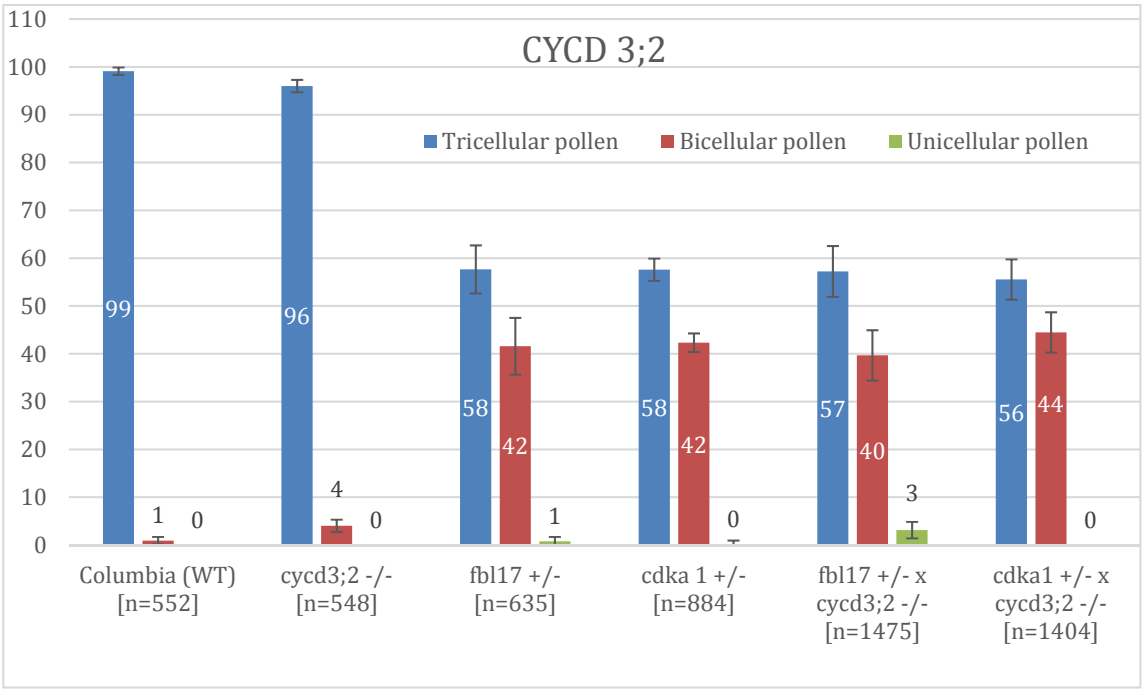

Figure 38. Pollen distribution in the *CYCD3;2* experiment

3.2.1.4. CYCLIND4;1 (CYCD4;1)

The last counting was performed for the *CYCLIND4;1*. There were again four types of controls used, such us wild type Columbia, single mutant of the *cycd4;1* itself and single mutants of *fbl17+/-* and *cdka;1+/-*. In the preparatory work (made by B.Gloecke) the *cycd4;1* mutant was crossed with both *fbl17+/-* and *cdka;1+/-* . In the process of counting of wild type pollen counting, three plants were used and in total 655 pollen grains in total were checked, from which 100% were tricellular. In case of the *cycd4;1* three different plants were used with 600 pollen grains counted, from which 3% of pollen grains showed mutant bicellular phenotype whereas the remaining 98% was characterized as wild type-like pollen with three cells. Likewise, for single *fbl17+/-* and *cdka;1+/-* mutants three plants were used for counting each genotype. The amount of tricellular pollen was at 64% for *fbl17+/-* and 58% for *cdka;1+/-* while the level of bicellular pollen was at 34% and 42%, respectively. Representing 4% of the whole population of *fbl17+/-* mutant a new class of unicellular pollen appeared. For the cyclin and *fbl17+/-* cross the graph is demonstrating no significant difference in regard to the *fbl17+/-* control. For this genotype two different plants were chosen and 1274 pollen grains were counted. The *cdka;1+/- x cycd4;1* double mutant showed a non-significant decrease in the bicellular class by 1 percent altogether, with an increase in the tricellular class by 1%. The number of pollen grains was 1404, coming from two plants (Figure 39).

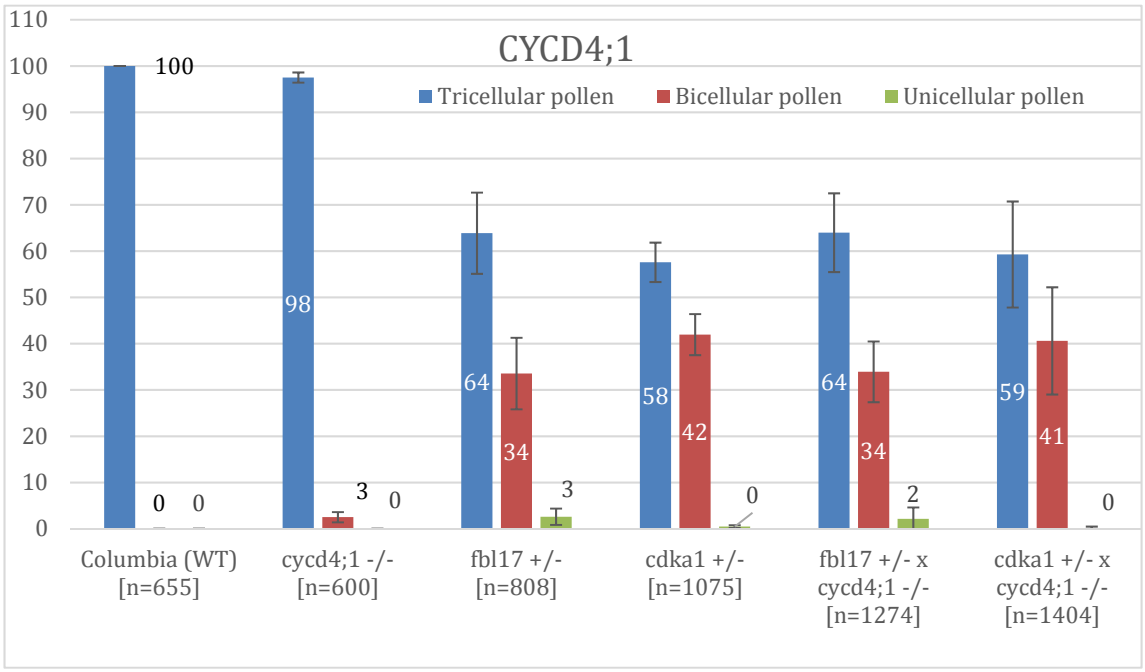

Figure 39. Pollen distribution in the *CYCD4;1* experiment

3.2.2. Transposons are active in single celled pollen after the second mitosis

In my experiments I used transposon enhancer trap line ET11075 and crossed it with double cell cycle mutant *e2fa* $^{-/-}$ *fbl17*$^{+/-}$. A similar experiment was performed by Barbara Gloecke, where she crossed the ET13889 line with *cdka;1*$^{-/-}$ *fbl17*$^{+/-}$ double mutant. Both of the transposon lines have a GUS marker that shows up in pollen when the repression is lifted. Both of experiments demonstrated similar results. The signal was present in all types of cells including the monocellular pollen (Figure 40). This further proves the hypothesis that the single celled pollen has a vegetative fate.

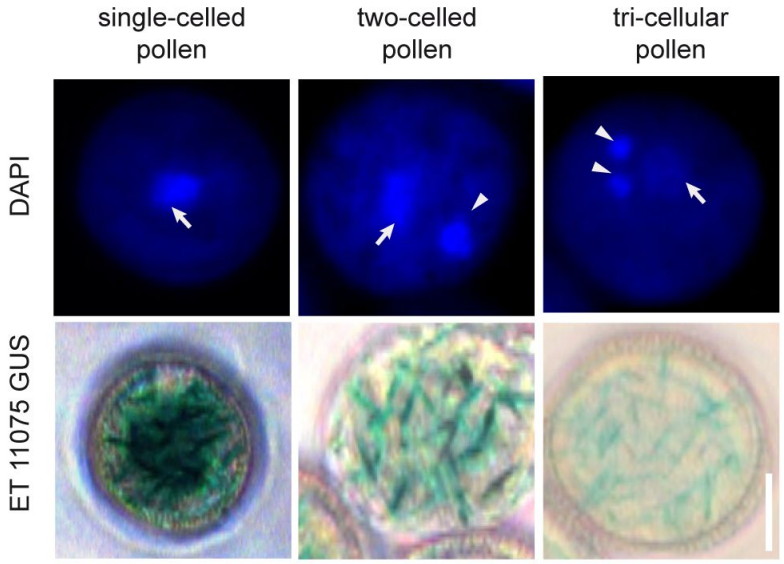

Figure 40. Activation of transposon expression in single-celled pollen of e2fa -/- fbl17-/+ plants.

Fluorescent- and light micrographs of single-celled, two-celled and tri-cellular pollen of e2fa+/- fbl17+/- plants expressing the Ds transposon Enhancer trap line ET11075 GUS reporter. All three pollen types of e2fa+/- fbl17+/- plants express the GUS reporter. In the upper row DAPI staining is shown, the lower show GUS staining. The arrowheads indicate the sperm cell, arrows indicate the vegetative nucleus. Scale bar is 10 µm.

3.2.3. Generation of reporter lines for pollen tube tracking

Although the importance of the vegetative cell is evident, nobody so far has addressed the question whether a vegetative cell, without the presence of sperms, can grow a pollen tube and reach an ovule. To address that issue, Barbara Gloecke started an experiment by crossing a *e2fa -/- fbl17+/-* double mutant with the FB037 line, which has a GFP marker expressed only in the sperm cells (*PRO*$_{MGH}$*:MGH3:eGFP*) and an RFP marker

expressed solely in the vegetative nucleus (*PRO$_{ACTII}$:H2B:mRFP*; Figure 41; Borges et al.,2012).

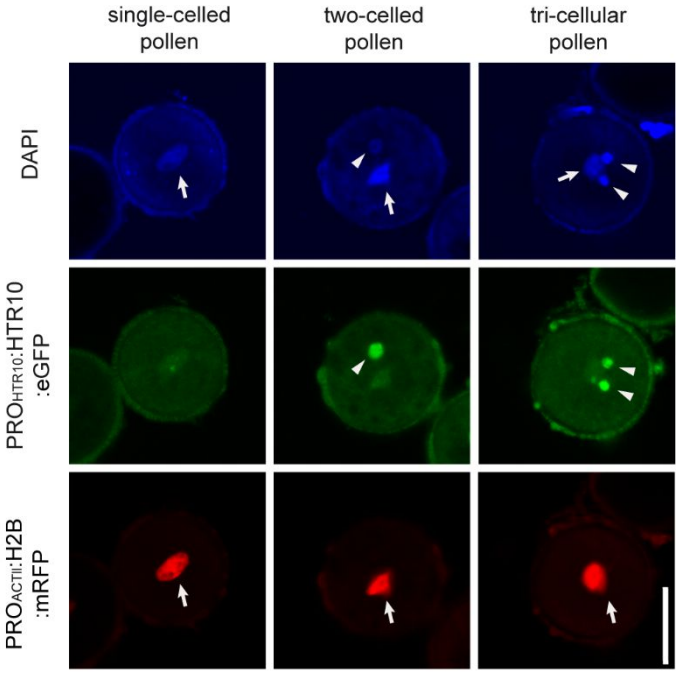

Figure 41. Cell fate analysis of single-celled pollen of *e2fa -/- fbl17+/-* plants. Fluorescent micrographs of pollen from *e2fa -/- fbl17+/-* plants carrying FB037 reporters *PRO$_{HTR10}$:HTR10:eGFP* and *PRO$_{ACT11}$:H2B:mRFP*. The columns represent, DAPI staining of all nuclei in the pollen grain, *PRO$_{HTR10}$:HTR10:eGFP* marking the generative nuclei and *PRO$_{ACT11}$:H2B:mRFP* marking the vegetative nucleus. The first, second and third row show panels with single celled pollen, two celled pollen and tricellular pollen, respectively. Arrowheads indicate sperm cell nuclei, arrows designate vegetative nuclei. Scale bar is 10 µm.

After propagating the cross three times I managed to obtain two lines from the cross of *e2fa -/- fbl17+/-* with FB037 that were homozygous in terms of GFP and RFP signal. It was possible to conduct further experiments with both lines because of significantly high levels of monocellular pollen (around 15 percent each). Tricellular pollen was between 66 and 69% and the bicellular class was represented by 16 to 20% of pollen. After the lines were established, seeds were sent to Japan to Tetsuya Higashiyama lab where they were regrown to check how single cell pollen behaves in the company of ovules in a special medium (Figure 42).

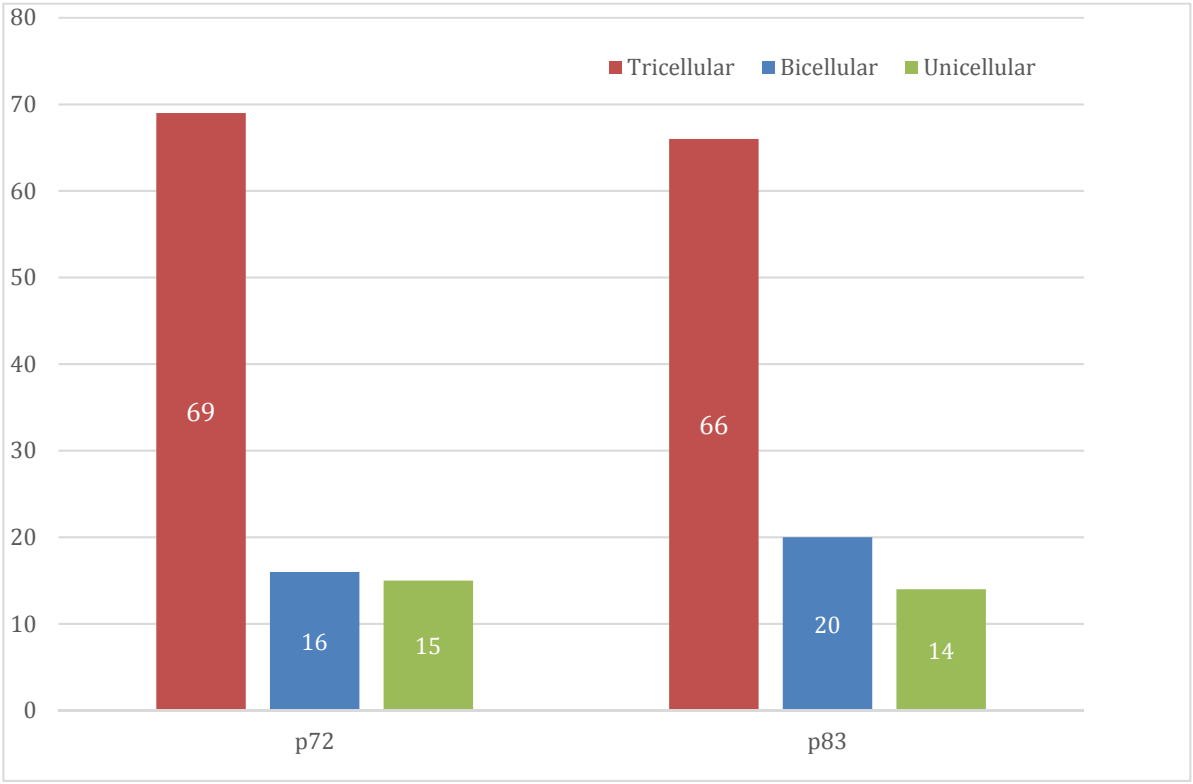

Figure 42. Pollen distribution in FB037 cross

3.2.4. Pollen tube tracking

To finally answer the question if sperm cells have an influence on pollen tube germination, Shiori Nagahara from Higashiyama lab performed an semi in vivo fertilization experiment. Firstly, two experiment involving controls were performed, in which only pollen from uncrossed FB037 line was used. Ovules used in those experiments were taken from WT plants and plants transformed with a *PRO$_{RPS5A}$:H2B:tdTomato* construct. When both pollen from FB037 plants and ovules from WT or *PRO$_{RPS5A}$:H2B:tdTomato* plants were placed together on the same medium, pollen tubes started to germinate and move towards the ovules (Figure 43.A1), whereas the vegetative nucleus marked with RFP started to lead the sperm cells towards the ovule's micropyle. Upon arriving at the destination we could observe a sudden discharge of both sperms and the vegetative nucleus (Figure 43.A2). After that the vegetative nucleus stayed in the resting zone and the sperms moved towards the central and egg cells where the double fertilization occurred (Figure 43.A3). Secondly, pollen from the cross between FB037 line and our double mutant - e2fa$^{-/-}$ fbl17$^{+/-}$ was used. In that case it was possible to observe

pollen grains that were bicellular or even unicellular, apart from wild type like pollen. The detected movements of bicellular pollen were similar to wild type. The pollen tube was moved toward the ovule (Figure 43.B1) and after that it discharged (Figure 43.B2). Subsequently, the vegetative nucleus traveled to the resting zone and the sperm cell moved towards the central cell nucleus to fertilize it (Figure 43.B3). An intriguing phenomenon has been noticed during the observation of the monocellular pollen, which had only the vegetative cell nucleus. Moreover, there were no discrepancies in pollen tube growth and targeting in regard to the wild type pollen (Figure 43.C1). The pollen tube discharged normally (Figure 43.C2) and the vegetative cell moved to the resting zone (Figure 43.C3). This result proves that the single-celled pollen mutant with only the vegetative cell present can grow, guide and successfully discharge a pollen tube.

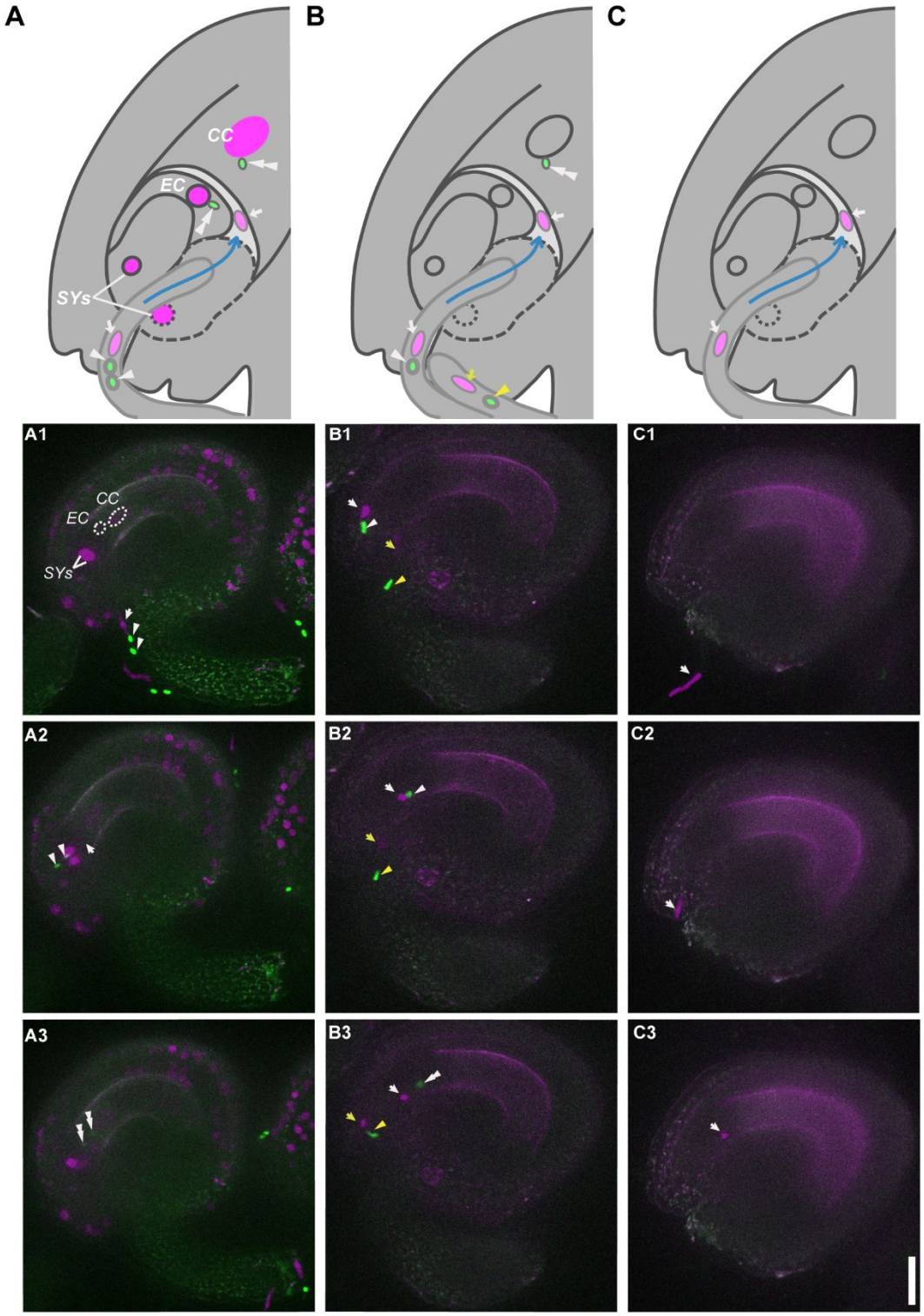

Figure 43. Fertilization by singled-celled pollen. First row depicts a summary sketch of the fertilization process shown in the column below. Numbers from 1 to 3 represent specific fertilization process time points. 1 –pollen tube entry into the ovule; 2 – post pollen tube discharge; 3 – (double) fertilization. Arrowheads, sperm cell nuclei moving towards the egg cell and the central cell; double arrowheads, sperm cell nuclei fertilizing egg- and central cell; arrows, vegetative nucleus. EC, egg cell; CC, central cell; SYs, synergid cells. Scale bar, 20 µm.

A. Fertilization of a *PRO$_{RPS5A}$:H2B:tdTomato* expressing wild-type ovule with a tricellular wild-type pollen tube possessing FB037 marker genes. The RFP-labeled vegetative nucleus and the two GFP-labeled sperm nuclei are visible.

B. Fertilization of a *PRO$_{RPS5A}$:H2B:tdTomato* expressing ovule with a two-celled (single sperm) *e2fa-/- fbl17-/+* mutant pollen tube possessing FB037 markers . An RFP-labeled vegetative nucleus and a single GFP-labeled sperm cell nucleus were observed in both the first and second pollen tube approaching (white and yellow arrow and arrowheads). Note that only one fertilization event is observed. The rod shape appearance of the nuclei result from their movement during image acquisition.

C. Fertilization of a *PRO$_{RPS5A}$:H2B:tdTomato* expressing ovule with a single-celled *e2fa-/- fbl17-/+* mutant pollen tube possessing FB037 markers. Only one RFP-labeled vegetative nucleus (arrow) was observed. Note that no fertilization occurs due to the lack of a male gamete.

4. Discussion

The present PhD thesis was divided in two main parts, the meiosis and mitosis project. The meiosis project focused on the investigation of translational control of meiosis in Arabidopsis. The mitosis project comprised of two subprojects - the first on the role of cyclins in male gametophyte development and the second one aiming to discover the developmental capacities of single cell pollen.

4.1. Translation control

During this thesis, I started a project addressing two genes that exhibited expression patterns, which are not correlated with protein appearance observed in our laboratory. *REC8* transcripts were detected with qRT-PCR three days before the REC8:GFP protein could be observed. Moreover, the *TAM* mRNA was present all the time, while the protein was visible only in meiosis. Additional *in silico* experiments demonstrated that *REC8* and *TAM* genes are expressed in tissues other than those undergoing meiosis. This preliminary data obtained in our lab gives rise to a presumption that those genes might be controlled on a translational level. In comparison to other organisms, such as yeast or mammals, translational control in plants is a relatively unexplored topic.

Starting with the first gene, *REC8*, there are no known cases for translational control of its homologs from organisms, such as yeast, mammals etc. However, this does not exclude the possibility that this kind of regulation is present in plants. The second gene – *TAM,* belongs to cyclins, which are a large group of genes represented by a number of translationally regulated genes in other organisms, in spite of the fact that they are not known to be translationally controlled in plants. *CYCLIN* (*CYE-1*) in *C. elegans* is repressed by *GLD-1* (*GERMLINE DIFFERENTIOATION 1*) through its interaction with the GLD-1 binding element located in the 3'UTR of *CYE-1* (Bidermann et al, 2009). Its homolog was investigated in mammalian cells lines, where it was discovered that a different gene called *DDX3* (*DEAD BOX 3*) regulates its expression by interacting with the 5'UTR of this cyclin (Lai et al., 2010). In Drosophila, a gene called *BRUNO* inhibits translation of mitotic *CYCLIN A* at the beginning of meiosis, which happens again by interaction with a specific responsive element located in the 3'UTR (Sugimura and Lilly 2006). Another example of a cyclin that is translationally controlled via its UTR is *CLB3 (CYCLINB 3*) from yeast. In

this case, translational control is restricting protein synthesis until the second meiotic division while the transcripts already start to accumulate in anaphase I (Carlie et al., 2008). This discrepancy between the appearance of transcript and protein was very similar to what was observed in our lab with *TAM* and *REC8* genes. All this examples also illustrate the importance of both UTRs as locations for different translation regulation elements. Maintaining those sequences might be crucial for full investigation of mRNA regulation mechanisms. Unfortunately, this has proven to be problematic because the initial vector for *REC8,* which was a starting point for my cloning experiments, was already lacking the 3'UTR. Therefore, any potential binding motifs that could interact with factors responsible for regulating *REC8* mRNA were omitted.

Another interesting mechanism of translation control was observed in rice, where a short upstream open reading frame was consisting only from six nucleotides - namely start and stop codon (AUG-stop). This ORF is located in the 5'UTR and influences translation of the *NIP5;1* gene (*NOD26-LIKE INTRINSIC PROTEIN 5;1*), which encodes a boric acid channel, although the mechanisms behind this regulation remain unclear. (Tanaka et al 2016). Interestingly, a short AUG-stop frame is located approximately 150 bp before the 5'UTR of *TAM* gene. Although the current state of art states that the uORFs can influence translation only when they are located in the UTR of a gene, it is not fully investigated if they can control translation when they are located before the UTR. Likewise, it is not clear whether the uORF located before the *TAM* 5'UTR is transcribed during meiosis or not. If the transcript during meiosis is different, the uORF might be included in the UTR and therefore influence the translation of this cyclin. Alternative splicing variants like that could be detected, for example by RT-PCR, through designing specific primer sets for different fragments. This would make it possible to distinguish if a certain fragment is included or skipped during the pre-mRNA maturation process (Harvey and Cheng, 2016). *REC8* in this matter should also be investigated since it possesses two different variants, one of which has a slightly longer 5'UTR that may harbour some binding motifs influencing *REC8* translation.

After confirming that *TAM* and *REC8* have alternative splicing variants, and whether they have influence on translation control, it would be conceivable to perform some experiments to visualise this process. Gurskaya et al., in 2012 created a technique that uses a specially constructed "minigene" that encodes two fluorescent proteins and the investigated gene of interest. On one hand, when all of the exons of the investigated

gene are included, both fluorescent proteins can be detected. On the other hand, when one of the fragments is skipped a frameshift occurs, resulting in a stop codon before GFP and therefore the obtained signal will be only red. If this stop inducing frameshift does not occur naturally, it is necessary to add some nucleotides to induce the appearance of the stop codon artificially. The artificial splicing can be then observed by fluorescence microscopy or quantified by flow cytometry (Gurskaya et al., 2012). Nevertheless, it would be beneficial to investigate the possibility of different splicing variants in both genes since it may influence the presence of some binding motifs that might be omitted or included during the pre-mRNA maturation.

The methods I have chosen to visualise *TAM* and *REC8* mRNA particles are utilising components of the PP7 and MS2 bacteriophages, namely their coating proteins and stem loops. The first technique I used is called MS2-tag, it only uses components from the MS2 bacteriophage and it was already tested in plants for various purposes. Hamada with colleagues in 2003 used it while researching rice and its proline mRNA transport. Another group utilised it for discovering the mechanisms of cytoplasmic redistribution of a nuclear ribosome binding protein protein caused by *ENOD40* (*EARLY NODULIN 40*) gene in *Medicago truncatula* plants (Compalans et al 2004). MS2-tag was also used for detecting the turnip circle virus in Arabidopsis (Zhang et al. 2003). In multiple other labs it was used for a general purpose of localising or co-localising specific mRNA particles (Fujioka et al., 2007; Fang and Spector, 2007; Sambade et al., 2008).

This method combined with *REC8*/*TAM* – GFP constructs created in our lab opens the possibility to compare transcript levels and protein levels of those genes. However, this combination would fail to give us any data in case something happened in the timeframe before the GPF is folded and observable. The protein might have been degraded before that happened or the folding itself could have been blocked by some other proteins.

To cope with this problem, knowing when the first round of translation happens would tell us if there is some kind of control occurring at this point. The second technique I used is called TRICK and by implementing components coming form an additional bacteriophage it can demonstrate us when exactly the first round of translation occurs.

There are some general aspects connected with the usage of bacteriophage hairpins components in mRNA research. The biggest advantages are in high specificity and non-invasive transgenic delivery. Among the disadvantages are: the large RNA tag

that may interfere with RNA function and low signal-to noise ratio detection (Christiansen et al 2010). Additionally, PP7 sequences were never tested in plants. Thus, although those hairpins are non-homologous to any known protein, it is currently not clear whether they interfere with any cellular processes.

In this study, I prepared two kinds of TRICK platforms and in one of them all of the crucial elements, so PP7 and MS2 sequences were followed by a separate terminator each. The second type is lacking the terminator after the PP7 fragment and was constructed because of initial problems with construction of the more complex vectors.

The results obtained from transforming *tam* mutants with the *TAM:GFP:MS2* construct are showing signals in the meiocyte cytoplasm, with an exception in the nucleus. For an unknown reason the autofluorescence in the GFP channel was very strong relatively to the GFP signal coming from the meiocyte, therefore some might argue if that signal was truly relevant. However, in the autofluorescence channel I could not find any fluorescence coming from the meiocytes. Some of those lines had also fully or partially restored WT phenotypes and I could genotype for the *GFP* coding sequence. Therefore, those lines were picked up for further experiments, regardless of the suspicious signal patterns.

After I've constructed the vectors coding the binding proteins (BP) and used them to transform plants, I began to search for the best lines that could be used in further experiments. Via confocal microscopy I was looking for signals present in the nuclei of all cells to see if the *CDKA;1* and *UBIQUITIN* promoters were correctly promoting the expression of either GFP or RFP. For the simple binding proteins from the MS2-tag experiments, it was relatively uncomplicated to find lines that had strong expression in all types of cells, including meiocytes. A completely different case was observed in the case of BP constructs from the TRICK experiments. In this instance, after screening more than 250 plants, I was able to find only two plants that had both signals in all nuclei. The rest of plants was showing either only GFP signal, only RFP signal or in a few rare cases – both signals present in all cells - except meiocytes. Moreover, I was able to witness some fluorescence in all promoters combinations, except from the example where both PP7 and MS2 proteins were preceded by the *CDKA;1* promoter. In this case, it was impossible to find either GFP or RFP signals in the nuclei of transformed plants, despite multiple repetitions of the experiment. There is a high possibility that those constructs, in particular, were either silenced because of the repeated *CDKA;1* sequence or simply the

vector with two *CDKA;1* promoters was too big (Hanahan, 1983; Hsieh and Fire, 2000; Pontier et al., 2005).

Nevertheless, the repetitive sequences present in the constructs were most probably the main reason for the low number of lines obtained at the end of the transformation process. Vectors with only one batch of repetitions, for MS-tag, were incomparably easier to obtain than vectors with two regions of repetitive sequences. Repetitive DNA is often silenced because it acts as a nucleation centre for heterochromatin formation and it is recognised by specific DNA binding proteins interacting with machinery responsible for heterochromatin formation (Twyman, 2016). Furthermore, at earlier steps of vector construction I encountered problems while performing simple cloning steps (like adding a promoter in front of the repetitive sequence). In one instance, bacteria recombined a fragment of the PP7 with a different sequence of the same length rendering the whole construct unfunctional. This example proved that working with constructs containing repetitive regions, requires thorough sequencing of the vector after each cloning step. In cases similar to mine, this problem could be also solved by using special vectors, designed for cloning fragments full of repeats, like pJAZZ created by Godiska et al in 2010.

After the preliminary screening for GFP and/or RFP in the nuclei and selecting the lines with the strongest signal, I noticed that the observed signal is not coming from the nucleus as it should, because of the NLS, but from the nucleolus. From the images presented in the original work of Halsted et al., it is visible that the nucleoli are brighter than the rest of the nucleus. It might be possible that in my lines the signal is much weaker than it potentially can be and therefore it is only visible in the nucleolus.

The other group of constructs that possessed an additional terminator in between the PP7 and MS2 fragments might exhibit stronger and more stable signals since, as in many cases, it was shown that transcription termination can influence the overall level of protein expression. Presence of a terminator adjusts the expression via terminating the transcription process and influencing the 3' end processing of the mRNA molecule. The latter has a huge effect on its stability and translation capacity (Carswell and Alwine, 1989; Ingelbrecht et al., 1989; West and Proudfoot, 2009; Nagaya et al. 2009). The effectiveness of this group of constructs will be tested by a student continuing this project after me. If the project would experience further problems with signal intensity, it would be reasonable to complement my studies with some other mRNA visualisation techniques.

For instance, a visualisation method has been developed in a separate laboratory and uses a probe based on a RNA binding protein domain - PUM-HD (pumilio homology domain). This probe is constructed to recognise a specific 8-base RNA sequence and detect targeted RNA with low background also in plant systems (Ozawa et al., 2007, Tilsner at al., 2009). Since it is possible to design multiple probes and target sequences, it would be also conceivable to use the components of this technique just like in the TRICK method. Instead of the coating proteins different PUM-HD probes would bind with specifically designed mRNA sequences that would be placed before and after a stop codon, instead of the PP7/MS2 stem loops. Interestingly, the authors report that they were able to capture single mRNA molecules by using only two 8-base recognition sequences. This would greatly decrease the size of any constructs, thus lessening the possible influence on all biological processes they partake in. Additionally, from a technical point of view, it would also make it easier to create and manipulate such vectors as well as abolish all the problems that could be caused by the many repeats present in my constructs. Naturally, it still remains a question whether the translation machinery can knock off those probes from the mRNA.

Nevertheless if we manage to fully establish the TRICK system in plants and successfully introduce it to the *ap1*/*cal* lines, which will allow us to produce many synchronised cells, we will create a powerful tool for translation control research in plant cells. This tool will allow us to monitor single translation events with high resolution and harvest large amounts of transcripts for further investigations.

4.2. Analysis of *CYCD x CDKA;1 / FBL17* double mutants

Second part of this thesis revolves around mitosis. Finding the major player among many cyclins that are active during the S-phase before mitosis was the prime objective. In this part of the project various cyclin mutants were crossed with *cdka;1+/-* and *fbl17+/-* mutants to asses if one of the combinations will show a stronger phenotype than single mutants. The way to determine the genetic interactions was the same as in Zhao et al. 2012, where other redundant regulators of the cell cycle, called *KRPs,* were investigated. It has been accomplished by comparing pollen distribution in double and single mutants of investigated genes, in this case - between *cdka;1+/-* and *krp*'s double mutant and *cdka;1+/-* alone. Distribution in *cdka;1+/-* mutants is divided between mutant - bicellular

and wildtype-like - tricellular pollen. When combined with another gene, it is expected to show a shift in the ratio between bicellular and tricellular pollen, in a direction depending on interaction type. If the investigated gene is an inhibitor of *CDKA;1*, a cross will result in a ratio shift in favor of tricellular pollen, thus rescuing *CDKA;1* phenotype. The abovementioned researchers managed to demonstrate that genes *KRP1* and *6* are able to do that, proving that among seven *KRP* genes those two are more influential than the rest of this gene family (Zhao et al., 2012).

This project was originally started by Barbara Gloecke, a former Ph.D. student, who analysed *in silico* which of the D-type cyclins have the highest expression in mature pollen grains. Among many preparatory experiments, she also performed a small scale counting experiment which showed that the *CYCD3;2* and *CYCD4;1* had slightly increased levels of bicellular pollen. This would indicate that they play a stronger role in interacting with the *CDKA;1* gene than other cyclins from the same group. After performing the same experiments on a different scale, the previously observed differences faded away, illustrating that the investigated genes do not show any stronger phenotypes than control lines. This result could indicate a couple of conclusions. Firstly, that there are other D-type cyclins, which were initially omitted in the *in silico* analysis and might be more important than the others. Secondly those D-type cyclins might be redundant and any stronger phenotype would be observed only when triple, quadruple etc. mutants are created. This kind of redundancy is well known among Arabidopsis cyclins (Wang et al., 2004). Finally, it might be the case that a completely different group of cyclins, for example A-type cyclins, plays a major role during the S-phase preceding mitosis. Cyclins from the A;3-group, just like D-type cyclins, are known to interact with the CDKA;1 during the G1/S transition and during the S-phase. At those same time points the A-type genes – *CYCA3;1*, *CYCA3;2* and *CYCA3;4* were also found to have upregulated expression (Menges et al 2005; van Leene et al., 2010)

4.3. Developmental potential of single celled pollen

At the beginning, the obtained data, consistent with previous analyses (Zhao et al., 2012) indicated that the double heterozygous mutant *cdka;1*$^{+/-}$ *fbl17*$^{+/-}$ produced approximately ten percent pollen at anthesis with only a single cell next to approximately 50 percent tri-cellular (wild-type like) and 40 percent pollen with two cells. Our second

mutant combination, the *e2fa*$^{-/-}$ *fbl17*$^{+/-}$ double mutant, produced even more, namely 25 percent of single celled pollen, which all together gave us a decent number of experimental samples to further investigate the nature and functionality of single celled pollen.

The reduction in cell number in pollen results from delayed/failed PMI and PMII of *cdka;1+/-* and *fbl17+/-* mutant microspores and pollen - at the time point when CDKA;1 protein levels, carried over from somatic cells, drop and the accumulation of CDK inhibitor proteins start due their reduced degradation in the absence of FBL17 (Nowack et al., 2006; Kim et al., 2008; Zhao et al., 2012).

First steps to understand the identity of single celled pollen were taken by Barbara Gloecke when she introgressed two reporters for generative/sperm cell fate into *cdka;1*$^{+/-}$ *fbl17*$^{+/-}$mutants. To this end, two histone reporters lines were used, i.e. *HTR10* (also called *MALE-GAMETE-SPECIFIC HISTONE H3* [*MGH3*]) and *HRT12* (also called *CENTROMERIC HISTONE H3* [*CENH3*]), which have been found to accumulate in the nucleus of the generative but not in the vegetative cell during pollen maturation (Fang and Spector, 2005; Okada et al., 2005; Ingouff et al., 2007; Aw et al., 2010).

Analysis of RFP (for PRO_{HTR10}*:HTR10:RFP*) and GFP (for PRO_{HTR12}*:HTR12:GFP*) fluorescence after staining the nuclear DNA with DAPI showed that single-celled pollen did not express these markers. Notably, *HTR12* accumulates in uni-cellular microspores in the wildtype (Chen et al., 2009; Ravi et al., 2011). It was also found, that HTR12 is also present in the uni-cellular microspores of *cdka;1*$^{+/-}$ *fbl17*$^{+/-}$mutants that is released after meiosis indicating that the single-celled pollen of *cdka;1*$^{+/-}$ *fbl17*$^{+/-}$mutants at anthesis is not just a developmentally delayed/arrested microspore.

To complement these studies, another reporter line, which indicates vegetative cell fate was developed by Barbara Gloecke. A promoter reporter line for *CSLD4*, previously found to be strongly expressed in vegetative cells after completion of PMI was generated (Bernal et al., 2008; Wang et al., 2011). Consistent with earlier analyses (Bernal et al., 2008; Wang et al., 2011), plants, which express *β-glucuronidase* (*GUS*) behind a 5' fragment of the *CSLD4* gene, demonstrated strong blue precipitates in pollen after incubation with the GUS substrate X-Gluc. When this line was introgressed to *cdka;1*$^{+/-}$ *fbl17*$^{+/-}$mutants, the single-celled pollen also showed strong GUS staining consistent with a vegetative fate of the single cell. These results are in accordance with earlier work, in which a chemically induced block of PMI gave rise to single-celled pollen grains in which

the vegetative-cell specific, tomato-derived *LAT52* promoter is active (Twell, 1992; Eady et al., 1995).

Another approach to validate the fate of single celled pollen was taken in Oslo by analyzing its chromatin state by immunostaining of H3K27me1. This revealed a pattern typical for vegetative cells, similar to the one seen in *cdka;1*$^{+/-}$ *fbl17*$^{+/-}$ single-celled pollen. Given that the sperm cells are enclosed within the vegetative cell of a pollen grain, a question still open is to what degree an interaction of the individual cells of the pollen is required for their differentiation and whether they collaborate in pollen functions, such as pollen tube growth and guidance. Evidence for a possibly intense communication between cells of the pollen came from the observation that the sperms in tobacco and other species are connected by a cytoplasmatic bridge (Yu and Russell, 1993). Moreover, sRNAs presumably originating from the vegetative cell can be detected in the sperm cells in Arabidopsis (Slotkin et al., 2009).

In the experiments I conducted, as part of the mitosis project, I discovered that the transposon repression of the enhancer trap line ET11075, which resides in an Athila3 transposon (Olmedo-Monfil et al., 2010), was released in the single-celled pollen of *e2fa*$^{-/-}$ *fbl17*$^{+/-}$ plants. This result was consistent with what Barbara Gloecke observed in her PhD thesis while using different lines (ET13889 – retrotransposon line and *cdka;1+/- fbl17+/-* plants). The transcriptional release, observed in both transposon enhancer trap lines, demonstrated that differentiation of the vegetative nucleus is independent of the presence of sperm cells. These results are also consistent with earlier work using the colchicine to block PMI or in mutants that interfere with pollen cytokinesis, such as *gem1* (Eady et al., 1995; Park et al., 1998). If the formative division is absent, differentiation of the vegetative cell proceeds independently of the presence of gametes or their precursors and progresses either autonomously promoted by an internal pace maker or is driven by an external signal. Regarding the first hypothesis, one of the most distinguishable differences between sperms and the vegetative cell is the chromatin condensation. However, it remains unclear whether it has any influence on the cell fate determination of either of those. Genes responsible for chromatin condensation might be the ones directly or indirectly influencing fate determination of the vegetative cell (Berger and Twell 2011). It might be possible that together with “transposon release” some other, not yet characterized, genes become active and are influencing pollen development (Hirsch and Springer, 2017). The vegetative cell’s special trait is that it is arrested in G_0 and lacks

the activity of genes responsible for forcing a cell into S-phase and sperm cells differentiation. Perhaps, while trying to investigate the network behind the G_0 arrest, it would be possible to discover the genes responsible for the vegetative cell fate (Berger and Twell 2011; Borg et al., 2011). The other possibility would be differentiation of the vegetative cell provoked by tapetum cells surrounding the microspores, either directly by delivering the components required for microspore growth or indirectly by signals created by maturation of those anther cells.

Another interesting extension of our experiments would be repeating them in other plant species. It is acknowledged that actually in most angiosperms the second mitotic division actually occurs after pollination in the growing pollen tube, not before. Furthermore, an entirely different case would occur in species like *Plumbago zeylanica* or *Brassica oleracea* when the second mitotic division is asymmetrical, just like the first one. There is a distinct polarization that is characterized by the volume, nucleus size and organelle types present in each sperm cell. In this case, the sperm cells are not completely separated but, on the contrary, one of them is directly connected with the vegetative nucleus via a long cytoplasmic appendix. Correspondingly, morphologically different sperm cells have different functions. For example in *P.zeylanica* one of the sperm cells is always targeting the egg cell and the other invariably fertilizes the central cell (Gou et al., 2009, McCue et al., 2011). Those variations in pollen development might be also present in the level of interaction between the sperms and the vegetative cell also in the case of pollen tube guidance. Moreover, it is crucial to mention that the level of connection between the sperms and the vegetative nucleus is different than in case of our model organism. Therefore, it would be highly interesting to see if we can obtain the same results in the species representing the developmental types presented above (McCue et al., 2011).

This comparison might allow us to discover if there are any important differences between sperm cells in Arabidopsis that have not yet been possible to observe because of their morphological identity. Various techniques that made it conceivable to isolate generative and/or sperm cells allowed us to obtain and compare characteristic transcriptomes from different species like *P.zeylanica* (Gou et al., 2009*), Nicotiana tabacum* (Wetering et al.,1992)*, Lilium longiflorum* (Okada et al.,2006) *or Zea Mays* (Engel et al., 2005). Being able to know if the transcriptomes from Arabidopsis sperm cells differ between each other and if indeed each of those sperms will fertilise a predestined female

gamete would allow us to further investigate double fertilisation in this model organism and improve our knowledge in that topic.

From a similar standpoint, with single celled mutants in our possession it would be interesting to investigate the transcriptome of such cells in comparison to wild-type. In a wild-type, a grain of pollen possesses a transcriptome which is showing expression of specific genes distinct to other tissues, with around seven thousand genes responsible mainly for signaling, vesicle transport and cytoskeleton formation (Becker et al., 2003; Honys and Twell, 2004; Pina et al., 2005). It is known that the vegetative cell is interacting with the sperm cells. From the example of *AHG3* gene (*ABA-HYPERSENSITIVE GERMINATION3*) we can deduce that the vegetative cell is providing transcripts, which are then translated into proteins in the sperm cells. The case of this gene illustrated that its promoter was transcriptionally active only in the vegetative cell but the AHG3:GFP fusion protein from the same promoter was observed in the sperm cells (Jiang et al. 2015). Therefore, it would be interesting to examine if our mutant behaves in the same way as in the WT situation and whether it is still trying to provide transcripts for the inexistent gametes or it recognises the fact that the pollen grain is lacking two cells (Borges et al 2008).

A different issue of pollen cell functionality that was addressed in this project was whether it can produce a pollen tube and guide it to the ovule without the presence of sperm cells. Previously, it has been shown that colchicine-treated single-cell pollen grains could germinate and grew a pollen tube *in vitro* (Eady et al., 1995). Matching these results, it was found by Barbara Gloecke that the *cdka;1*$^{+/-}$ *fbl17*$^{+/-}$ single-cell pollen could germinate a pollen tube. However, whether such a single-cell pollen tube can actually reach an ovule remained unclear. Subsequent step was to follow pollen tube growth and fertilisation by live cell imaging. In this instance, as a preparatory measure for subsequent live cell imaging, I had to establish the *FB037* reporter system in our single celled mutant lines (Borges et al., 2012), which contains both *PRO*$_{HTR10}$*:HTR10:eGFP and PRO*$_{ACT11}$*:H2B:mRFP* (Okada et al., 2005; Rotman et al., 2005; Ingouff et al., 2007). Those lines were then sent to Japan for final pollen tube germination and guidance experiments. Remarkably, results from Japan proved that the vegetative cell is sufficient for pollen tube guidance and discharge. The same conclusion was recently drawn from a completely independent experimental set using double mutants in *helix-loop-helix* (*bHLH*) transcription factor genes *DEFECTIVE REGION OF POLLEN 1* (*DROP1*), also known as *Lj-*

RHL1- LIKE (*LRL1*), and *DROP2* (*LRL2*) that also develop to approximately 40 percent single-celled pollen at anthesis (Zhang et al., 2017).

All these results correspond to the opposite approach taken by several laboratories which investigated pollen development by focusing on the vegetative cell instead of sperm cells. In 2014 Zhou and Meier proved that deactivating specific for the vegetative cell protein families, results in serious impairments of movement of the vegetative nucleus, which is influencing the pollen tube germination *ipso facto* decreasing the fertilisation rate (Zhou and Meier, 2014). As early as in 1996 Chen and McCormick presented data regarding the importance of vegetative cell in pollen tube germination and growth. Pollen grains of their mutants had an additional vegetative cell that was able to create a separate pollen tube (Chen and McCormick, 1996).

Taken together, my work and work of my colleagues, supported by work of other groups, demonstrates that the default state of microspores is a vegetative fate and the sperm cells are just a cargo for DNA which is transported by the vegetative cell.

5. Materials and methods

5.1. Plant work

5.1.1. Plant strains

Each line used in this thesis was acquired from Nothingam Arabidopsis Stock Center (NASC) unless stated otherwise. For all Gabi-Kat lines (GK) refer to Kleinboelting et. al. 2012 and for the SALK lines refer to Alonso et al. 2003. Single lines used in this thesis are represented in Table 1. Marker lines used in this thesis are shown in Table 2. Double lines used in this thesis are represented in Table 3. Table 4 shows transformed lines that were obtained during the time of this PhD.

Table 1 Single mutant lines used in this thesis

Gene	Line	Background ecotype
CDKA;1	SALK_106809	Col 0
FBL17	GABI-170E02	Col 0
E2Fa	GK-348E09	Col 0
CYCD1;1	GK-214D10	Col 0
CYCD2;1	Salk_049449	Col 0
CYCD4;1	GK344D08	Col 0
CYCD3;2	GK396C10	Col 0
tam-2	SAIL_505-C06	Col 0
rec8	SAIL_807B08	Col 0

Table 2 Marker lines used in this thesis

Line	Background ecotype	Source
ET13889	Ler	Slotkin et al.,2009
ET11075	Ler	Slotkin et al.,2009
ET11075 x e2fa-/- fbl17+/-	Ler	Crossed by W.Urban
FB037: $PRO_{MGH3:}$MGH3-GFP PRO_{ACTII}:H2B-RFP	Col 0	PI Jörg Becker, Ph.D (Instituto Gulbenkian De Ciência, Portugal)
FB037 x e2fa -/- fbl17+/-	Col 0	Crossed by W.Urban

Table 3 Double lines used in this thesis

Line	Background ecotype	Crossed by
cdka;1 +/-fbl17+/-	Col	XinAi Zhao, Ph.D
e2fa +/-fbl17+/-	Col	XinAi Zhao, Ph.D
cdka;1 +/- CYCD1;1	Col	Barbara Gloecke, Ph.D
cdka;1 +/- CYCD2;1	Col	Barbara Gloecke, Ph.D
cdka;1 +/- CYCD4;1	Col	Barbara Gloecke, Ph.D
cdka;1 +/- CYCD3;2	Col	Barbara Gloecke, Ph.D
fbl17+/- CYCD1;1	Col	Barbara Gloecke, Ph.D
fbl17+/- CYCD2;1	Col	Barbara Gloecke, Ph.D
fbl17+/- CYCD4;1	Col	Barbara Gloecke, Ph.D
fbl17+/- CYCD3;2	Col	Barbara Gloecke, Ph.D

Table 4 Transformed lines obtained in this thesis

Line	Background ecotype
TAM:GFP:MS2 pGW501	Col
REC8:GFP:MS2 pGW501	Col
$PRO_{CDKA:1}$:MCP:RFP pGW501	Col
$PRO_{UBIQUITIN}$:MCP:RFP pGW501	Col
TAM: PP7:MS2 pGW501	Col
REC8:PP7:MS2 pGW501	Col
$PRO_{CDKA;1}$:PCP:GFP:$PRO_{:CDKA;1}$:MCP:RFP (R4pGW501)	Col
$PRO_{CDKA;1}$:PCP:GFP:$PRO_{:UBIQUITIN}$:MCP:RFP (R4pGW501)	Col
$PRO_{UBIQUITIN}$:PCP:GFP:$PRO_{:CDKA;1}$:MCP:RFP (R4pGW501)	Col
$PRO_{UBIQUITIN}$:PCP:GFP:$PRO_{:UBIQUITIN}$:MCP:RFP (R4pGW501)	Col
$PRO_{CDKA;1}$:PCP:GFP:TER:$PRO_{:CDKA;1}$:MCP:RFP (pB7m34GW)	Col
$PRO_{CDKA;1}$:PCP:GFP:TER:$PRO_{:UBIQUITIN}$:MCP:RFP (pB7m34GW)	Col
$PRO_{UBIQUITIN}$:PCP:GFP:TER:$PRO_{:CDKA;1}$:MCP:RFP (pB7m34GW)	Col
$PRO_{UBIQUITIN}$:PCP:GFP:TER:PRO: $_{UBIQUITIN}$:MCP:RFP (pB7m34GW)	Col

5.1.2. Seed sterilization

In this thesis all seeds were sterilized before placing on a ½ Murashige&Skoog medium (check 5.1.3). The sterilization method was performed by using chlorine gas. I did it by inserting seeds in open 1.5ml Eppendorf tubes placed in a desiccator. Next to them I've located a beaker with either a mixture of 20ml H_2O and 20ml of bleach for overnight sterilization or 40ml of bleach for fast three hour sterilization. In both cases I was adding 2ml of HCL, then the dessicator was pressurized under the fume hood and left for a designated time period. After that time had passed it was opened and the seed were place under a dygestorium in order to evaporate the remaining gas from the tubes.

5.1.3. Growing conditions

After sterilizing the seed were placed on ½ Murashige & Skoog (1/2MS) with 0.5% sugar and 0.75% Phytoagar (Agar) concentration and pH of 5.8. In some cases also a proper antibiotic was added (check 5.1.4). After placing on plates the seeds were kept in darkness and 4°C for two days at least and transferred to light in long day conditions (18h day/6h night) at 20 °C. When the plants were big enough to develop 4 to 8 leaves they were transferred to soil and placed in growing chambers with short day conditions (12h day/12h night) at temperatures from 17 – 24 °C depending on the intended grow speed.

5.1.4. Antibiotics

Antibiotics or herbicides used for selection on ½ MS plates use 1 µl of stock solution per 1ml of medium.

Table 5 Antibiotics and herbicides used in this thesis

Antibiotics /herbicide	Stock
Kanamycin (kan)	50 mg/ml
Hygromycin (hyg)	15 mg/ml
Basta	10 mg/ml

5.1.5. Crossings

For crossings, flowers used as the female part of the cross were emasculated when anthers were still closed and far away from the pistil. The rest of neighboring flowers and/or siliques were cut off. After three days anthers from donor plants were used to pollinate the female part of the cross.

5.1.6. Alexander staining

This viability staining method (Table 6) was also used just for visualizing pollen grains under a light microscope. Anthers were placed in ~20µl of solution, covered with a cover slip and tapped on gently to release pollen grains.

Table 6 Alexander staining solution

Chemical	Concentration	Amount
Ethanol	96%	10ml
Malachite green	1% in 95% EtOH	1ml
Fuchsin acid	1% in H_2O	5ml
Orange G	1% in H_2O	0.5ml
Phenol	solid - 94.11g / mol	5g
Chloral hydrate	solid - 165.4g / mol	5g
Glacial acetic acid	60.05g / mol	2ml
Glycerol	92.09g / mol	25ml
Distilled H_2O		50ml

5.1.7. DAPI staining

For DAPI staining, pollen grains were lightly released into DAPI working solution afterwards incubated in 4 °C for 12 to 48 hours.

Table 7 DAPI staining solution

Chemical	Stock solution	Working solution	For 1ml
DAPI	250µg/ml	2.5 µg/ml	10 µl
Tween	10% in water	0.01%	1 µl
DMSO	100%	5%	50 µl
$NaHPO_4$ pH 7.2	1M	50mM	50 µl
H_2O	-	-	889 µl

5.1.8. Gus staining

For GUS Staining (100 mM NaP04, 10 mM EDTA, 0.1% Triton X-100, 1 mM X-Gluc, 1 mM Ferri-K, 1 mM Ferro-K) whole flowers were placed in the staining solution and vacuumed for 15-30 minutes and then incubated in room temperature in dark for 2 days. After that, the inflorescence was dissected and the anthers were placed in DAPI solution.

5.1.9. Microscopy

Fluorescent microscopy pictures were taken with the light microscope Axio lmager.Z1 with the AxioCamMR3 camera and the AxioVision software (Zeiss). For the confocal pictures they were obtained with Leica SP8.

5.2. DNA work

5.2.1. DNA isolation

DNA extraction was performed with the so called “magic buffer” (50 mM Tris-HCl pH 7.5, 300 mM NaCl, 300 mM sucrose). Sampled leaves were placed in deep well plates or 2ml Eppendorf tubes with metal beads and ~200 µl of magic buffer inside. Then they were shaked in a mixer mill at frequency of max 25/sec for 4 minutes, changing the orientation of blocks every 2 minutes. Afterwards the plates/tubes were centrifuged at 2,500 rpm for

3 minutes. In the last step 100 µl of supernatant was transfer to a 96 well plate and sealed with adhesive PCR film.

5.2.2. PCR

5.2.2.1. PCR mix

In my thesis I used two types of partially premade PCR master mixes. The first mix was used in the Genotyping experiments and the second one was used in cloning procedures (Table 8). Wild type specific primers used for genotyping are listed in Table 11. T-DNA specific primers used for genotyping are shown in Table 12. Primers used in cloning procedures are represented by Table 13. Primers used for sequencing of DNA are listed in Table 14.

Table 8 PCR master mix

Reagent	DreamTaq Green PCR master mix	Phusion High-Fidelity master Mix
H_2O	5,9 µl	22 µl
Primer 1 (10 µM)	0,3 µl	1 µl
Primer 2 (10 µM)	0,3 µl	1 µl
master mix	7,5 µl	25 µl
DNA	2 µl	1 µl

5.2.2.2. PCR programs and primers

For genotyping the PCR program presets there were always the same, only with small alternations depending on the primer set (Table 9). Regarding the PCR programs used for cloning procedures extension step was variable depending on the size of the fragment (Table 10). Primers used for genotyping are listed in Tables 11 and 12. The ones used in cloning procedures and for sequencing reactions are listed in tables 13 and 14 respectively.

Table 9 Genotyping PCR program

Step	Temp. in °C	Time	Go to
Initial denaturation	94	05:00	
Denaturation	94	00:30	
Annealing	56-60 (depending on primer pair)	00:30	
Extension	72	00:30	30x Step 2
Final extension	72	05:00	

Table 10 Cloning PCR program

Step	Temp. in °C	Time	Go to
Initial denaturation	94	05:00	
Denaturation	94	00:30	
Annealing	56-60 (depending on primer pair)	00:30	
Extension	72	20s per 1kb	30x Step 2
Final extension	72	05:00	

Table 11 Primers for "WT" Specific PCR

Plant line	Primer name	Sequence 5'-3'	Gene of interest
GK-214D10	Barb229_CYCD1;1_right	5'-TAACGATATGGATTTGTTTTGTGG-3'	*CYCD1;1*
	Barb230_CYCD1;1_left	5'-CGCTCCTGTTCTATCGTTTAC-3'	*CYCD1;1*
Salk_049449	Barb225_CYCD2;1_2right	5'-CACTAAAACCTCGATTTTCGACTC-3'	*CYCD2;1*
	Barb226_CYCD2;1_2left	5'-GAGACCACCCCAATAAACGA-3'	*CYCD2;1*
CDKA;1 (Salk)	108_SALK_106809LP	5'-TTTGGCTGGCTGCATTCCTTA-3'	*CDKA;1*
	14_N049-Intron_CDKA;1	5'-TGTACAAGCGAATAAAGACATTTGA-3'	*CDKA;1*
FBL17 (GK)	FBL17F	5'-GGTGGCATTCAATTTGCTAC-3'	*FBL17*
	FBL17R	5'-CAGATGTTCAAGGGATTACC-3'	*FBL17*
E2Fa (GK)	B256_GK-348E09_LP	5'-TTCCAGGTCTGTCTTTCCTATTTC-3'	*E2Fa*
	B257_GK-348E09_RP	5'-ATTCCTCCTACTTGCTCTTGC-3'	*E2Fa*

Table 11 Primers for "WT" Specific PCR - continued

Plant line	Primer name	Sequence 5'-3'	Gene of interest
GK344D08	Barb227_CYCD4;1_right	AAGGCTGCTTTATATGTGTGTGTG	*CYCD4;1*
	Barb228_CYCD4;1_left	CTTCAGGTTCTCCTCTAAACTCG	*CYCD4;1*
GK396C10	Barb233_CYCD3;2_right	TCTCATCTTTAACATTATAACTGGAC	*CYCD3;2*
	Barb234_CYCD3;2_left	GAAAGAGGCTTTAGATTGGGTTC	*CYCD3;2*

Table 12 Primers for "TDNA" Specific DNA

Plant line	Primer name	Sequence 5'-3'	Gene of interest
GK-214D10	Barb229_CYCD1;1_right	5'-TAACGATATGGATTTGTTTTGTGG-3'	*CYCD1;1*
	Gabi-KAT 8409	5'-ATATTGACCATCATACTCATTGC-3'	T-DNA left border
Salk_049449	Barb225_CYCD2;1_2right	5'-CACTAAAACCTCGATTTTCGACTC-3'	*CYCD2;1*
	Salk (S*) T-DNA2	5'-ATTTTGCCGATTTCGGAAC-3'	T-DNA left border
CDKA;1 (Salk)	108_SALK_106809LP	5'-TTTGGCTGGCTGCATTCCTTA-3'	*CDKA;1*
	Salk T-DNA Primer	5'-GCGTGGACCGCTTGCTGCAACTCTCTCAGG-3'	T-DNA left border
FBL17 (GK)	Gabi-KAT 8409	5'-ATATTGACCATCATACTCATTGC-3'	T-DNA left border
	FBL17R	5'-CAGATGTTCAAGGGATTACC-3'	F*BL17*
E2Fa (GK)	T-DNA_BORDER_GABIKAT	5'-CCCATTTGGACGTGAATGTAGACAC-3'	T-DNA left border
	B256_GK-348E09_LP	5'-TTCCAGGTCTGTCTTTCCTATTTC-3'	*E2Fa*
GK344D08	Barb227_CYCD4;1_right	AAGGCTGCTTTATATGTGTGTGTG	*CYCD4;1*
	Gabi-KAT 8409	5'-ATATTGACCATCATACTCATTGC-3'	*CYCD4;1*
GK396C10	Barb233_CYCD3;2_right	TCTCATCTTTAACATTATAACTGGAC	*CYCD3;2*
	Gabi-KAT 8474:	5'-ATAATAACGCTGCGGACATCTACATTTT-3'	*CYCD3;2*

Table 13 Primers for cloning

Primer name	Sequence 5'-3'
gTAM-AscI-F	TTGGCGCGCCTGATAGTGTTTCTGGATACGTTTTT
C6-Rec-AscI-F	TTGGCGCGCCGGAGGTGGACCCGGGTAAGGTTTGA
C7 - AtUBQ10-634pro-NotI-F	ATAAGAATGCGGCCGCGTCGACGAGTCAGTAATAAACG
C8-AtUBQ10-634pro-NotI-R	ATAAGAATGCGGCCGCCTGTTAATCAGAAAAACTCAG
C9 Ligation check pp7 R	TTCCAGCCTGATGTAGTCGG
C10 Ligation chceck TAM RFP F	TGCAGAAGAAAACACTCGGC
C11-MS2-AscI-R	TTGGCGCGCCTGGTTTGTCCAAACTCATCGGATCT
C12-PP7-PacI-F	CCTTAATTAAGCCTGGTCACTGTCTCCGTCGAC
C12a-PP7-PacI-F	CCTTAATTAACCTGGTCACTGTCTCCGTCGAC
C13-6Trick-PP7/MS2-PacI-F	CCTTAATTAACGAGTGATAAGGATCTCGGATCC
C13a-6Trick-PP7/MS2-PacI-F	CCTTAATTAAGCGAGTGATAAGGATCTCGGATCC
C14a-tagGFP-T-PacI-R	CCTTAATTAAGCTTGTACAGCTCGTCCATGCCGT
C14-REC8green-AscI-F	TTGGCGCGCCGGAGGTGGACCCGGGTAAGGTTT
C16- pENTRY2B -TAM-GFP-AscI-F	TTGGCGCGCCGGAGGTGGACCCGGGTGATAGTG
C17 - pENTRY2B - TAM-AscI-F	TTGGCGCGCCTGATAGTGTTTCTGGATACGTTT
C 18 - pENTRY2B -TAM-PacI-R	CCTTAATTAAGGAGGAAAAGCTCTTGCGGTAGTG
C 18a - pENTRY2B -TAM-PacI-R	CCTTAATTAAGAGGAAAAGCTCTTGCGGTAGTG
C19-AtCDKA1-2075pro-NotI-F	ATAAGAATGCGGCCGCGGGAAGATAGAAGGGAAGAGAGA
C20-AtCDKA1-2075pro-NotI-R	ATAAGAATGCGGCCGCCAATTCCTGAATAATAAAGCTGA
C21-pDONOR221-ASY3/ASY3+meGFP-AscI-F	TTGGCGCGCCGCAAAGTTGGCATTATAAGAAAGC
C22-pDONOR221-ASY3/ASY3+meGFP-Pac-R	CCTTAATTAAGTACAAGAAAGCTGGGTTCCCGGG
C25-pentry2b-Tam-del-f	TTAAGCCTGGTCACTGTCTCCG
C26-pentry2b-Tam-del-R	ATTAAGGAGGAAAAGCTCTTGCG
C27-pENTRY2B-Rec8only-AscI-F	TTGGCGCGCCGGTTTGATTTCTAAATTATAAAA
C28-pENTRY2B-Rec8only-PacI-r	CCTTAATTAAGTTACATGTTGGGTCCTCTTGCAA
C29 - attB4-Ubi-PCP	GGGGACAACTTTGTATAGAAAAGTTGTTGCGTCGACGAGTCAGTAATAAAC
C30-attB1r-GFP-PCP	GGGGACTGCTTTTTTGTACAAACTTGTTTACTTGTACAGCTCGTCCATGC
C31-attB1-terminator	GGGGACAAGTTTGTACAAAAAAGCAGGCTTTGAGCTCGAATTTCCCCGATCGTT
C32-attB2-terminator	GGGGACCACTTTGTACAAGAAAGCTGGGTTAGTTAGCTCACTCATTAGGCACC

Table 13 Primers for cloning continued

Primer name	Sequence 5'-3'
C33-attB2r-Ubi-MCP	GGGGACAGCTTTCTTGTACAAAGTGGTTGCGTCGACGAGTCAGTAATAAAC
C34-attB3-RFP-MCP	GGGGACAACTTTGTATAATAAAGTTGTTTACTTGTACAGCTCGTCCATGC
C35-attB1-MCP-Ubi	GGGGACAAGTTTGTACAAAAAAGCAGGCTTTGCGTCGACGAGTCAGTAATAAAC
C36a-attB2-MCP-Ubi	GGGGACCACTTTGTACAAGAAAGCTGGGTTTTACTTGTACAGCTCGTCCATGCC
H8-MCP-Ubi-R	TTAACGGCTAGCATATGGCGGCCTT
C65 - attB4-CDKA-PCP	GGGGACAACTTTGTATAGAAAAGTTGTTGCGGGAAGATAGAAGGGAAGAGA
C67-attB2r-CDKA-MCP	GGGGACAGCTTTCTTGTACAAAGTGGTTGCGGGAAGATAGAAGGGAAGAGA
C69-attB1-MCP-CDKA	GGGGACAAGTTTGTACAAAAAAGCAGGCTTTGCGGGAAGATAGAAGGGAAGAGA
C71 CDKA Promoter-R-beginning 169	CGGTTATCAGTTGTAAGTAAG
C72 CDKA Promoter-R-beginning 95	GGATATCAGTTCTTTTTCCTT
C76 deletion PCR REC 8 f	GACCCAGCTTTCTTGTACAAAG
C77 deletion PCR REC 8 r	CACCCTTTGTGTGATTCAGGGG
N874380U WT	GACTTGATGGATCCACAGC
N874380L WT	CAGAAATCCTCCACTTGCG
LB3Sail TDNA (works with N874380L)	TAGCATCTGAATTTCATAACCAATCTCGATACAC
C78 - Long TAM Primer	ATCGCGAGCCATTTCATTGAA
REC 8 REVERSE FROM SHINI	GGGCATGTTGGGTCCTCTTGCAAT

Table 14 Primers for sequencing

Primer name	Sequence 5'-3'
C37-Seq primer for Rec GFP	CAGATAAAACGAAAGGCCCAG
C38-Seq primer for Rec GFP	CTAACCAGAGGTGCAAATTAG
C39-Seq primer for Rec GFP	ACATTCGTCACGAGCATATAC
C40-Seq primer for Rec GFP	CACTCGAGGCGGCGCGTAGGT
C41-Seq primer for Rec GFP	TTCCTTTTGAGTAAGTTTCTC
C42-Seq primer for Rec GFP	CAGCTTCTTCTCCACGCAAAG
C43-Seq primer for Rec GFP	GGACGTAATTAAACACCAAAG
C44-Seq primer for Rec GFP	ACTAGATAAGCTCGATATCAT
C45-Seq primer for Rec GFP	ATTGCCTGAGAACGAAGAAGC

Table 14 Primers for sequencing - continued

Primer name	Sequence 5'-3'
C46-Seq primer for Rec GFP	CTGATGAGACTCTGCTCTTTT
C47- Seq primer for Rec GFP	ATGAACTCAAACCAAAATCAT
C48- Seq primer for Rec GFP	AGACCAACAATGAAACATATG
C49- Seq primer for Rec GFP	AGCAAGAAAGACAGCTACTTC
C50 - Seq primer for Rec GFP	GTCAAAGATGAAATTGTTTTC
C51 - Seq primer for Rec GFP	GATCATAGCTTGGTATTGTGG
C52 – Seq primer for Rec GFP	CATTTGGAAATGTCGATACAG
C53 - Seq primer for Rec GFP	AAAGGTAGAAGTTTTTAATTG
C54 - Seq primer for Rec GFP	ATGATTATTGTTTATATGTCC
C55 – Seq primer for Rec GFP	ATTATAAAAGATTCTGGTG
C56 - Seq primer for Rec GFP	CGGCGCGCGCGCCCACCCTTT
C57 – Seq primer for Rec GFP	CTTTTATAATTTAGAAATCAA
C58 – Seq primer for Rec GFP	CAAAAGGACCAAACAGAGGAA
C59 - Seq PP7/MCP - Upstream promoter	ATCGCTGTGATCGTCACTTGG
C60 - Seq PP7/MCP - 1200	TAACTCAACATTTAACATATG
C61 - Seq PP7/MCP - 800	GGCTTATGTTTAATATTTTTG
C62 - Seq PP7/MCP - 1600	AAACCATTTTCATCATAAAAG
C63 - Seq PP7/MCP - 2000	GAAATTCTGACTTGAACTTTG
C64 - Seq PP7/MCP - 2468	TGTTGTGTGCTGATATACAGC
C73 PP7 GFP seq for att site-end	AAGACCCCAACGAGAAGCGCG
C74 MCP RFP seq for att site end1 (Beginning of the RFP seq)	ATGGTGAGCAAGGGCGAGGAG
C75 MCP RFP seq for att site end2 (Middle of the RFP seq)	GACACCAGCCTCCAGGACGGC
S1-pENTR2B300bTAM-F	ATCCGCCGGGAGCGGATTTGAAC
S2-TAM-400-F	ACGGTGTTCGTGGTGGCTTGAGC
S3-TAM-1100-F	GCTCTAAAACAGAGTTAGAGCAC
S4-TAM-1800-F	ATATATCAGAATCACAACTTTTG
S5-TAM-2500-F	GAACTTAGCCAAGACTCGAACCT
S6-TAM-3200-F	TCTGAATTGTCAAAGTTGAAATT
S7-TAM-3900-F	CTACTTGAAGTTCGAATTAACAA
S8-TAM-4500-F	GATGTGGTTGCAATCAGAAAGAA
S9-TAM-5200-F	CACAACATCGAGGACGGCAGCGT
S10-TAM-5100-F	GATCTCTCGACAGATCCTACCTG
S11-TAM-5500-F	ATCTCTCGAGTGATAAGGATCCT
H2-seq-TAM-12TRICK-R	TCCCAGAAACTATCAACATTCTA

5.2.3. Gel electrophoresis

Agarose gels were typically prepared with TBE buffer in a final concentration of 1%. I was usually using a 1kb plus DNA ladder from Ferments Thermos Scientific. The amount of PCR reaction placed in wells varied from 7,5 µl to 50 µl.

5.3. Cloning work

5.3.1. Growing conditions for bacteria

The LB (Luria-Bertani) Medium was prepared by combining all of the reagents listed in Table 15 until the soluble components are dissolved. Afterword the pH was adjusted so in the end it would equal 7.0. At the end everything was sterilized by autoclaving.

Table 15 LB medium reagents

Reagent	Amount
H_2O	950ml
Tryptone	10g
NACL	10g
Yeast extract	5g

5.3.2. BP reaction

For the BP reactions 100ng of donor vector was used together with from 50 to 100ng of fragment, 4 to 4,5 µl of TE buffer and 0.5 to 1 µl of BP clonase. At the end the sample was incubated overnight in 25°C

5.3.3. LR reaction

DNA concentrations for the LR reactions were calculated accordingly to the equation:

$$ng=(xfmoles)(N)(\frac{660fg}{fmoles})(\frac{1ng}{10^6fg})$$

Where x is the number of fmoles and N is the size of the fragment in bp, for all, the destination vectors and all 3 donors. Additionally 4 to 4,5 µl of TE buffer and 0.5 to 1 µl of LR clonase added to the mix . At the end the sample was incubated overnight in 25°C

5.3.4. Enzyme restriction

All enzymes, used in this thesis and their incubation/inactivation temperatures and times are listed in Table 17, the reaction ratios are viewed in Table 16 .

Table 16 Reagent ratios for enzyme restriction

Reagent	Reaction mix
H_2O	up to 10 µl
DNA	1ng
Buffer	2 µl
Enzyme	0,2 - 0,3 µl

Table 17 Enzymes used in this thesis

Enzyme name	Incubation	Inactivation	Buffer	Company
FastDigestPACI	37°C for 1h	65°C for 10 min	10xFastDigest	Thermo Fisher Scientific
FastDigestASCI (SGSI)	37°C for 1h	65°C for 20 min	10xFastDigest	Thermo Fisher Scientific
FastDigestEcoRI	37°C for 1h	80°C for 5 min	10xFastDigest	Thermo Fisher Scientific
FastDigestBamHI	37°C for 1h	80°C for 5 min	10xFastDigest	Thermo Fisher Scientific
KpnI	37°C for 1h	no	1XNEBuffer1.1	New England Biolabs

Table 17 Enzymes used in this thesis - continued

Enzyme name	Incubation	Inactivation	Buffer	Company
XmnI	37°C for 1h	65°C for 20 min	1XCutSmart	New England Biolabs
FastDigestXbaI	37°C for 1h	no	10xFastDigest	Thermo Fisher Scientific
FastDigestNotI	37°C for 1h	80°C for 5 min	10xFastDigest	Thermo Fisher Scientific
FastDigestNcoI	37°C for 1h	65°C for 15 min	10xFastDigest	Thermo Fisher Scientific
BstAPI	60°C for 1h	80°C for 20 min	1XCutSmart	New England Biolabs

5.3.5. Alkaline phosphatase (AP) reaction

For this reaction, in the case of this thesis, two mixes were prepared. Mix I with the alkaline phosphatase (Table 18) and mix II for the promoter sequence (Table19). In the first mix the NotI site was prevented from self-ligation by the AP. In the second one a fragment was created with the same enzyme. The incubation for both mixes was for 1 hour in 37 °C. At the end both pieces were ligated and the direction of the promotor was checked.

Table 18 Mix I with AP

Reagent	Amount
H_2O	38 µl
Plasmid	1-2 µg
10x Buffer	5 µl
FastDigestNotI	1 µl
AP (Fast)	2 µl

Table 19 Mix II for the promoter sequence

Reagents	Amount
H_2O	up to 50 µl
DNA	40 µl (whole tube)
10x Buffer	2 µl
FastDigestNotI	1 µl

5.3.6. Klenow-Fragment reaction

For the Klenow reaction I used the mix from Table 20, incubation was 10 minutes long in 37 °C. After that the Klenow enzyme needed to be inactivated in 75°C for 10 min.

Table 20 Klenow reaction mix

Reagents	Amount
H_2O	20 µl
DNA	10-15 µl
Klenow Buffer	2 µl
2 mM dNTP-Mix	0,5 µl
Klenow fragment	0,5 µl

5.3.7. Ligation

For the ligation process the "ligation mix" was used in amount of 5 µl. Ligated fragments were used in concentration of 50ng each (vector and fragment) and everything was filled up with water up to 10 µl. Afterwards everything was incubated in 16°C overnight.

5.3.8. Plasmid extraction

Extracting the plasmids starts from collecting the bacteria from the LB medium into 2ml Eppendorf tubes, centrifuging at 8000 rpm for 1 min and discarding the supernatant. Afterwards 200 µl of PD1 with RNA-ase was added and everything was resuspended by

vortexing. Later 200 µl of the next buffer (PD2) and mixed in hand, next the last PD buffer was added(PD3 – 300 µl), again everything was mixed in hand (one tube at a time) and centrifuged for 10 min at 14000 rpm. In the next part of the protocol the supernatant was transferred to the columns centrifuged for 30s at 8000rpm, then 400 µl of W1 buffer was added and the columns were centrifuged for 30s at 10000rpm. Afterwards 600 µl of washing buffer was added and the tubes were centrifuged like last time, everything was then discarded and the membranes were dried by centrifuging for 2 min at 14000rpm. In the last steps the tubes were opened so the ethanol could evaporate, then 50 µl of warm ddH_2O was added and everything was centrifuged at 13500 rpm for 2 min.

5.3.9. Gel extraction

Gel extraction in my thesis was perform in accordance to NucleoSpin Gel and PCR Clean up protocol. This clean up started with extracting the band of interest from a agarose gel and placing it in tube with the NTI buffer in order to incubate it at 50°C until the gel melts away. The resulting mix was loaded on cleanup columns and centrifuged for 30s at 11000 x g. Afterwards the silica membrane of the column was twice washed with 700 µl of NT3 buffer and centrifuged again. Later the membrane was dried by 1 min centrifugation at 11000 x g. In the last step the DNA from the membrane was eluted in hot water by last centrifugation step (1 min at 13000 x g).

5.3.10. E.coli transformation

An adequate amount of vector (1,5-3 µl) was added to *E.coli* competent cells (TOP10 from Invitrogen). When bacteria were thawed they were mixed in hand and kept in ice for 30 minutes. Afterwards they were heat shocked at 42°C for 1 min and placed in ice for 5 min. Next 1ml of LB medium was added and everything was incubated in 37 °C for 1 hour. Subsequently the tubes were centrifuged at 8000 rpm for 1 min, the supernatants were discarded, pellet resuspended and everything was spread on LB plates with proper antibiotic.

5.3.11. Agrobacterium transformation

1µg of plasmid was added to frozen *Agrobacterium tumefaciens* cells (GV3101 (pMP90)). I was Afterwards it the mix was incubated at 37 °C for 5 min, then after 2 min mixed gently. Later incubated for about 15-30 min on ice. Then 1 ml of LB medium was added and kept at 28 °C for 1 to 3 hours. In the meantime LB-agar plates were prepared with appropriate antibiotics, for example spectinomycin (100 µg/ µl) for the destination vector and gentamycin and rifampicin (working concentration) for Agrobacterium. After the incubation in 28 °C was done the tubes needed to be centrifuged at 8,000 rpm for 1 min. Then the pellet was resuspend in 100 µl of LB medium. Finally everything was plated and a clone was picked up after 2 days of incubation in 28 °C.

5.3.12. Plant transformation

E.coli were incubated (28°C) in 10-15ml of LB medium, with two kinds of antibiotic (Gentamicin and bacterial resistance antibiotic). After two days of incubation liquid cultures were centrifuged for 5 min at 4000 rpm and the supernatant was discarded. The pellet was then resuspended in transformation solution (5% sucrose, 0,02% Silvet L77). Later the pellets were resuspended and dropped on flowers with a pipette. Next the plants were kept in dark overnight.

6. Literature

Alonso, J. M., Stepanova, A. N., Leisse, T. J., Kim, C. J., Chen, H., Shinn, P., ... & Gadrinab, C. (2003). Genome-wide insertional mutagenesis of Arabidopsis thaliana. *Science*, *301*(5633), 653-657.

Andreuzza, S., Nishal, B., Singh, A., & Siddiqi, I. (2015). The chromatin protein DUET/MMD1 controls expression of the meiotic gene TDM1 during male meiosis in Arabidopsis. *PLoS genetics*, *11*(9), e1005396.

Aw, S. J., Hamamura, Y., Chen, Z., Schnittger, A. and Berger, F. (2010). Sperm entry is sufficient to trigger division of the central cell but the paternal genome is required for endosperm development in Arabidopsis. Development 137, 2683-2690.

Barakate, A., Higgins, J. D., Vivera, S., Stephens, J., Perry, R. M., Ramsay, L., ... & Armstrong, S. J. (2014). The synaptonemal complex protein ZYP1 is required for imposition of meiotic crossovers in barley. *The Plant Cell*, tpc-113.

Barbosa, C., Peixeiro, I., & Romão, L. (2013). Gene expression regulation by upstream open reading frames and human disease. *PLoS genetics*, *9*(8), e1003529.

Becker, J. D., Boavida, L. C., Carneiro, J., Haury, M., & Feijó, J. A. (2003). Transcriptional profiling of Arabidopsis tissues reveals the unique characteristics of the pollen transcriptome. *Plant physiology*, *133*(2), 713-725.

Berger, F., & Twell, D. (2011). Germline specification and function in plants. *Annual review of plant biology*, *62*, 461-484.

Bernal A. J., Yoo C.-M., Mutwil M., Jensen J. K., Hou G., Blaukopf C., Sørensen I., Blancaflor E. B., Scheller H. V. and Willats W. G. (2008). Functional analysis of the cellulose synthase-like genes CSLD1, CSLD2, and CSLD4 in tip-growing Arabidopsis cells. *Plant Physiol.* 148, 1238-1253. 10.1104/pp.108.121939

Biedermann, B., Wright, J., Senften, M., Kalchhauser, I., Sarathy, G., Lee, M. H., & Ciosk, R. (2009). Translational repression of cyclin E prevents precocious mitosis and embryonic gene activation during C. elegans meiosis. *Developmental cell*, *17*(3), 355-364.

Borg M., Brownfield L. and Twell D. (2009). Male gametophyte development: a molecular perspective. *J. Exp. Bot.* 60, 1465-1478. 10.1093/jxb/ern355

Borg, M., Brownfield, L., Khatab, H., Sidorova, A., Lingaya, M., & Twell, D. (2011). The R2R3 MYB transcription factor DUO1 activates a male germline-specific regulon essential for sperm cell differentiation in Arabidopsis. *The Plant Cell*, tpc-110.

Borges, F., Gardner, R., Lopes, T., Calarco, J. P., Boavida, L. C., Slotkin, R. K., ... & Becker, J. D. (2012). FACS-based purification of Arabidopsis microspores, sperm cells and vegetative nuclei. *Plant Methods*, *8*(1), 44.

Borges, F., Gardner, R., Lopes, T., Calarco, J. P., Boavida, L. C., Slotkin, R. K., ... & Becker, J. D. (2012). FACS-based purification of Arabidopsis microspores, sperm cells and vegetative nuclei. *Plant Methods*, *8*(1), 44.

Borges, F., Gardner, R., Lopes, T., Calarco, J. P., Boavida, L. C., Slotkin, R. K., ... & Becker, J. D. (2012). FACS-based purification of Arabidopsis microspores, sperm cells and vegetative nuclei. *Plant Methods*, *8*(1), 44.

Borges, F., Gomes, G., Gardner, R., Moreno, N., McCormick, S., Feijó, J. A., & Becker, J. D. (2008). Comparative transcriptomics of Arabidopsis sperm cells. *Plant Physiology*, *148*(2), 1168-1181.

Browning, D. F., & Busby, S. J. (2004). The regulation of bacterial transcription initiation. *Nature Reviews Microbiology*, *2*(1), 57.

Cai, X., Dong, F., Edelmann, R. E., & Makaroff, C. A. (2003). The Arabidopsis SYN1 cohesin protein is required for sister chromatid arm cohesion and homologous chromosome pairing. *Journal of Cell Science*, *116*(14), 2999-3007.

Calarco, J. P., Borges, F., Donoghue, M. T., Van Ex, F., Jullien, P. E., Lopes, T., Gardner, R., Berger, F., Feijó, J. A., Becker, J. D. et al. (2012). Reprogramming of DNA methylation in pollen guides epigenetic inheritance via small RNA. Cell 151, 194-205.

Campalans, A., Kondorosi, A., & Crespi, M. (2004). Enod40, a short open reading frame–containing mRNA, induces cytoplasmic localization of a nuclear RNA binding protein in Medicago truncatula. *The Plant Cell*, *16*(4), 1047-1059.

Cardarelli, M., & Cecchetti, V. (2014). Auxin polar transport in stamen formation and development: how many actors?. *Frontiers in plant science*, *5*, 333.

Carlile, T. M., & Amon, A. (2008). Meiosis I is established through division-specific translational control of a cyclin. *Cell*, *133*(2), 280-291.

Carswell, S., & Alwine, J. C. (1989). Efficiency of utilization of the simian virus 40 late polyadenylation site: effects of upstream sequences. *Molecular and Cellular Biology*, *9*(10), 4248–4258.

Chen, Y. C., & McCormick, S. (1996). sidecar pollen, an Arabidopsis thaliana male gametophytic mutant with aberrant cell divisions during pollen development. *Development*, *122*(10), 3243-3253.

Cheung, A. Y. (1995). Pollen-pistil interactions in compatible pollination. *Proceedings of the National Academy of Sciences*, *92*(8), 3077-3080.

Christensen, N. M., Oparka, K. J., & Tilsner, J. (2010). Advances in imaging RNA in plants. *Trends in plant science*, *15*(4), 196-203.

Cifuentes, M., Jolivet, S., Cromer, L., Harashima, H., Bulankova, P., Renne, C., ... & Schnittger, A. (2016). TDM1 regulation determines the number of meiotic divisions. *PLoS genetics*, *12*(2), e1005856.

Criqui, M. C., & Genschik, P. (2002). Mitosis in plants: how far we have come at the molecular level?. *Current opinion in plant biology*, *5*(6), 487-493.

Cromer, L., Heyman, J., Touati, S., Harashima, H., Araou, E., Girard, C., ... & Mercier, R. (2012). OSD1 promotes meiotic progression via APC/C inhibition and forms a regulatory network with TDM and CYCA1; 2/TAM. *PLoS genetics*, *8*(7), e1002865.

da Costa-Nunes, J. A., Bhatt, A. M., O'shea, S., West, C. E., Bray, C. M., Grossniklaus, U., & Dickinson, H. G. (2006). Characterization of the three Arabidopsis thaliana RAD21 cohesins reveals differential responses to ionizing radiation. *Journal of experimental botany*, *57*(4), 971-983.

De Muyt, A., Mercier, R., Mezard, C., & Grelon, M. (2009). Meiotic recombination and crossovers in plants. In *Meiosis* (Vol. 5, pp. 14-25). Karger Publishers.

d'Erfurth, I., Cromer, L., Jolivet, S., Girard, C., Horlow, C., Sun, Y., ... & Mercier, R. (2010). The cyclin-A CYCA1; 2/TAM is required for the meiosis I to meiosis II transition and cooperates with OSD1 for the prophase to first meiotic division transition. PLoS genetics, 6(6), e1000989.

Desvoyes, B., de Mendoza, A., Ruiz-Trillo, I., & Gutierrez, C. (2013). Novel roles of plant RETINOBLASTOMA-RELATED (RBR) protein in cell proliferation and asymmetric cell division. *Journal of experimental botany*, *65*(10), 2657-2666.

Dick, F. A., & Rubin, S. M. (2013). Molecular mechanisms underlying RB protein function. *Nature reviews Molecular cell biology*, *14*(5), 297.

Dong, J., Kim, S. T., & Lord, E. M. (2005). Plantacyanin plays a role in reproduction in Arabidopsis. *Plant Physiology*, *138*(2), 778-789.

Dresselhaus, T., & Franklin-Tong, N. (2013). Male–female crosstalk during pollen germination, tube growth and guidance, and double fertilization. *Molecular plant*, *6*(4), 1018-1036.

Eady, C., Lindsey, K., & Twell, D. (1995). The significance of microspore division and division symmetry for vegetative cell-specific transcription and generative cell differentiation. *The Plant Cell*, *7*(1), 65-74.

Edlinger, B., & Schlögelhofer, P. (2011). Have a break: determinants of meiotic DNA double strand break (DSB) formation and processing in plants. *Journal of experimental botany*, *62*(5), 1545-1563.

Engel, M. L., Holmes-Davis, R., & McCormick, S. (2005). Green sperm. Identification of male gamete promoters in Arabidopsis. *Plant physiology*, *138*(4), 2124-2133.

Fang, Y., & Spector, D. L. (2005). Centromere positioning and dynamics in living Arabidopsis plants. *Molecular biology of the cell*, *16*(12), 5710-5718.

Fang, Y., & Spector, D. L. (2007). Identification of nuclear dicing bodies containing proteins for microRNA biogenesis in living Arabidopsis plants. *Current Biology*, *17*(9), 818-823.

Ferdous, M., Higgins, J. D., Osman, K., Lambing, C., Roitinger, E., Mechtler, K., ... & Franklin, F. C. H. (2012). Inter-homolog crossing-over and synapsis in Arabidopsis meiosis are dependent on the chromosome axis protein AtASY3. PLoS genetics, 8(2), e1002507.

Freire, M. A. (2005). Translation initiation factor (iso) 4E interacts with BTF3, the β subunit of the nascent polypeptide-associated complex. *Gene*, *345*(2), 271-277.

Freire, M. A., Tourneur, C., Granier, F., Camonis, J., El Amrani, A., Browning, K. S., & Robaglia, C. (2000). Plant lipoxygenase 2 is a translation initiation factor-4E-binding protein. *Plant molecular biology*, *44*(2), 129-140.

Fujioka, Y., Utsumi, M., Ohba, Y., & Watanabe, Y. (2007). Location of a possible miRNA processing site in SmD3/SmB nuclear bodies in Arabidopsis. *Plant and cell physiology*, *48*(9), 1243-1253.

Gebauer, F., & Hentze, M. W. (2004). Molecular mechanisms of translational control. *Nature reviews Molecular cell biology*, *5*(10), nrm1488.

Glöckle, B., Urban, W. J., Nagahara, S., Andersen, E. D., Higashiyama, T., Grini, P. E., & Schnittger, A. (2017). Pollen differentiation as well as pollen tube guidance and discharge are independent of the presence of gametes. Development, dev-152645.

Godiska, R., Mead, D., Dhodda, V., Wu, C., Hochstein, R., Karsi, A., ... & Ravin, N. (2009). Linear plasmid vector for cloning of repetitive or unstable sequences in Escherichia coli. *Nucleic acids research*, *38*(6), e88-e88.

Gou, X., Yuan, T., Wei, X., & Russell, S. D. (2009). Gene expression in the dimorphic sperm cells of Plumbago zeylanica: transcript profiling, diversity, and relationship to cell type. *The Plant Journal*, *60*(1), 33-47.

Grebnev, G., Ntefidou, M., & Kost, B. (2017). Secretion and endocytosis in pollen tubes: models of tip growth in the spot light. *Frontiers in Plant Science*, *8*, 154.

Gurskaya, N. G., Pereverzev, A. P., Staroverov, D. B., Markina, N. M., & Lukyanov, K. A. (2016). Analysis of nonsense-mediated mRNA decay at the single-cell level using two fluorescent proteins. In *Methods in enzymology* (Vol. 572, pp. 291-314). Academic Press.

Gusti, A., Baumberger, N., Nowack, M., Pusch, S., Eisler, H., Potuschak, T., ... & Genschik, P. (2009). The Arabidopsis thaliana F-box protein FBL17 is essential for progression through the second mitosis during pollen development. *PloS one*, *4*(3), e4780.

Gutzat, R., Borghi, L., & Gruissem, W. (2012). Emerging roles of RETINOBLASTOMA-RELATED proteins in evolution and plant development. *Trends in plant science*, *17*(3), 139-148.

Hamamura, Y., Saito, C., Awai, C., Kurihara, D., Miyawaki, A., Nakagawa, T., ... & Higashiyama, T. (2011). Live-cell imaging reveals the dynamics of two sperm cells during double fertilization in Arabidopsis thaliana. *Current Biology*, *21*(6), 497-502.

Hanahan, D. (1983). Studies on transformation of Escherichia coli with plasmids. *Journal of molecular biology*, *166*(4), 557-580.

Harashima, H., & Sugimoto, K. (2016). Integration of developmental and environmental signals into cell proliferation and differentiation through RETINOBLASTOMA-RELATED 1. *Current opinion in plant biology*, *29*, 95-103.

Harashima, H., & Schnittger, A. (2012). Robust reconstitution of active cell-cycle control complexes from co-expressed proteins in bacteria. *Plant Methods*, *8*(1), 23.

Hartung, F., & Puchta, H. (2000). Molecular characterisation of two paralogous SPO11 homologues in Arabidopsis thaliana. *Nucleic acids research*, *28*(7), 1548-1554.

Harvey, S. E., & Cheng, C. (2016). Methods for characterization of alternative RNA splicing. In *Long Non-Coding RNAs* (pp. 229-241). Humana Press, New York, NY.

He, Y., Wang, C., Higgins, J., Yu, J., Zong, J., Lu, P., ... & Liang, W. (2016). MEIOTIC F-BOX is essential for male meiotic DNA double strand break repair in rice. *The Plant Cell*, tpc-00108.

Higgins, J. D., Sanchez-Moran, E., Armstrong, S. J., Jones, G. H., & Franklin, F. C. H. (2005). The Arabidopsis synaptonemal complex protein ZYP1 is required for chromosome synapsis and normal fidelity of crossing over. *Genes & development*, *19*(20), 2488-250

Higgins, J. D., Vignard, J., Mercier, R., Pugh, A. G., Franklin, F. C. H., & Jones, G. H. (2008). AtMSH5 partners AtMSH4 in the class I meiotic crossover pathway in Arabidopsis thaliana, but is not required for synapsis. *The Plant Journal*, *55*(1), 28-39.

Hirsch, C. D., & Springer, N. M. (2017). Transposable element influences on gene expression in plants. *Biochimica et Biophysica Acta (BBA)-Gene Regulatory Mechanisms*, *1860*(1), 157-165.

Honys, D., & Twell, D. (2004). Transcriptome analysis of haploid male gametophyte development in Arabidopsis. *Genome biology*, *5*(11), R85.

Hou, Y., Guo, X., Cyprys, P., Zhang, Y., Bleckmann, A., Cai, L., ... & Dong, J. (2016). Maternal ENODLs are required for pollen tube reception in Arabidopsis. *Current Biology*, *26*(17), 2343-2350.

Hsieh, J., & Fire, A. (2000). Recognition and silencing of repeated DNA. *Annual review of genetics*, *34*(1), 187-204.

Ibarra, C. A., Feng, X., Schoft, V. K., Hsieh, T. F., Uzawa, R., Rodrigues, J. A., ... & Rojas, D. (2012). Active DNA demethylation in plant companion cells reinforces transposon methylation in gametes. *Science*, *337*(6100), 1360-1364.

Ingelbrecht, I. L., Herman, L. M., Dekeyser, R. A., Van Montagu, M. C., & Depicker, A. G. (1989). Different 3'end regions strongly influence the level of gene expression in plant cells. *The Plant Cell*, *1*(7), 671-680.

Ingouff, M., Hamamura, Y., Gourgues, M., Higashiyama, T., & Berger, F. (2007). Distinct dynamics of HISTONE3 variants between the two fertilization products in plants. *Current Biology*, *17*(12), 1032-1037.

Jiang, H., Yi, J., Boavida, L. C., Chen, Y., Becker, J. D., Köhler, C., & McCormick, S. (2015). Intercellular communication in Arabidopsis thaliana pollen discovered via AHG3 transcript movement from the vegetative cell to sperm. *Proceedings of the National Academy of Sciences*, *112*(43), 13378-13383.

Johnson, S. A., & McCormick, S. (2001). Pollen germinates precociously in the anthers of raring-to-go, an Arabidopsis gametophytic mutant. *Plant Physiology*, *126*(2), 685-695.

Kalyna, M., Simpson, C. G., Syed, N. H., Lewandowska, D., Marquez, Y., Kusenda, B., ... & Dinh, H. Q. (2011). Alternative splicing and nonsense-mediated decay modulate expression of important regulatory genes in Arabidopsis. *Nucleic acids research*, *40*(6), 2454-2469.

Kim, H. J., Oh, S. A., Brownfield, L., Hong, S. H., Ryu, H., Hwang, I., ... & Nam, H. G. (2008). Control of plant germline proliferation by SCF FBL17 degradation of cell cycle inhibitors. *Nature*, *455*(7216), 1134.

Kleinboelting, N., Huep, G., Kloetgen, A., Viehoever, P., & Weisshaar, B. (2011). GABI-Kat SimpleSearch: new features of the Arabidopsis thaliana T-DNA mutant database. *Nucleic acids research*, *40*(D1), D1211-D1215.

Kronja, I., & Orr-Weaver, T. L. (2011). Translational regulation of the cell cycle: when, where, how and why?. *Phil. Trans. R. Soc. B*, *366*(1584), 3638-3652.

Kuwabara, A., & Gruissem, W. (2014). Arabidopsis Retinoblastoma-related and Polycomb group proteins: cooperation during plant cell differentiation and development. *Journal of experimental botany*, *65*(10), 2667-2676.

Lai, M. C., Chang, W. C., Shieh, S. Y., & Tarn, W. Y. (2010). DDX3 regulates cell growth through translational control of cyclin E1. *Molecular and cellular biology*, *30*(22), 5444-5453.

Lam, W. S., Yang, X., & Makaroff, C. A. (2005). Characterization of Arabidopsis thaliana SMC1 and SMC3: evidence that AtSMC3 may function beyond chromosome cohesion. *Journal of cell science*, *118*(14), 3037-3048.

Lázaro-Mixteco, P. E., & Dinkova, T. D. (2012). Identification of proteins from Cap-binding complexes by mass spectrometry during maize (Zea mays L.) germination. *Journal of the Mexican Chemical Society*, *56*(1), 36-50.

Lu, X., Liu, X., An, L., Zhang, W., Sun, J., Pei, H., ... & Zhang, C. (2008). The Arabidopsis MutS homolog AtMSH5 is required for normal meiosis. *Cell research*, *18*(5), 589.

Martínez, G., Panda, K., Köhler, C., & Slotkin, R. K. (2016). Silencing in sperm cells is directed by RNA movement from the surrounding nurse cell. *Nature plants*, *2*(4), 16030.

McCormick, S. (2004). Control of male gametophyte development. *The Plant Cell*, *16*(suppl 1), S142-S153.

McCue, A. D., Cresti, M., Feijó, J. A., & Slotkin, R. K. (2011). Cytoplasmic connection of sperm cells to the pollen vegetative cell nucleus: potential roles of the male germ unit revisited. *Journal of experimental botany*, *62*(5), 1621-1631.

Menges, M., De Jager, S. M., Gruissem, W., & Murray, J. A. (2005). Global analysis of the core cell cycle regulators of Arabidopsis identifies novel genes, reveals multiple and highly specific profiles of expression and provides a coherent model for plant cell cycle control. *The Plant Journal*, *41*(4), 546-566.

Mercier, R., Mézard, C., Jenczewski, E., Macaisne, N., & Grelon, M. (2015). The molecular biology of meiosis in plants. *Annual review of plant biology*, *66*, 297-327.

Muench, D. G., Zhang, C., & Dahodwala, M. (2012). Control of cytoplasmic translation in plants. *Wiley Interdisciplinary Reviews: RNA*, *3*(2), 178-194.

Nagaya, S., Kawamura, K., Shinmyo, A., & Kato, K. (2009). The HSP terminator of Arabidopsis thaliana increases gene expression in plant cells. *Plant and cell physiology*, *51*(2), 328-332.

Noir, S., Marrocco, K., Masoud, K., Thomann, A., Gusti, A., Bitrian, M., ... & Genschik, P. (2015). The control of Arabidopsis thaliana growth by cell proliferation and endoreplication requires the F-box protein FBL17. *The Plant Cell*, tpc-114.

Nowack, M. K., Grini, P. E., Jakoby, M. J., Lafos, M., Koncz, C., & Schnittger, A. (2006). A positive signal from the fertilization of the egg cell sets off endosperm proliferation in angiosperm embryogenesis. *Nature genetics*, *38*(1), 63.

Okada, T., Bhalla, P. L., & Singh, M. B. (2006). Expressed sequence tag analysis of Lilium longiflorum generative cells. *Plant and Cell Physiology*, *47*(6), 698-705.

Okada, T., Endo, M., Singh, M. B., & Bhalla, P. L. (2005). Analysis of the histone H3 gene family in Arabidopsis and identification of the male-gamete-specific variant AtMGH3. *The Plant Journal*, *44*(4), 557-568.

Olmedo-Monfil, V., Durán-Figueroa, N., Arteaga-Vázquez, M., Demesa-Arévalo, E., Autran, D., Grimanelli, D., ... & Vielle-Calzada, J. P. (2010). Control of female gamete formation by a small RNA pathway in Arabidopsis. *Nature*, *464*(7288), 628.

Osman, K., Higgins, J. D., Sanchez-Moran, E., Armstrong, S. J., & Franklin, F. C. H. (2011). Pathways to meiotic recombination in Arabidopsis thaliana. *New Phytologist*, *190*(3), 523-544.

Ozawa, T., Natori, Y., Sato, M., & Umezawa, Y. (2007). Imaging dynamics of endogenous mitochondrial RNA in single living cells. *Nature methods*, *4*(5), 413.

Park, S. K., Howden, R., & Twell, D. (1998). The Arabidopsis thaliana gametophytic mutation gemini pollen1 disrupts microspore polarity, division asymmetry and pollen cell fate. *Development*, *125*(19), 3789-3799.

Pawlowski, W. P., Sheehan, M. J., & Ronceret, A. (2007). In the beginning: the initiation of meiosis. *Bioessays*, *29*(6), 511-514.

Pina, C., Pinto, F., Feijó, J. A., & Becker, J. D. (2005). Gene family analysis of the Arabidopsis pollen transcriptome reveals biological implications for cell growth, division control, and gene expression regulation. *Plant physiology*, *138*(2), 744-756.

Pontier, D., Yahubyan, G., Vega, D., Bulski, A., Saez-Vasquez, J., Hakimi, M. A., ... & Lagrange, T. (2005). Reinforcement of silencing at transposons and highly repeated sequences requires the concerted action of two distinct RNA polymerases IV in Arabidopsis. *Genes & development*, *19*(17), 2030-2040.

Ravi, M., Shibata, F., Ramahi, J. S., Nagaki, K., Chen, C., Murata, M., & Chan, S. W. (2011). Meiosis-specific loading of the centromere-specific histone CENH3 in Arabidopsis thaliana. *PLoS genetics*, *7*(6), e1002121.

Rotman, N., Durbarry, A., Wardle, A., Yang, W. C., Chaboud, A., Faure, J. E., ... & Twell, D. (2005). A novel class of MYB factors controls sperm-cell formation in plants. *Current Biology*, *15*(3), 244-248.

Sabelli, P. A., & Larkins, B. A. (2009). Regulation and function of retinoblastoma-related plant genes. *Plant science*, *177*(6), 540-548.

Sambade, A., Brandner, K., Hofmann, C., Seemanpillai, M., Mutterer, J., & Heinlein, M. (2008). Transport of TMV movement protein particles associated with the targeting of RNA to plasmodesmata. *Traffic*, *9*(12), 2073-2088.

Sesma, A., Castresana, C., & Castellano, M. (2017). Regulation of translation by TOR, eIF4E and eIF2α in plants: current knowledge, challenges and future perspectives. Frontiers in plant science, 8, 644.

Shi, D. Q., & Yang, W. C. (2010). Pollen germination and tube growth. In *Plant developmental biology-biotechnological perspectives* (pp. 245-282). Springer, Berlin, Heidelberg.

Slotkin, R. K., Vaughn, M., Borges, F., Tanurdžić, M., Becker, J. D., Feijó, J. A., & Martienssen, R. A. (2009). Epigenetic reprogramming and small RNA silencing of transposable elements in pollen. *Cell*, *136*(3), 461-472.

Sugimura, I., & Lilly, M. A. (2006). Bruno inhibits the expression of mitotic cyclins during the prophase I meiotic arrest of Drosophila oocytes. *Developmental cell*, *10*(1), 127-135.

Tanaka, M., Sotta, N., Yamazumi, Y., Yamashita, Y., Miwa, K., Murota, K., ... & Naito, S. (2016). The minimum open reading frame, AUG-stop, induces boron-dependent ribosome stalling and mRNA degradation. *The Plant Cell*, tpc-00481.

Tilsner, J. et al. (2009) Live-cell imaging of viral RNA genomes using a Pumilio-based reporter. Plant J. 57, 758–770

Twell D. (1992). Use of a nuclear-targeted -glucuronidase fusion protein to demonstrate vegetative cell-specific gene expression in developing pollen. *Plant J.* 2, 887-892.

Twell D. (2011). Male gametogenesis and germline specification in flowering plants. *Sex. Plant Reprod.* 24, 149-160.

Twyman R.M. (2009), Transcriptional Silencing, Editor(s): Larry R. Squire, Encyclopedia of Neuroscience, Academic Press, Pages 1099-1104,

Van Leene, J., Hollunder, J., Eeckhout, D., Persiau, G., Van De Slijke, E., Stals, H., ... & De Bodt, S. (2010). Targeted interactomics reveals a complex core cell cycle machinery in Arabidopsis thaliana. *Molecular systems biology*, *6*(1), 397.

Vandepoele, K., Raes, J., De Veylder, L., Rouzé, P., Rombauts, S., & Inzé, D. (2002). Genome-wide analysis of core cell cycle genes in Arabidopsis. *The Plant Cell*, *14*(4), 903-916.

Von Arnim, A. G., Jia, Q., & Vaughn, J. N. (2014). Regulation of plant translation by upstream open reading frames. *Plant Science*, *214*, 1-12.

Wang, G., Kong, H., Sun, Y., Zhang, X., Zhang, W., Altman, N., & Ma, H. (2004). Genome-wide analysis of the cyclin family in Arabidopsis and comparative phylogenetic analysis of plant cyclin-like proteins. *Plant physiology*, *135*(2), 1084-1099.

Wang, M., Wang, K., Tang, D., Wei, C., Li, M., Shen, Y., ... & Cheng, Z. (2010). The central element protein ZEP1 of the synaptonemal complex regulates the number of crossovers during meiosis in rice. The Plant Cell, 22(2), 417-430.

Wang, W., Wang, L., Chen, C., Xiong, G., Tan, X. Y., Yang, K. Z., ... & Chen, L. Q. (2011). Arabidopsis CSLD1 and CSLD4 are required for cellulose deposition and normal growth of pollen tubes. Journal of experimental botany, 62(14), 5161-5177.

West, S., & Proudfoot, N. J. (2009). Transcriptional termination enhances protein expression in human cells. *Molecular cell*, *33*(3), 354-364.

Weterings, K., Reijnen, W., van Aarssen, R., Kortstee, A., Spijkers, J., van Herpen, M., ... & Wullems, G. (1992). Characterization of a pollen-specific cDNA clone from Nicotiana tabacum expressed during microgametogenesis and germination. *Plant molecular biology*, *18*(6), 1101-1111.

Wilson, Z. A., & Zhang, D. B. (2009). From Arabidopsis to rice: pathways in pollen development. *Journal of experimental botany*, *60*(5), 1479-1492.

Yamashita, A., & Takeuchi, O. (2017). Translational control of mRNAs by 3′-Untranslated region binding proteins. *BMB reports*, *50*(4), 194.

Yu, H. S., & Russell, S. D. (1993). Three-dimensional ultrastructure of generative cell mitosis in the pollen tube of Nicotiana tabacum. *European journal of cell biology*, *61*(2), 338-348.

Zemach, A., Kim, M. Y., Hsieh, P. H., Coleman-Derr, D., Eshed-Williams, L., Thao, K., ... & Zilberman, D. (2013). The Arabidopsis nucleosome remodeler DDM1 allows DNA methyltransferases to access H1-containing heterochromatin. *Cell*, *153*(1), 193-205.

Zhang J., Huang Q., Zhong S., Bleckmann A., Huang J., Guo X., Lin Q., Gu H., Dong J., Dresselhaus T. et al. (2017). Sperm cells are passive cargo of the pollen tube in plant fertilization. *Nat. Plants* 3,

Zhang, F., & Simon, A. E. (2003). A novel procedure for the localization of viral RNAs in protoplasts and whole plants. *The Plant Journal*, *35*(5), 665-673.

Zhao, X. A., Harashima, H., Dissmeyer, N., Pusch, S., Weimer, A. K., Bramsiepe, J., ... & Sprunck, S. (2012). A general G1/S-phase cell-cycle control module in the flowering plant Arabidopsis thaliana. *PLoS genetics*, *8*(8), e1002847.

Zhou, X., & Meier, I. (2014). Efficient plant male fertility depends on vegetative nuclear movement mediated by two families of plant outer nuclear membrane proteins. *Proceedings of the National Academy of Sciences*, *111*(32), 11900-11905.

Zhou, Z. D., & Tan, E. K. (2017). Iron regulatory protein (IRP)-iron responsive element (IRE) signaling pathway in human neurodegenerative diseases. *Molecular neurodegeneration*, *12*(1), 75.

7. Appendix

7.1. Publication

Pollen differentiation as well as pollen tube guidance and discharge are independent of the presence of gametes

Published by The Company of Biologists Ltd | Development (2018) 145, dev152645. doi:10.1242/dev.152645

Barbara Glöckle, Wojciech J. Urban, Shiori Nagahara, Ellen D. Andersen, Tetsuya Higashiyama, Paul E. Grini and Arp Schnittger

For this paper I propagated and genotyped the *e2fa -/- fbl17+/-* FB037 cross three times and managed to obtain two lines that were homozygous in terms of GFP and RFP signal. I made pictures of PRO_{HTR12}HTR12:GFP and PRO_{HTR10}HTR10:RFP single celled pollen. I crossed *e2fa-/– fbl17+/–* plants with ET11075 Ds transposon enhancer trap line and made pictures of single-celled microspores, and two-celled and tri-cellular pollen. I have also made the pictures of single-celled microspores, and two-celled and tri-cellular pollen coming from the *cdka;1+/– fbl17+/–* crossed with ET13889 line. Additionally I performed an pollen counting experiment on the PRO_{CSLD4}GUS line.

7.2 Erklarung

Eidesstattliche Versicherung

Declaration on oath

Hiermit erkläre ich an Eides statt, dass ich die vorliegende Dissertationsschrift selbst verfasst und keine anderen als die angegebenen Quellen und Hilfsmittel benutzt habe.

I hereby declare, on oath, that I have written the present dissertation by my own and have not used other than the acknowledged resources and aids.

Hamburg, den Unterschrift

TAMWORTH10.08.2018

Linguistic accuracy declaration

I Dee Kemp, as a native speaker (United Kingdom), confirm the linguistic accuracy of the dissertation – "Towards the analysis of translational regulation during male meiosis and dissection of pollen development via mutants in cell cycle control factors in Arabidopsis thaliana." written by Wojciech Urban (matriculation number 6737874).

Signature and date

D L Kemp 10/8/18.